MODELLING, ANALYSIS AND COMPARISON OF HYDRAULIC DRIVE CONFIGURATIONS FOR THE FRONT WHEELS OF AN ALL WHEEL DRIVE MOTOR GRADER

UFUK AKPINARLI

JULY 2020

MODELLING, ANALYSIS AND COMPARISON OF HYDRAULIC DRIVE CONFIGURATIONS FOR THE FRONT WHEELS OF AN ALL WHEEL DRIVE MOTOR GRADER

A THESIS SUBMITTED TO
THE GRADUATE SCHOOL OF NATURAL AND APPLIED SCIENCES OF
ÇANKAYA UNIVERSITY

BY
UFUK AKPINARLI

IN PARTIAL FULFILLMENT OF THE REQUIREMENTS FOR THE DEGREE OF
MASTER OF SCIENCE
IN
MECHATRONICS ENGINEERING
DEPARTMENT

JULY 2020

STATEMENT OF NON-PLAGIARISM PAGE

I hereby declare that all information in this document has been obtained and presented in accordance with academic rules and ethical conduct. I also declare that, as required by these rules and conduct, I have fully cited and referenced all material and results that are not original to this work.

Name, Last Name: Ufuk AKPINARLI

Signature:

Date: 19.08.2020

ABSTRACT

MODELLING, ANALYSIS AND COMPARISON OF HYDRAULIC DRIVE CONFIGURATIONS FOR THE FRONT WHEELS OF AN ALL WHEEL DRIVE MOTOR GRADER

AKPINARLI, Ufuk

M.Sc., Department of Mechatronics Engineering

Supervisor: Assist. Prof. Dr. Ulaş BELDEK

JULY 2020, 104 pages

The subject of this study is the hydrostatic driving system that will drive the front wheels of a motor grader vehicle whose rear wheels are driven by a diesel engine. This system, referred to as All-Wheel-Drive, will increase the traction force and operating efficiency of the vehicle. The hydraulic components required for the system are characterized and calculations of the hydrostatic system and hydraulic circuit diagram are included. The hydrostatic system is modeled in Matlab / Simscape environment and the outputs are compared with theoretical calculations. In addition, the mathematical model of the motor grader vehicle and hydrostatic driving system was created in Matlab / Simulink environment. Feedforward control and feedback linearization are used in the controller design based on torque control. The test results of the system applied on the motor grader vehicle were compared with the simulations and the hydrostatic drive system was verified.

Keywords: Motor Grader, All Wheel Drive, Torque Control, Feedforward Control

ÖZ

TÜM TEKERLEKLERDEN ÇEKİŞLİ MOTOR GREYDERİN ÖN TEKERLEKLERİ İÇİN HİDROLİK SÜRÜŞ KONFİGÜRASYONLARININ MODELLENMESİ, ANALİZİ VE KARŞILAŞTIRILMASI

AKPINARLI, Ufuk

Yüksek Lisans, Mekatronik Mühendisliği Anabilim Dalı

Tez Yöneticisi: Dr. Öğr. Üyesi Ulaş BELDEK

TEMMUZ 2020, 104 sayfa

Bu çalışmanın konusu, arka tekerlekleri dizel motorla sürülen bir motor greyder aracının ön tekerleklerine tahrik kazandıracak hidrostatik sürüş sistemidir. Tüm Tekerleklerden Çekiş olarak anılan bu sistem aracın çekiş kuvvetinin ve çalışma verimliliğinin artmasını sağlamaktadır. Çalışmada, sistem için gerekli olan hidrolik komponentler (birimler) karakterize edilmiş ve hidrostatik sistemin hesaplamalarına ve hidrolik devre şemasına yer verilmiştir. Hidrostatik sistem Matlab/Simscape ortamında modellenerek çıktılar teorik hesaplamalarla karşılaştırılmıştır. Ayrıca motor greyder aracının ve hidrostatik sürüş sisteminin matematiksel modeli Matlab/Simulink ortamında oluşturulmuştur. Tork kontrolüne dayanan kontrolcü tasarımında ileri beslemeli kontrol ve geri besleme linearizasyonu (doğrusallaştırma yöntemi) kullanılmıştır. Motor greyder aracı üzerinde uygulanan sistemin test sonuçları simülasyonlar (benzetimler) ile karşılaştırılarak hidrostatik sürüş sistemi doğrulanmıştır.

Anahtar Kelimeler: Motor Greyder, Tüm Tekerleklerden Çekiş, Tork Kontrolü, İleri Besleme Kontrolü

ACKNOWLEDGEMENTS

I would like to take this chance to acknowledge who have mentored, helped and supported me along this period.

Foremost, I would like to thank my thesis supervisor Assistant Professor Ulaş Beldek for his guidance, support and encouragement throughout this research. Your support and encouragement provided me great learning opportunities. I am grateful for your mentorship.

I would like to thank Professor Klaus Werner Schmidt and Professor Yavuz Samim Ünlüsoy for their helped, support and guidance.

I would also like to express my appreciation to Hasan Basri Bozkurt, Founder of Hidromek Inc. and Mustafa Bozkurt, Chairman of Hidromek Inc., Ahmet Bozkurt, General Manager of Hidromek Inc. and Dr. İlhan Varol, Motor Grader Engineering Department Manager of Hidromek Inc.

I would like thank my colleagues for their helped, support. Their feedback about the research are significant to augment the quality of research.

This study is supported by Hidromek Inc.

TABLE OF CONTENTS

LIST OF FIGURES

LIST OF TABLES

LIST OF ABBREVIATIONS

AWD	All Wheel Drive
PTO	Power Take Off
VPDVM	Variable Pump Driving Variable Motor

CHAPTER 1

INTRODUCTION

1.1. Background

Motor Grader are construction machines used in roads and runways repair for grading, scarifying, ditching and snow removal solutions. The first graders were either pulled by horses or a power generating component were used for this purpose [1]. With the developing engine technology, internal combustion engines were integrated to graders and these grades are named as motor graders [1]. A typical motor grader is shown in Figure 1.1. There are two different frame types of motor graders: these are rigid and articulated frames. Recently, articulated frames are preferred for motor grader applications. Articulated frames generally have six wheels and they possess different attachments such as riper, scarifier, front blade and angling plow.

Figure 1.1. *Motor Grader*

In general, motor grader has single diesel engine which actuates the hydraulic functions of the grader and it also drives the rear wheels. Motor graders have three main powertrain components which are transmission, differential and tandem. Diesel engine and powertrain components are given in Figure 1.2. The engagement between diesel engine and transmission is provided by inching pedal which acts as a clutch. Inching pedal is used during take-off and stopping however it is not used for shifting gears.

Motor grader chassis design is different from many vehicles. There is a blade mechanism that performs the grading function between the front frame and the rear frame. It moves in three axes. The blade mechanism rotates around its axis with circle drawbar. In addition, the blade is able to move to right and left by the help of blade side shift cylinder and up and down by the help of blade lift cylinder. The blade mechanism has accumulators to damp unexpected forces. Due to its structure, the blade is one of the important features that make a motor grader different from other vehicles. Therefore, front axle mechanism has two different movements which are steering and leaning. Also, there are cooling and hydraulic systems for machine functions. The components of the motor grader are examined below with details:

Diesel engine is connected directly to the transmission without any other connection member. This connection is known as direct drive which is the common connection type of motor graders. Other output of diesel engine is connected to main hydraulic pump which drives the machine functions by the power delivered from it.

Damper is located between the engine and the transmission and it absorbs the vibration of the engine hence ensures the stability of the system.

Transmission has planetary gear mechanisms and transfer gears. A planetary gear system consists of planet gear, sun gear and ring gear. In this gear system, first movement starts with sun gear that is the input. Planet gears are fastened by carriers. Clutches hold ring or planet gears in respect to desired gear option.

Differential transmits power equally in both sides, so rear wheels turn same amount of revolutions. Bevel pinion gear is the major component for the differential. When a wheel enters the skid in difficult terrain, the differential lock is activated with a clutch and the power is distributed evenly to the rear wheels.

Tandem is final powertrain element which is like a chain mechanism. The sprocket gears that ensure the drive of the rear wheels are connected by the chain mechanism. Tandem can oscillate until a certain degree for grading applications.

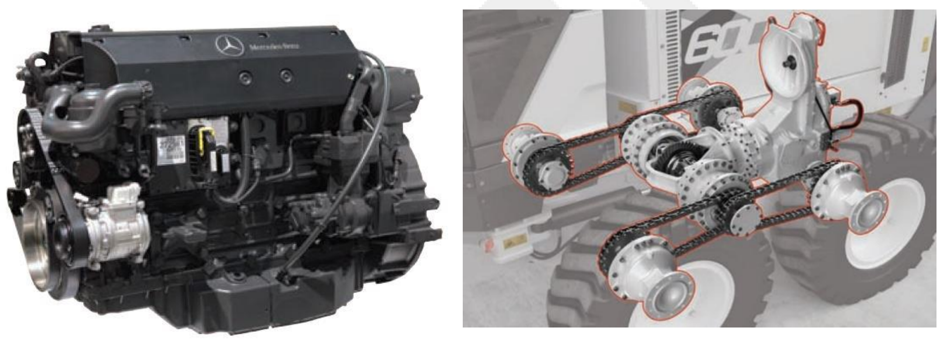

Figure 1.2. *Diesel Engine and Powertrain*

Brake system can be air-brake or hydraulic brake system. In hydraulic brake systems, brake is activated by hydraulic pressure otherwise air pressure locks clutches in air brake system.

Hydraulic system carries out significant functions of motor grader such as blade functions, articulated frame movement and front axle movements. There are three hydraulic pumps: one hydraulic variable pump is used for blade functions and the other one is employed in cooling system. The last hydraulic pump is the gear pump and it is used for steering system. Moreover, main control valve is located in the front frame and provides movement of the cylinders in reference to valve positions. Main pump provides hydraulic flow and pressure to realize the functions of motor grader vehicle.

Cooling system is precaution for overheating of diesel engine and includes a fan and an intercooler. There are three section of the intercooler which refrigerates used liquids such as oil and water in these sections separately. Rear output of diesel engine actuates the cooling pump. The flow of the cooling pump is related with the number of revolutions of the diesel engine. Fan directional control valve determines the flow direction of the fan. The flow of the pump drives the fixed displacement hydraulic motor which in total creates a hydrostatic system.

Steering system is propelled by the gear pump. Also, there is the orbitrol valve which adjusts the flow that is supplied from the pump according to the direction and the quantity of rotation of the steering shaft. Hydraulic lines of steering cylinders are connected in cross. Hydraulic flow actuates the piston side of one cylinder and rod side of the other cylinder. Steering movement is provided by this flow.

The motor grader has a complex structure and it is versatile for this reason besides it must meet expectations in the field. It has a great importance especially in road, tunnel and forest works. Many different functions of the motor grader are also needed in construction area. These functions are constantly changing and improving in line with the needs. AWD system is the most needed system in the field for motor grader with the traction it brings to the front wheels.

1.2. All Wheel Drive Application

Nowadays, motor graders are used in rough terrain conditions to grade heavy loads in parallel with the construction requirements. In difficult terrain conditions, more traction force is required to perform applications otherwise, there can be big problems for vehicle and construction process. Without AWD application, motor grader is just a rear wheel drive system which is called hydrodynamic drive. In this case, there is no traction for front wheels of motor grader and for this reason the front axle is defined as a dead axle. This means that the movement of the front wheels only depends on the rear wheels and hence the front wheels create an extra load for the rear wheels.

Due to the vehicle structure, the front wheel drive (thus AWD) is provided by hydraulic components instead of mechanical parts. That is to say, it is not feasible and applicable to direct the transmission from the diesel engine output to the front wheels with a driveshaft due to its distance and kinematic structure. Hydrostatic drive system reaches high pressure values so; more traction force is occurred. Also, the applicability of a hydraulic system is more conceivable because the steering is carried out through the front wheels. Besides, in general, in terms of controllability, the response of the hydraulic system is faster than a mechanical system.

AWD is a system for increasing the traction force by providing traction to front wheels of motor grader. Front axle can be able to carry some of its own weight due to the traction provided by AWD. Thus, the load on the rear wheels will be reduced. The load distribution on the motor grader will be driven from all wheels instead of just the rear wheels and a more powerful driving configuration will be created with AWD which enable better vehicle performance and efficiency in working areas. Moreover, the fuel consumption of the vehicle will be directly affected by the load ratio of the driving systems.

AWD is a hydrostatic drive mechanism which is defined as a closed loop hydraulic circuit to transmit force for the front wheels. Hydrostatic drive systems involve hydraulic pump(s) and hydraulic motors which are mounted in wheels. Also, hydraulic motor can contain gear or gearbox which can be used in these driving systems according to traction need. In motor grader application, hydraulic pump is actuated by diesel engine or power take-off. There are two drive configurations for this application. First one includes two hydraulic pumps and two hydraulic motors. In this drive configuration, PTO is the necessary component because diesel engine output must increase for two hydraulic pumps. At the same time, PTO can solve packaging problems. Diesel engine is connected to PTO that has a gear ratio and transmit power to hydraulic pump. Each two hydraulic pump sends flow to each hydraulic motor. Second drive configuration involves one hydraulic pump and two hydraulic motor. Hydraulic motor is actuated by diesel engine and hydraulic flow must be divided into two for hydraulic motors. Flow divider component is necessary to supply hydraulic flow equally for two hydraulic motor. Also, flushing valve is very important component for hydrostatic transmission. It can be located in hydraulic pump or hydraulic motor. It prevents overheat in closed loop circuit. Moreover, other flushing valve can be used in hydrostatic drives to cool bearings of hydraulic motors. Other feature of this drive system is free-wheeling. Free-wheeling means that front wheels do not engage hydraulic motor or gearbox which is independent by clutch or valve.

Motor graders with AWD system have two different traction systems: normal mode and creep mode. In normal mode, traction force occurs on all wheels of the machine. Especially, this application is used in snow removal operations and poor conditions. During these conditions, the vehicle needs better adhesion to the surface. Since the weight distribution on the vehicle is carried in a more balanced way in all-wheel drive system and hence this system is preferred in operations such as snow removal. In creep mode, rear wheels are not actuated this means gear is neutral, only front wheels rotate and pull vehicle. There is also the creep mode of operation where traction is provided only from the front wheels [2]. This mode is used in fine grading applications.

In general, AWD is needed for the motor grader vehicle in operations where excessive traction force is required and because AWD system is applicable for motor grader and provides desired requirements.

1.3. Literature Survey

There are very few publications about applications of motor graders and most of these limited publications focuses on hydrostatic drive of motor graders. Generally, hydrostatic drive transmission is preferred about this drive configuration.

Backas et al [3] presented feedback velocity control of hydrostatic drive transmission. Vehicle is evaluated in terms of translational dynamic that includes effects of forces. Hydrostatic circuit properties and schematic, drive configuration and velocity control methods of hydrostatic actuated wheel loader was examined in this study. Two different control methods are considered about hydrostatic drive. These are constant gain state feedback controller and PID controller. In control system, system matrix, input vector and disturbance input are described and pole placement techniques is used to calculate the gain. Then, state-feedback control loop is created with D-implementation method. Therefore, PID controller is designed for hydrostatic drive. Outputs of controllers are compared and analyzed.

Zeman et al [4] analyzed hydrostatic drive train mathematically. Firstly, axial piston pump with electro-hydraulic system including two hydraulic cylinders and 3/3 way spool valve is modelled in detail and reduced order model is created for hydrostatic drive. Also, all components that compose hydrostatic system are explained. Moreover, pump is analyzed in terms of its characteristic and implemented in all drive train system.

Kayzad et al [5] mentioned about circuit design and calculations of hydrostatic transmission actuated by electric motor. Hydrostatic transmission design is implemented for four-wheeled heavy vehicle. In calculations, hydraulic pump and motor selection is explained in detail depending on requirements. Under heavy loads, the circuit is developed and simulated in Automation Studio in order to check stability of system. Automation Studio is used to determine the gain value. Moreover, pump, motor, cooling and braking hydraulic circuits are analyzed in this study. Speed, power and power-torque graphics are evaluated and system behavior are examined. It is foreseen that the system is suitable for high accuracy and precise control.

Likaj et al [6] emphasized that hydrostatic systems work with high accuracy and performance. A circuit belonging to hydrostatic driving system is shared and calculations are made according to the requirements of this circuit. Frequency analysis of the automatic control system was performed. Then, the system model is expressed with the state space equation. Stability of the system was evaluated using Lyapunov method. Outputs of LQR and PID controller designs and system behaviors were compared.

Stroempl [7] mentioned about flow divider-combiner valves in closed loop hydrostatic transmission applications. Especially, one pump-multiple motor including hydrostatic transmissions are analyzed in this study. Also, cavitation and pressure intensification problems are explained with solutions. According to problems, solutions are determined and detailed in hydraulic circuit. Valve selection factors and the applications made with the valve selected related to these factors are interrelated. In valve operation, work conditions of flow divider-combiner valve is defined with figures which include orifices, spool etc. and hydraulic circuit with detail. When vehicle is cornering, hydraulic motors rotates at synchronous speed thanks to flow divider.

Kumbasar [8] presented design criteria of closed loop hydrostatic circuits. Firstly, closed loop circuit is defined with hydraulic circuit which is includes all components. Then, hydrostatic drive calculation is emphasized and critical points in determination of the conversion range are highlighted. Pump-motor configuration and calculations depends on conversion range. At the same time, working range and transport range is determined in traction force-speed diagram. Finally, hydraulic circuit is figured with all components in detail.

In their study, Aschemann et al [9] examine the mathematical model and control of a hydrostatic transmission circuit. In this process, hydraulic pump, hydraulic motor, pressure and torque relationships are formulated. After examining the dynamics of the actuator, the state space representation of the entire model was made. Different methods were used for nonlinear control in the control phase. These include flatness-based control of the tilt angle of the hydraulic motor and state feedback design using extended linearization techniques. In the linearization phase, eigenvalue, feedforward control and dynamic disturbance techniques were used. The simulation and test outputs obtained as a result of these methods were evaluated.

Song et al [10] introduce HydraulicAddiDrive system features and components. In addition, studies on speed synchronization are mentioned. The system consists of a hydraulic pump and two hydraulic motors. The system configuration is as shown in the Figure 1.3.

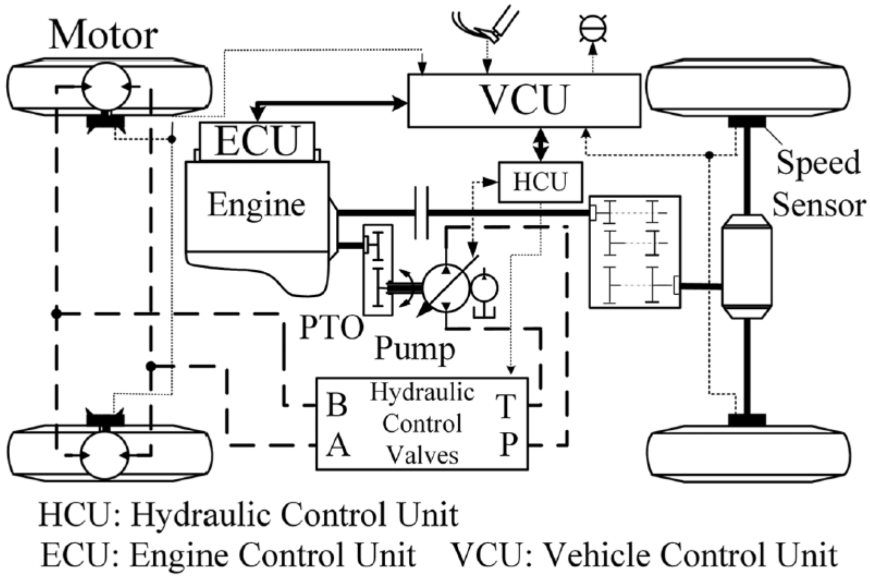

Figure 1.3. *System Configuration [10]*

The system will be applied to the front axle in a manner similar to the motor grader application and the purpose of the system is to increase the traction force. Feedforward and feedback control strategies were examined in speed synchronization. A controller design consisting of a combination of these two structures was realized. The controller structure is given in Figure 1.4. PI algorithm is used to eliminate errors in the control algorithm. Amesim and Matlab programs were used for simulations during the activities carried out in the studies. The resulting speed, torque and displacement graphs were analyzed.

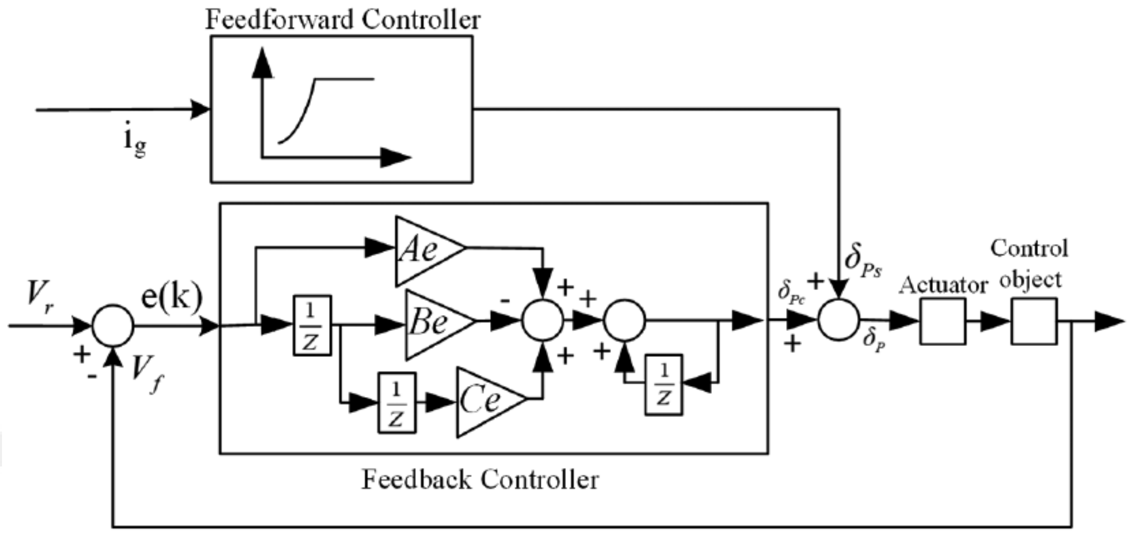

Figure 1.4. *Compound of Feedback and Feedforward Control [10]*

Aschemann et al [11] has described hydrostatic transmission system as a mechatronic system. Modeling is divided into two subsystems, Mechanical and Hydraulic. The actuator dynamics of the system formulated as mechanical and hydraulic are determined and the situation is expressed as state space representation. Ljapunov method was used to eliminate the error in the control application. In this control method, separate control systems have been created for the hydraulic motor and hydraulic pump. Model outputs were evaluated by using observer based disturbance compensation method for model uncertainties.

Yan et al [12] evaluate variable pump driving variable motor (VPDVM) system which is given in Figure 1.5. VPDVM is a hydrostatic transmission system designed for an unmanned vehicle. A fourth order state space model was obtained for the VPDVM system. Feedback linearization is used to make this nonlinear system linear. The bang-bang control method is used for the hydraulic pump. Hydraulic motor displacement and hydraulic pump displacement are controlled according to the desired hydraulic motor speed with this control method. In the simulation outputs obtained according to these control methods, the desired hydraulic motor speed, hydraulic motor speeds at different engine loads and different pump speeds were examined.

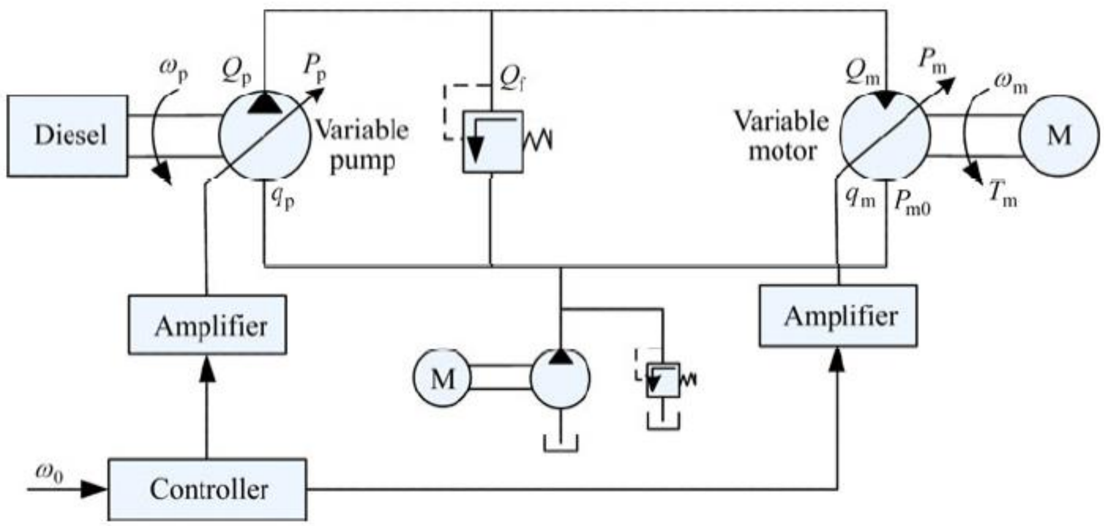

Figure 1.5. *VPDVM System (12)*

Jedrzykiewicz et al [13] improve mathematical model of hydrostatic drive system. Simulations were carried out by giving the appropriate values to the parameters of the model. Hydraulic motor speed, load applied to hydraulic motor and swash plate angle of variable displacement pump were observed.

Akkaya [14] construct a hydrostatic driving model in detail. Two different controller designs were made for this system. These are PID and fuzzy controllers. The simulations results are compared. When comparing these results, the variability of the bulk coefficient in the model was observed. The simulation results and model bulk coefficient were evaluated according to whether they were fixed or variable.

1.4. Thesis Objective

In this study, the design of the hydrostatic drive system has been realized in order to supply traction force to the front wheels of the motor grader vehicle. At the same time, the designed system was mathematically modeled. In order to test it on the vehicle and create a final product, its software was also implemented in an embedded software environment.

Initially, two different configurations were emphasized for the hydraulic drive system and components for these configurations were specified. These two configurations were assessed according to the characteristics of the vehicle and the configuration suitable for the vehicle was selected. This process was followed by the selection of the components that form the selected hydraulic system and calculations of hydrostatic drive system were realized accordingly. Moreover, the maximum power that the hydrostatic drive system can consume from the diesel engine has been calculated. Therefore, the hydraulic circuit diagram was created. Comparing the theoretical calculation results and simulation results in Matlab-Simscape environment, the first observations of the created hydrostatic drive system were obtained. Then, the mathematical model of the system was created in Matlab-Simulink. At the same time, other components and dynamics of the vehicle were modeled mathematically and the controller was designed. Feedback linearization and feed forward control methods were used during the controller design. The controller performs the displacement control with the torque parameter.

Thanks to this system, the motor grader vehicle, which gained more traction, will be able to operate more efficiently in many difficult terrain conditions.

1.5. Organization of thesis

Chapter 1 gives information about the definition of motor grader and AWD system and literature research. Chapter 2 includes the AWD hydraulic system, the components of the hydraulic system and hydraulic calculations. In addition, there are studies evaluating the simulation and study cases of this hydraulic system. Chapter 3 describes the mathematical model of the AWD system. Chapter 4 includes the controller design according to the mathematical model created. The last part, the Chapter 5, consists of a general evaluation of the thesis.

CHAPTER 2

SYSTEM DESCRIPTION

2.1. AWD Hydraulic System

AWD hydraulic system is a hydrostatic drive system which is preferred especially in construction and agricultural machines. Hydrostatic transmission systems are special energy transmission systems, which convert mechanical energy into pressure energy in the incompressible working fluid and then converts it into mechanical energy in the output shaft and performs the movement in the system [15]. Hydrostatic drive system is a closed loop hydraulic system and reaches high pressure levels in order to create high torque values. Also, it is more advantageous than mechanical drive system in terms of cost and efficiency. The absence of gear stoppages, efficient use of diesel engine power and the system, the use of additional brake components due to hydrostatic brakes, controlled acceleration and high traction are among the important advantages [8].

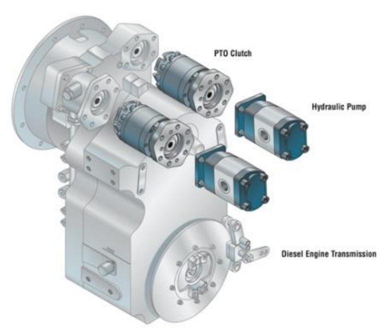

Figure 2.1. *PTO Application [16]*

In motor grader AWD hydrostatic application, there are two drive configurations. Firstly, dual pump and dual hydraulic motor is used for this drive system. In order to use dual pump, diesel engine output should be increased with power take off (PTO) which is mounted to diesel engine shaft and transmit power to two outputs thanks to gears. PTO is a component that has gears and is frequently used for power transmission in construction machinery applications. PTO application is illustrated in Figure 2.1.

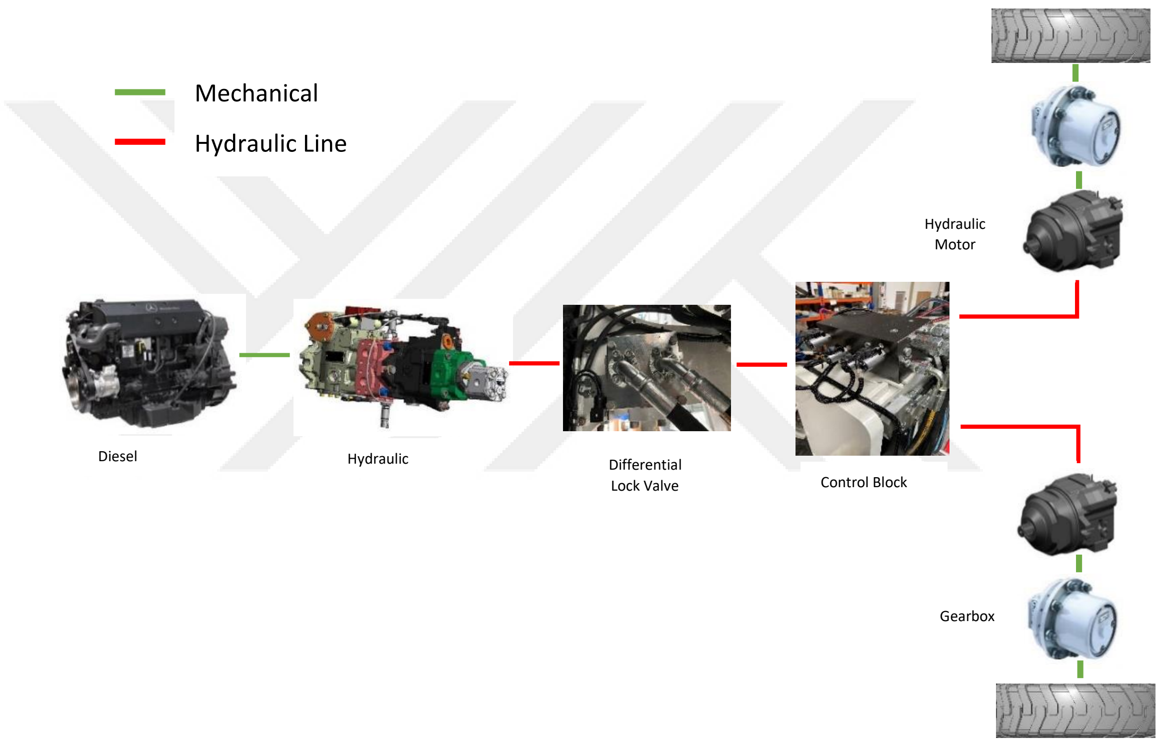

Figure 2.2. *General Structure of AWD System*

In other configuration, one pump actuates two hydraulic motors. With the cardan shaft, the pump is directly connected to the diesel engine. This configuration is chosen because of packaging problems. In hydrostatic transmission, flow divider is necessary to divide flow equally. In each configuration, hydraulic motors are packaged in wheels and hence the front axle structure changes which requires mechanism’s re-design and optimization. At the same time, flushing valve is used in hydraulic pump or hydraulic motor for this drive system to prevent overheat. Moreover, freewheeling is integrated to activate or de-activate drive system. Freewheeling is provided by valve or clutch.

Hydrostatic transmission scheme, the basic diagram of which is given in Figure 2.2, consists of a single pump double engine and it is the main drive element in diesel engine.

2.2. AWD Hydrostatic System Calculations

In hydrostatic systems, hydraulic pump and hydraulic motor selection is calculated and evaluated according to the conversion range. The ratio of largest output torque to the smallest at a constant power is described as a conversion range and that is the most practical method to determine hydraulic motor-pump configuration in hydrostatic drive [17].

In hydrostatic transmission circuits, hydrostatic drive characteristic curve given in Figure 2.3 should be taken into account during calculations. In hydrostatic transmission circuits, higher pressure and force values can be obtained in regions with low speed. As the vehicle speed increases, the traction force produced by the hydrostatic transmission circuit decreases.

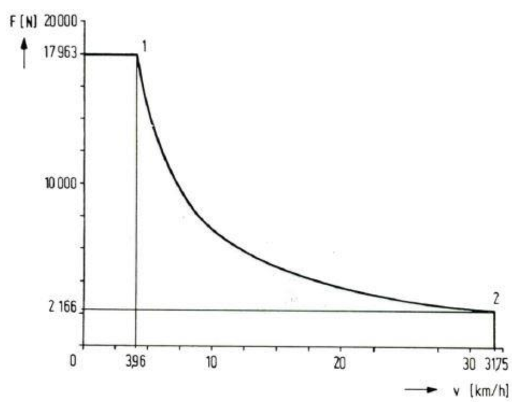

Figure 2.3. *Hydrostatic Drive Characteristic Curve [17]*

The conversion range value determines the type of hydraulic pump and hydraulic motor. Hydraulic pump and hydraulic motor can be variable or fixed displacement. Conversion range formula is given in Equation 2.1.

$$R = \frac{V_{maximum} * F_{maximum}}{3600 * \eta_{\mathrm{t}} * \eta_g * P} \tag{2.1}$$

In Equation 2.1, $V_{maximum}$ is maximum speed of travel in km/h, $F_{maximum}$ is traction force in Newton, and P is drive power that is determined with power regulation. η_t is overall efficiency, η_g is mechanical transmission efficiency. By using R value in Equation 2.1, system configuration is selected as given in Table 2.1.

R ≤ 3	***conversion by variable pump***
R > 3	***conversion by variable pump and variable motor***

Table 2.1. *Hydraulic Pump and Hydraulic Motor Selection According to Conversion Range [17]*

The conversion range for this drive system is greater than three, so the hydraulic pump and hydraulic motor have variable displacement. Variable displacement hydraulic pump and double displacement hydraulic motors are also used in hydrostatic drive systems for construction machines. These configurations provide variable speed variation, but the fact that the hydraulic pump and hydraulic motor are variable enables more efficient power usage for each speed change. The maximum speed and maximum force values in the conversion range formula depend on the vehicle's requirement. The square root of the calculated conversion range gives the conversion ratio of the hydraulic pump and hydraulic motor. This calculation is given in Equation 2.2.

$$R_{motor} = R_{pump} = \sqrt{R} \tag{2.2}$$

Hydraulic pump displacement formula which is given in equation 2.3, mainly depends on the maximum pressure change, maximum force, maximum speed and conversion range of the hydraulic pump.

$$\mathrm{V_{pump}} = \frac{170 * \mathrm{V_{maximum}} * \mathrm{F_{maximum}}}{\Delta p_{maximum} * n_{pump} * \eta_t * \eta_g * R_{pump}} \tag{2.3}$$

Hydraulic motor displacement formula is similar to the hydraulic pump displacement formula and is given in Equation 2.4.

$$\mathrm{V_{motor}} = \frac{170 * \mathrm{V_{maximum}} * \mathrm{F_{maximum}}}{\Delta p_{maximum} * n_{motor} * \eta_{hm} * \eta_g} \tag{2.4}$$

Hydraulic motor and the wheel are connected directly to each other and they rotate at the same speed. The speed of the hydraulic motor depends on the ratio of gearbox and wheel radius. The maximum speed value determined for the system is critical in the displacement selection of the hydraulic motor. Speed calculation of hydraulic motor is given in Equation 2.5.

$$n_{motor} = \frac{2.65 * V_{maximum} * i_{gearbox}}{r_w} \tag{2.5}$$

In Equation 2.5, n_{motor} is maximum hydraulic motor speed in rpm, r_w is wheel radius in meter, $i_{gearbox}$ is planetary mechanism gear ratio of gearbox, n_{hm} is hydro mechanical efficiency.

The following method can be used to determine the velocity and force values found in these selections. Firstly, required traction force is obtained according to resistance forces, which are summation of rolling, climbing and acceleration forces. Relation of these forces are given in Equation 2.6.

$$F_{req} = F_{rolling} + F_{climbing} + F_{acceleration} \tag{2.6}$$

Required traction force must be less than the limit traction force which depends on weight. Otherwise, the wheel will skid because the force on the wheel is excessive. Traction force to be obtained also depends on the force determined for the system.

Some of the power generated by the vehicle engine is reserved for this system. The power and priority of the other components on the vehicle are chosen while determining the power to be allocated to this system. The power regulation of the system is specified by designating the power to be transferred from the diesel engine for the AWD system according to the maximum power spent by hydraulic and mechanical drive systems. Power calculation is given in Equation 2.7.

$$P = \frac{\Delta p * Q}{600} \tag{2.7}$$

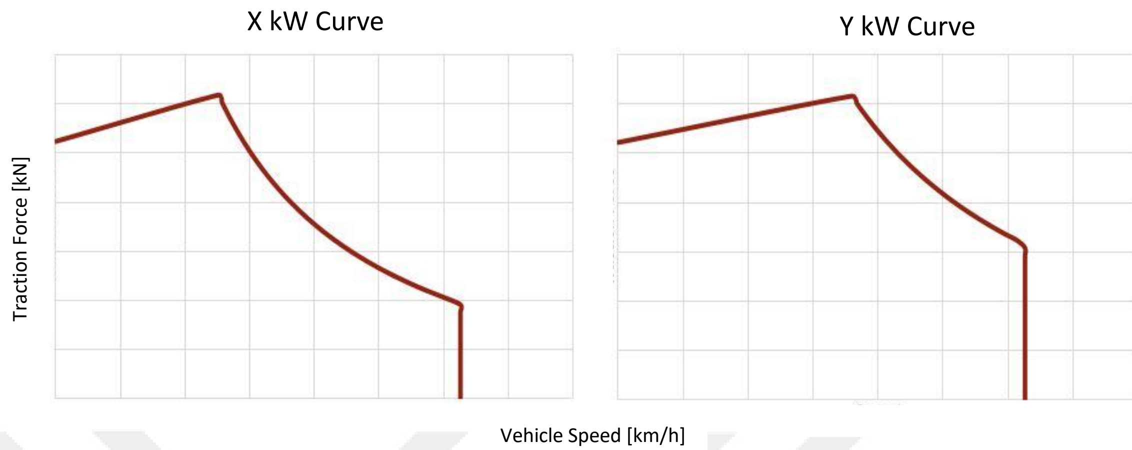

Figure 2.4. *Comparison of Different Power Curves*

In Equation 2.7, P is power in kW, Δp is pressure difference in bar and Q is flow in l/min. The power regulation determined for the system enables to determine the maximum power that can be spent during speed changes. When calculating the power regulation, the flow-pressure relationship that may occur in the system is taken into consideration. While the pressure value is decreased from the maximum value to the minimum, the flow regulation is increased and the power regulation in the system is completed and maximum power is chosen. During this calculation, the effect of power on traction force velocity graph can be observed. As it is seen in the Figure 2.4, as the system power increases, the power value that the system reaches at the same speed value increases. The power value used on the y curve is greater than the power value used on the x curve.

2.3. System Components

2.3.1. Variable Displacement Pump

Variable displacement pump(s) is actuated by diesel engine. Hydraulic pump provides flow which depends on diesel engine angular speed and displacement of pump. Pump flow equation is given in Equation 2.8. Q is pump flow in l/min, n is input speed of pump and n_{vol} is volumetric efficiency.

$$Q = \frac{V * n * \eta_{vol}}{1000} \tag{2.8}$$

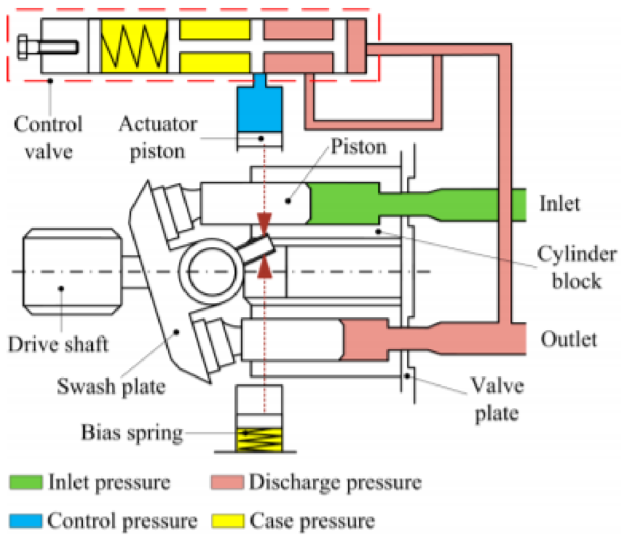

Figure 2.5. *Swash Plate Mechanism [18]*

Variable displacement hydraulic pump is preferred to reach different speeds. The swash plate mechanism inside the pump allows us to control the flow by adjusting the displacement. This mechanism shown in Figure 2.5 consists of control valve, pistons, driveshaft and plate.

The drive of this mechanism is carried out by a piston. As the stroke of the piston moves, the pump displacement changes according to the relationship between the stroke and displacement. The piston is driven by a control valve. In this system, there are solenoid valves on the pump. These valves, energized by current, provide movement of the piston. The angle of the swash plate mechanism is calculated with the linear variable displacement transducer sensor placed in the piston. This calculated angle value is sent to the pump controller as a feedback signal to ensure the precise operation of electronically controlled variable displacement pumps as a closed circuit system and the pump displacement is controlled. Control structure of variable displacement pump is given in Figure 2.6. A PID controller is designed to minimize the margin of error between the displacement value corresponding to the current value used to control and the displacement value corresponding to the plate angle taken as feedback. Also, the plate can be activated on both sides, the direction in which the plate is inclined determines the direction of rotation of the pump. After the pump shaft rotates with the determined pump displacement, the flow is started to be produced for the hydraulic system.

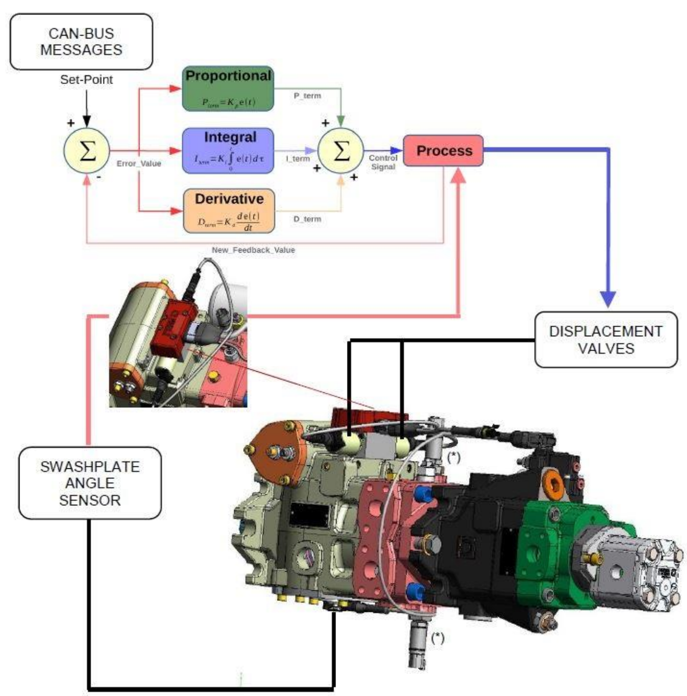

Figure 2.6. *Variable Displacement Pump Control Structure*

There is a relationship between the current value of the solenoid valve and the pump displacement. This relationship is given in Figure 2.7.

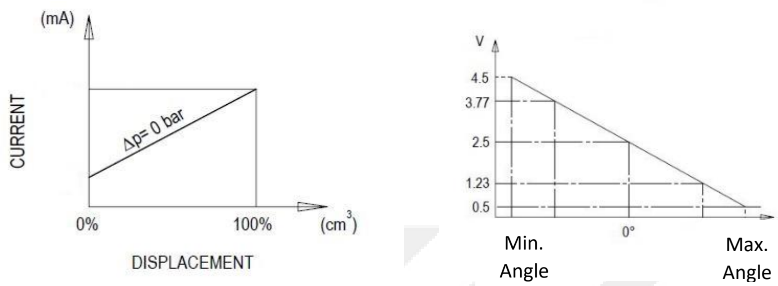

Figure 2.7. *Current-Displacement and Voltage-Swash Plate Angle Relation*

2.3.2. Variable Displacement Motor

Variable displacement hydraulic motors have been used to provide variable speed range and power regulation in this system. Variable hydraulic motor is actuated by pump flow and includes swash plate mechanism like hydraulic pump. This hydraulic motor has axial pistons. Radial piston motors produce more torque than axial pistons. So, hydraulic motors are connected to gearbox to generate more traction force. Adaptation of the AWD system to the front wheels is given in Figure 2.8.

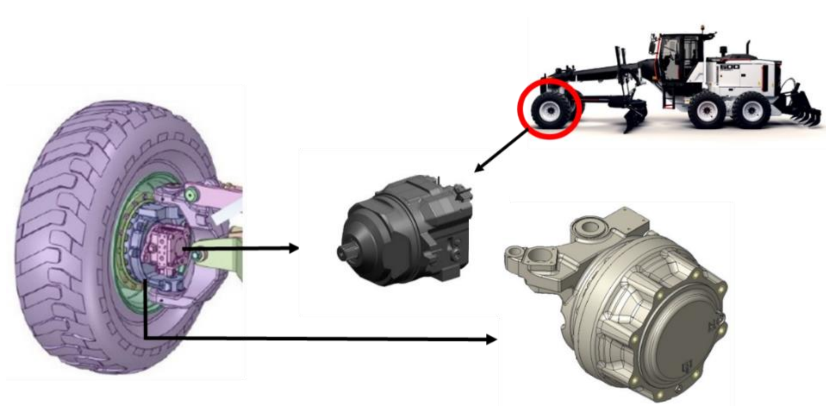

Figure 2.8. *Adaptation of the AWD system to the front wheels*

The control mechanism of the valve is different from the pump. A gear pump is also used to ensure the control pressure of the engine. The hydraulic motors are controlled by the pressure coming from the pilot line. Depending on the relationship between the current value of the solenoid valve and the incoming pressure value, the valves are energized to control the displacement of hydraulic motors within a certain pressure range.

Hydraulic motor displacement and speed are critical parameters for control algorithm of hydrostatic drive system. For this application, hydraulic motor speed is measured by speed sensor whose working principle depend on Hall Effect logic. Speed parameter are used as feedback for speed synchronization and power limitation in AWD control system. The speed difference between the wheels is calculated by the speed sensors and the skidding condition is determined. In such a case, the second position of the differential lock valve is energized and the flow sent to both sides is equalized. In addition, the first position of the valve is active in the case of drive.

2.3.3. Gearbox

The gearbox is a component mounted in the rim to increase the torque generated and provide connection to the wheels. At the same time, the gearbox which contains the steering arm carries the steering mechanism of the vehicle. It involves planetary type gear mechanism and clutch which provides freewheeling function. Thanks to freewheeling function, the wheel is joined or separated by the gearbox and hydraulic motor. Gearbox pressure port is related to hydraulic pressure line of system to pressurized clutch. A schematic representation of the gearbox is given in Figure 2.9. The maximum flow, maximum speed and maximum torque values must be taken into consideration when selecting the gearbox.

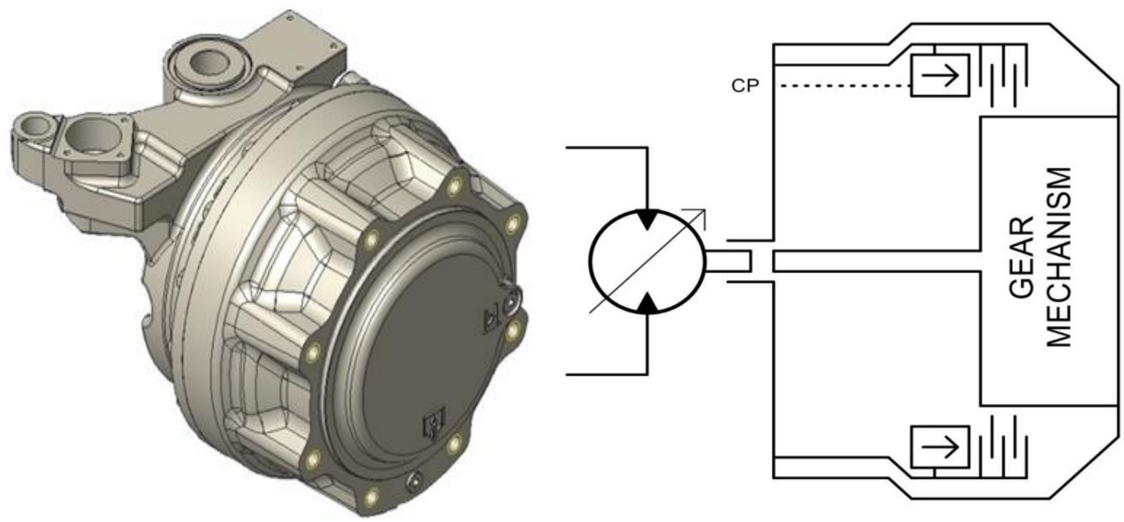

Figure 2.9. *Gearbox Mechanism*

2.3.4. Differential Lock Valve

Differential lock valves are applied in hydrostatic drive system for one pump-two motor configuration. It is mainly used to separate the flow equally with regulating motor speeds in the hydraulic line and eliminate slipping for different land conditions with variable orifices. Differential lock valve schematic representation is given in Figure 2.10.

Firstly, default position divides the flow according to the wheel speeds, that valve is non-energized. There is orifice between A and B hydraulic lines, which synchronizes wheel speeds during steering. In this case, the inner and outer wheels will spin at different speeds. It acts as a differential between the A and B lines of the valve, thus distributing the flow according to the speed of the wheels. Thanks to it, system controller does not adjust speed parameters in this case. When size of orifice is determined, maximum steering angles are critical parameters for synchronization. Inside and outside wheel speeds are different from each other with regards to dynamics of front axle. The amount of flow that can pass through the orifice is directly related to the rotation angles of the axle. So, balancing orifice size have importance for steering control.

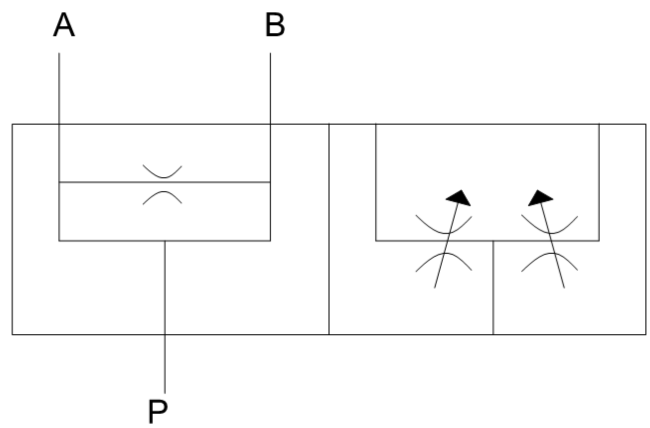

Figure 2.10. *Differential Lock Valve Schematic*

There is also another function than dividing the flow into two equally. Thanks to its variable orifices, the wheel skid condition can be controlled hydraulically. When different wheel speeds are measured by speed sensors, the second position is activated by energizing the valve. With the second position of the valve activated, flow is sent equally to both wheels.

Secondly, cavitation and pressure intensification in flow divider can create problems for hydrostatic drive systems. If the flow divide ratio is not selected correctly, cavitation may occur in the system when performing vehicle turns. Moreover, pressure intensification is possible during flow combination if the flow combiner is engaged and all of the wheels have good adhesion with the ground [7]. To prevent these problems, the choice of orifices should be made according to the front axle maximum rotation angle. The amount of flow division error should be minimized for proper transmission.

2.3.5. Hydraulic Control Block

Hydraulic control block provides flow control for forward and reverse direction. In this block, high stability valves should be preferred. Solenoid valves are available for controlling forward and reverse movements. The pressure in these lines is controlled by transmitters that measure the pressure sent to activate the clutch in the gearbox.

Ball valves are used in the lines used for the control of forward and reverse solenoids. The pressure value coming from the line of the activated valve moves the ball valve mechanism and pressure is sent to the clutch. Control block schematic representation is given in Figure 2.11.

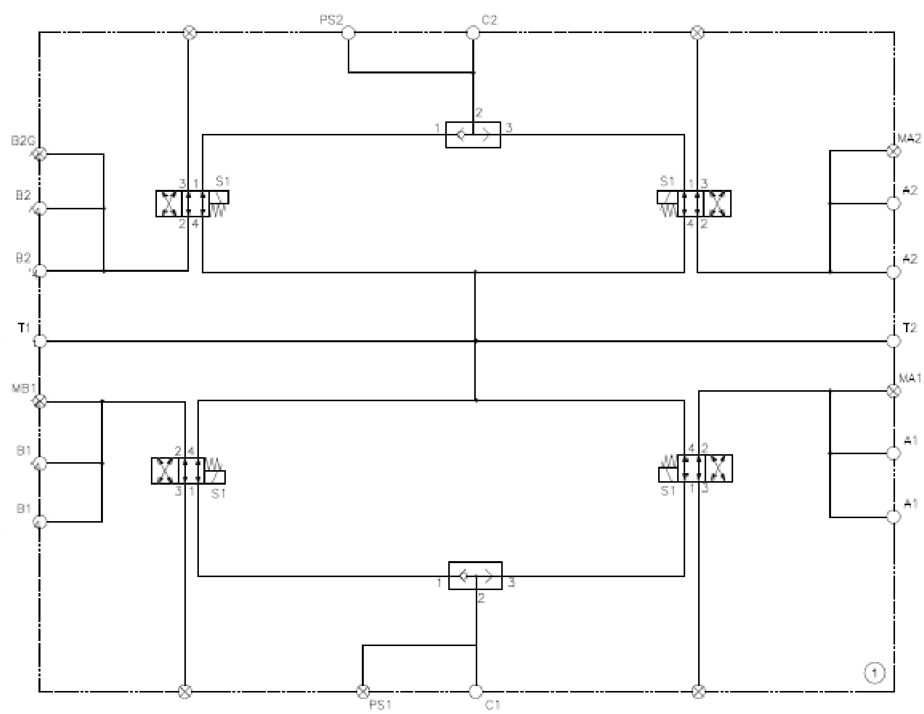

Figure 2.11. *Control Block Schematic*

2.3.6. Flushing Valve

Hydrostatic drive circuits are designed to work in a way that is not affected by cold oil taken from the tank. In these systems which can operate at high pressure and high speeds, the oil temperature can rise to high levels. Cooling component is needed in the system to prevent the oil temperature from rising to high temperatures.

Flushing valve cools the hydraulic oil by allowing a certain part of the oil in the system to be sent to the tank. The position of the valve changes according to the pressure between lines A and B in the hydraulic system. Therefore, the flow rate of the oil that the flushing valve will drain from the system to the tank is critical. Orifice or relief valve can be used to control the flow after the flushing valve while the hydraulic oil is drained into the tank. If this flow rate is large, the system will remain cold, and if it is small, there will be heating in the system [20]. In such a case, the system will not work at the expected efficiency. In this type of drive systems, it is sufficient to use a flushing valve in the pump or motor. In this system, the flushing valve is located on the pump. If the power loss and flow in the system is known, temperature change is calculated and valve selection is made [20].

2.4 Hydraulic Scheme

The hydraulic diagram of the system, which includes all the system components described in the previous section, is shared in this section. The system can be examined in more detail on the hydraulic scheme which is given in Figure 2.12.

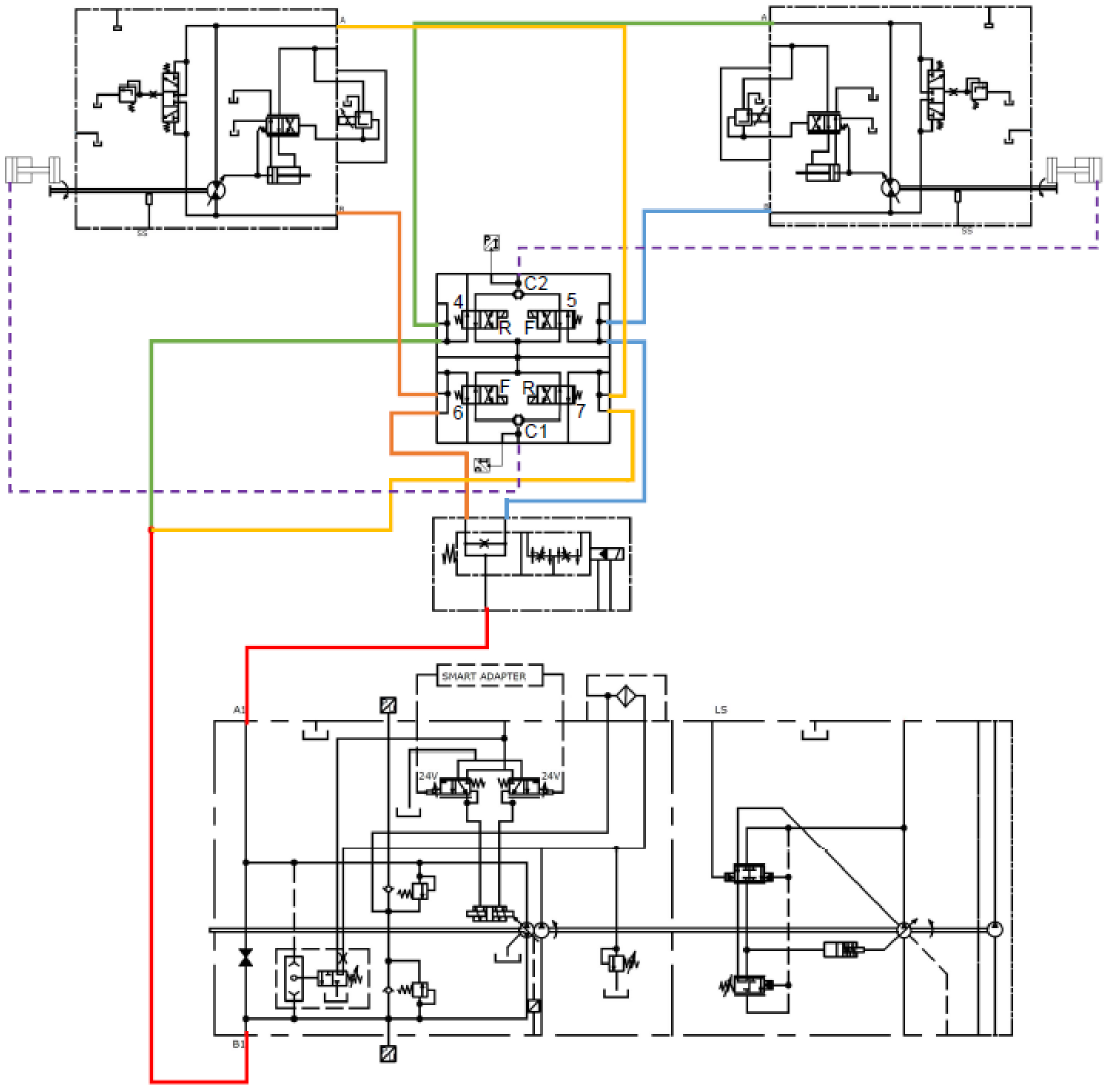

Figure 2.12. AWD Hydraulic Scheme

2.5 Hydraulic Simulation

A simulation was performed in Matlab-Simscape environment to test the hydraulic system's accuracy and how it works in the specified scenario. The most suitable blocks in Matlab environment were chosen for the components in the system. Components that are not available in Matlab were created using other blocks in Matlab. For example, since the flushing valve and differential lock valve in the system are not available in Matlab-Simscape, these valves are modeled using orifices. The hydraulic model includes the hydrostatic front drive system that extends from the hydraulic pump to the hydraulic motors and located on the front frame.

In the model, angular velocity source symbolizes the rotational speed of the diesel engine and is directly connected to the pump shaft. Then, inertia block contains diesel engine inertia with flywheel. These are showed in Figure 2.13.

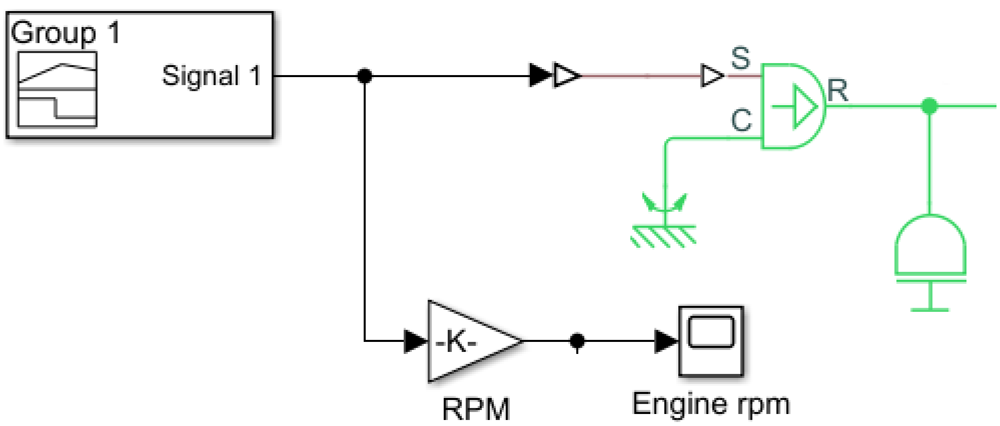

Figure 2.13. *Angular Velocity Source*

Variable displacement hydraulic pump block is used to create flow. The charge pump is connected to the pump shaft and feeds the system with the hydraulic oil in the tank. Fixed displacement hydraulic pump is used for charge pump. P line of block links system hydraulic network, T line of block connects to hydraulic reference. These blocks are related to equations that are given in Equation 2.9, 2.10, 2.11.

$$q = q_{ideal} + q_{leak} \tag{2.9}$$

$$T = T_{ideal} + T_{friction} \quad (2.10)$$

$$K_{HP} = \frac{v_{nom} * \rho_{nom} * w_{nom} * D_{MAX}}{\rho * v * \Delta p_{nom}} * (1 - \eta_{v_{nom}}) \quad (2.11)$$

For variable displacement pump,

$$q_{ideal} = D_{sat} * w \quad (2.12)$$

$$T_{ideal} = D_{sat} * \Delta p \quad (2.13)$$

$$q_{leak} = K_{HP} * \Delta p \quad (2.14)$$

$$T_{friction} = (\mathrm{T}_0 + K_{TP} * \left|\frac{\mathrm{D_{SAT}}}{D_{MAX}}\right| * |\Delta p|) * \tan(\frac{4 * w}{w_{thresh}}) \quad (2.15)$$

For fixed displacement pump,

$$q_{ideal} = D * w \quad (2.16)$$

$$T_{ideal} = D * \Delta p \quad (2.17)$$

$$q_{leak} = K_{HP} * \Delta p \quad (2.18)$$

$$T_{friction} = (\mathrm{T}_0 + K_{TP} * |\Delta p|) * \tan(\frac{4 * w}{w_{thresh}}) \quad (2.19)$$

These pumps are illustrated in Figure 2.14.

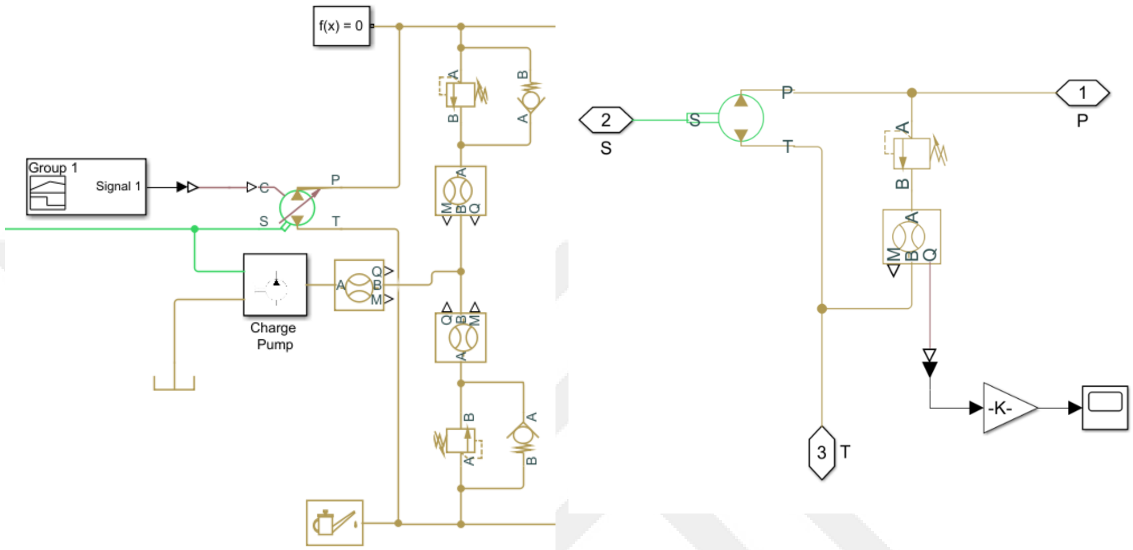

Figure 2.14. *Variable Displacement Pump and Charge Pump*

Sequence valves connected to lines A and B are available after the pump. Sequence valve consisting of relief valve and check valve is used to control the pressure. Relief valve flow rate is related to valve opening distance, which are determined as linear area-opening relationship parameterization in block. Related formulas are given in Equations 20, 21, 22.

$$q = \mathrm{C_d} * S * \sqrt{\frac{2}{\rho}} * \frac{\Delta \mathrm{p_{AB}}}{(\Delta \mathrm{p_{AB}^2} + \Delta p_{crit}^2)^{\frac{1}{4}}} \tag{2.20}$$

$$p_{crit} = \frac{\rho}{2} * \left(\frac{Re_{crit} * \nu}{C_d * D_h}\right)^2 \quad (2.21)$$

$$D_h = \sqrt{4 * \frac{S}{\pi}} \quad (2.22)$$

In check valve block, valve opening dynamic is linearly proportional to pressure difference between hydraulic lines A and B. There is not any load case on the valve. Equations of check valve are similar with relief valve equations. Thanks to the pressure sensor connected between the A and B lines, the ΔP pressure of the system is measured. Valve actuator is driven with this pressure and flushing valve operation is provided in the model. Pressure sensor, valve actuator, sequence valves and loop flushing valve are given in Figure 2.15.

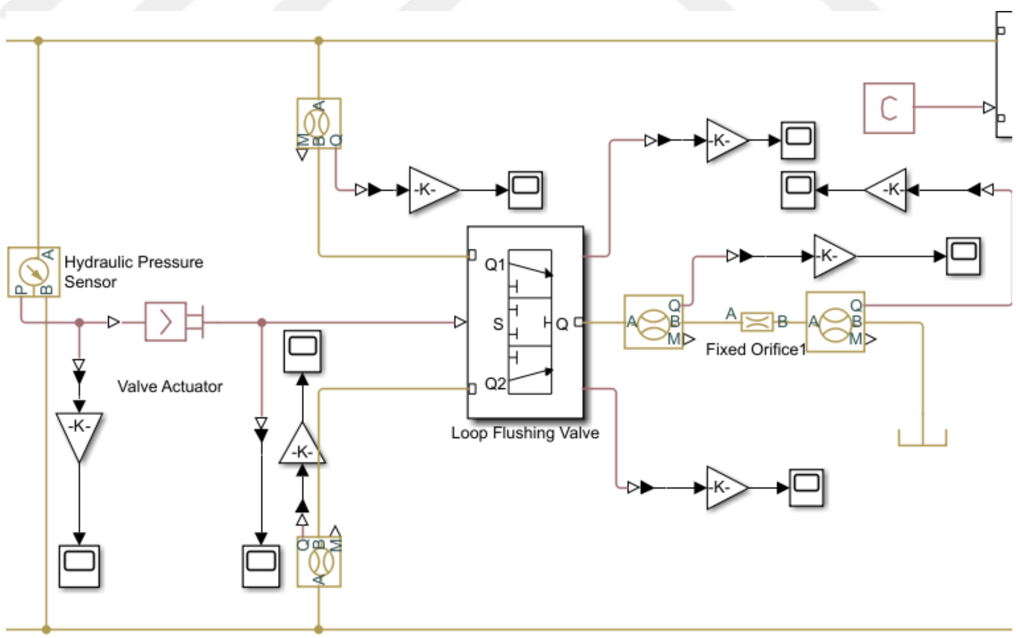

Figure 2.15. *Flushing Valve*

Valve actuator block is created with Simscape blocks that is showed in Figure 2.16. First PS gain block build the steady-state relationship between input and output signals. Moreover, first order control loop with feedback mechanism is generated. Saturation block inside valve actuator is determined valve stroke range, second gain refers "1/TimeConstant" and first order lag is created with the combination of PS Subtract and PS Integrator blocks. Thanks to the first order lag, a filter or damping is realized. Transfer function of valve actuator block is given in Equation 2.23.

$$H(s) = \frac{1}{Ts + 1} \tag{2.23}$$

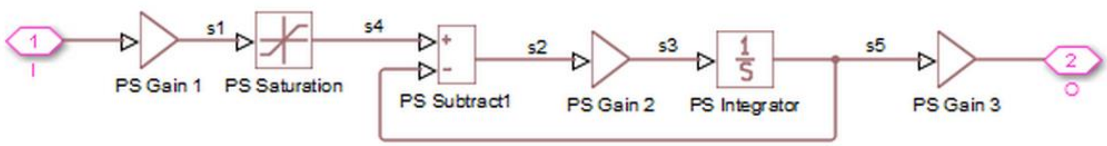

Figure 2.16. *Valve Actuator*

Flushing valve designed with orifices are including in Simscape. It includes two orifices for each direction. Respectively, the first orifice represents the first position of flushing valve and the second orifice represents the third position of flushing valve. The zero value of the valve on the S line is the middle position of the valve, that is to say the position where the flow does not pass. Opposite directions were chosen for the orifices used to design the valve. In other words, one orifice is opened while the other is closed. According to pressure differential, flushing valve position can change and hydraulic flow of A or B lines drains to tank. Thus, it is of great importance in cooling the oil in the system. After flushing valve, fixed orifice is used to control hydraulic flow. If orifice is not used, the amount of flow discharged from the system to the tank increase. The system may not reach the required flow rate by draining excess oil. Flushing valve design is given in Figure 2.17.

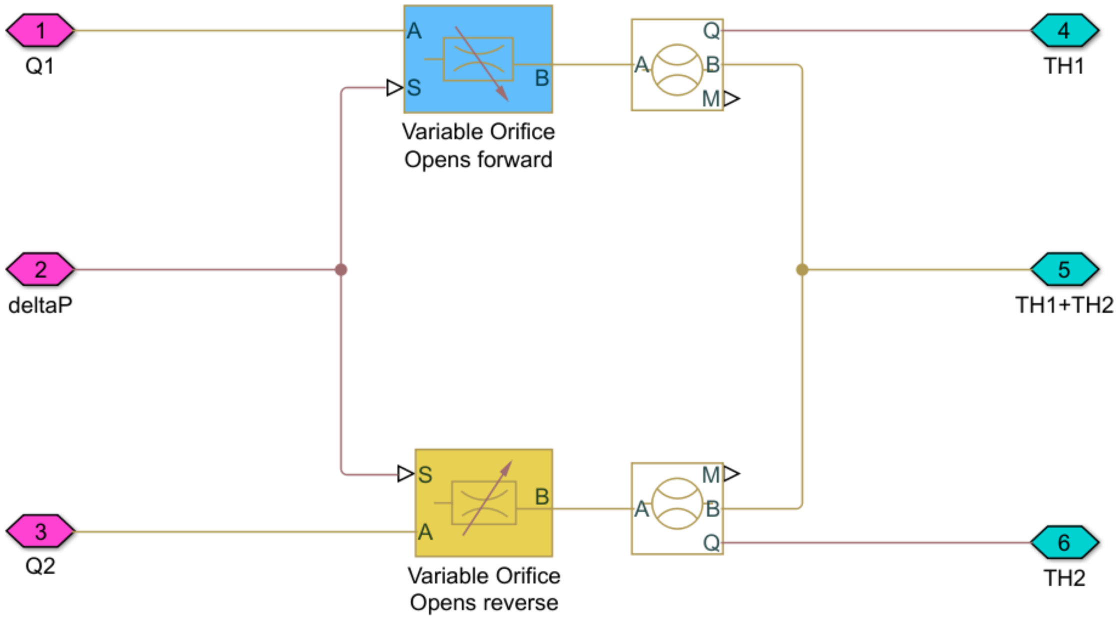

Figure 2.17. *Flushing Valve Design*

Differential lock valve designed using orifices such as flushing valve. During steering and skidding, this valve controls hydraulic flow and these cases are simulated to evaluate synchronous rotation of the wheels. The position of the valve completely depends on the driving situation. If the machine is in normal driving, the first position of the valve is used. If the spinning situation is to be evaluated in a scenario in the simulation, the second position of the valve can be used. The flow to the valve will move to the first position or the second position according to the signal value. In the first position, there is a fixed orifice between the lines leading to the motor, while in the second position there are two variable orifices that are constantly open and move in the same direction. Differential lock valve design is given in Figure 2.18.

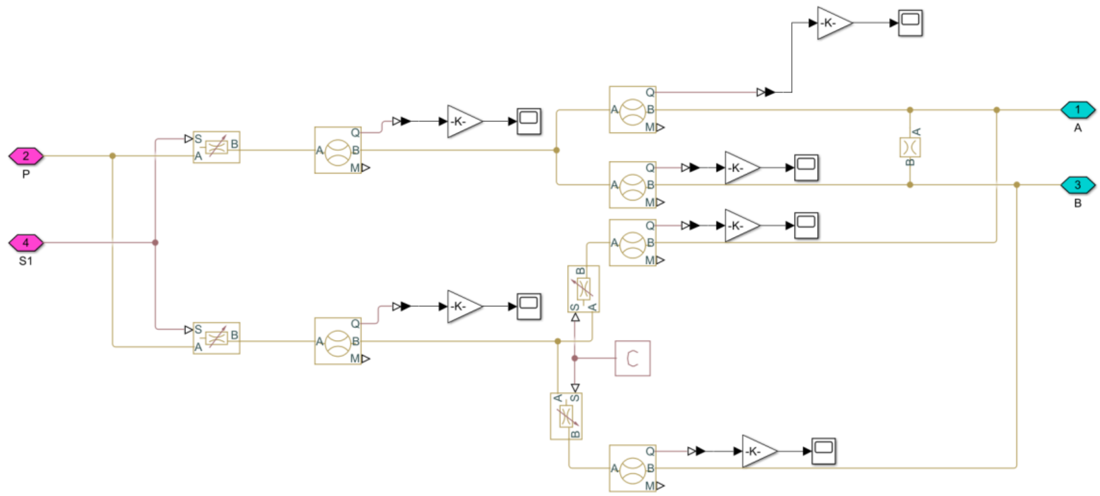

Figure 2.18. *Differential Lock Valve Design*

Flow from this valve is transmitted to hydraulic motors. Also, “Ideal Torque Source” blocks were used to simulate the load on the hydraulic motor. In addition, rotational damper block is linked with ideal torque source to eliminate instantaneous reactions. The load on the hydraulic motor has been used as it will cause an increase in the hydraulic system pressure and it is desired to observe this pressure increase. Due to the pressure sensor, how the hydraulic system pressure changes in response to the applied torque can be observed. Load case blocks are given in Figure 2.19.

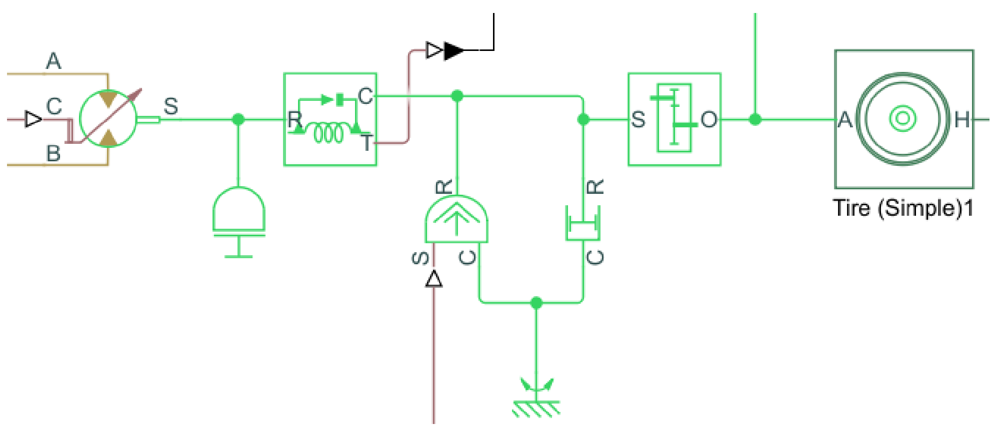

Figure 2.19. *Torque Source Block for Load Cases*

A torque sensor is connected to the hydraulic motor output to calculate the traction force. The torque value generated by the hydraulic motor in the no-load condition was determined and added with the torque value measured. In the first case, the initial condition block is used to indicate that it is zero. Torque sensor, gearbox and tire blocks are given in Figure 2.20.

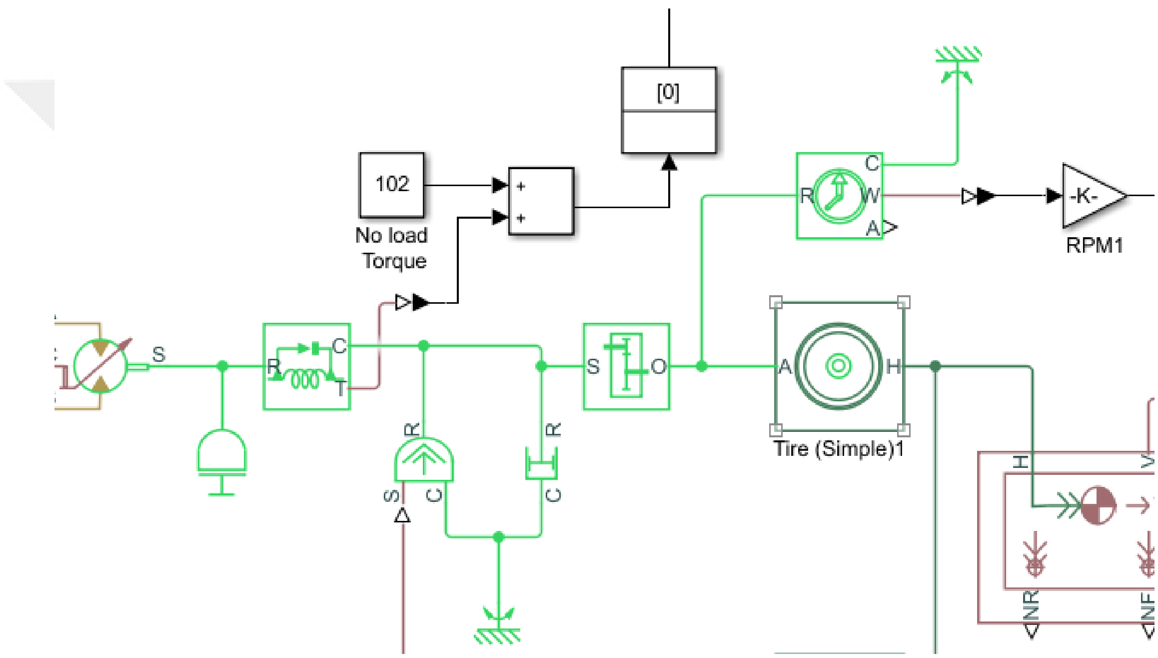

Figure 2.20. *Torque Sensor, Gearbox and Tire Blocks*

There are gearboxes connected to hydraulic motors. Gearboxes lines follow wheels which are attached to “Vehicle Body” block. There are additional rolling resistance blocks connected to the wheels as the blocks representing the front wheels and vehicle body neglect the rolling resistance parameter.

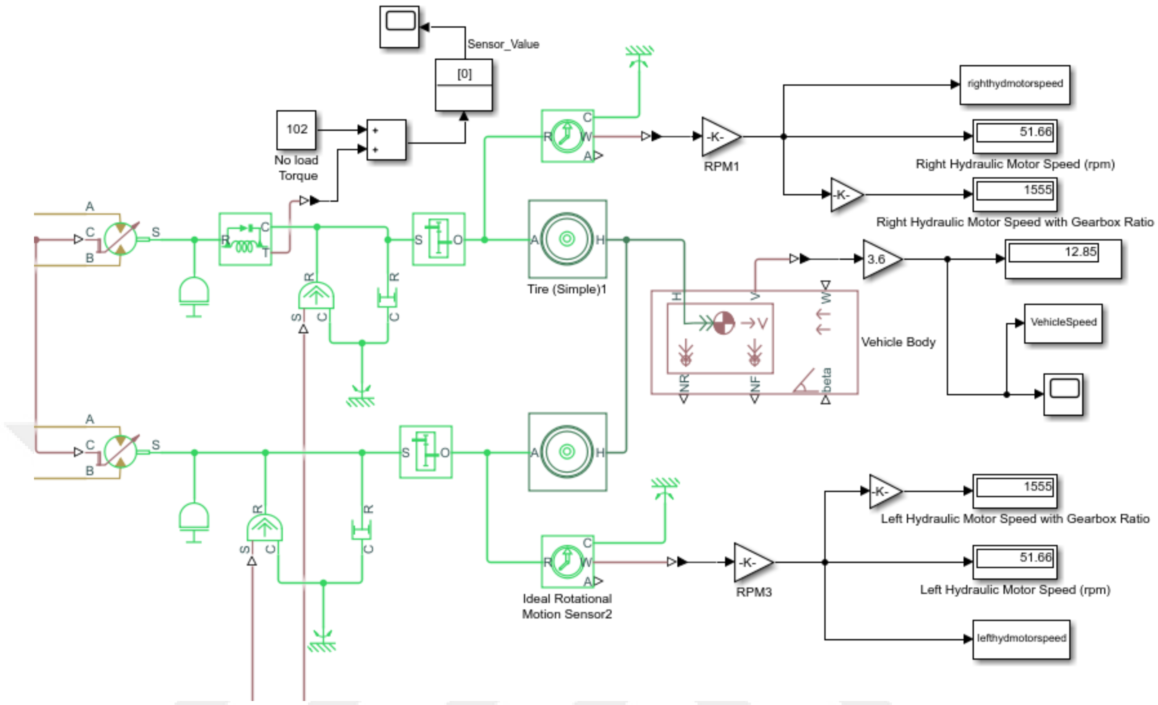

Figure 2.21. *Components from Variable Hydraulic Motor to Wheels and Vehicle Body Block*

The vehicle body block symbolizes a two-axle vehicle and longitudinal movement. Vehicle body block includes weight of vehicle, axle distances, aerodynamic drag force parameters and road grade force parameters. The rear axle of the motor grader is considered to be a single axle, and the rear axle is chosen as the exact midpoint of the rear two axles. It is stated that the vehicle may have the same or different number of wheels on each axle. In addition, it contains suspension dynamics, but this feature was not used since there was no suspension in the motor grader vehicle. Vehicle body block is given in Figure 2.21. Equations 2.24, 2.25 and 2.26 represent vehicle body block.

$$m\dot{v} = F_x - F_d - m * g * sin\beta \qquad (2.24)$$

$$F_x = n * \left(F_{xf} + F_{xr}\right) \tag{2.25}$$

$$F_d = \frac{1}{2} * C_d * \rho * A * (V_x + V_w)^2 * sgn(V_x + V_w) \tag{2.26}$$

2.6. Case Studies

In this section, case studies in hydraulic simulation are described and outputs of simulation are evaluated. Simulation results are compared with theoretical calculations. These values are verified and they are illustrated in different figures.

The purpose of this system is to increase the efficiency of the work done in the field by providing the vehicle with a traction force from the front wheels during operation. In each case, the speed of the front and rear wheels must be synchronized with the traction force it gains. Therefore, depending on the amount of flow produced by the pump and the scenario determined, the speed and synchronization of the vehicle were examined. The system should work properly without any loss of flow during speed synchronization. In addition, flushing valve and charge pump, which may affect flow, were modeled and evaluated.

Moreover, the variation of traction force and traction force with respect to pressure has been observed. At the same time, the load applied to create the pressure change is specified. Relief valve operation has been evaluated to prevent damage to the system under excess pressure.

2.6.1. Speed and Differential Lock Valve

The vehicle performs different grading applications at different speed ranges. Therefore, the maximum speed of the hydrostatic system and the synchronous movement of the wheel speeds is an issue to be considered. The differential lock valve has a critical role in speed synchronization, so valve positions have been analyzed.

A theoretical speed calculation was made according to the target values determined in the conceptual design of the system. During component selection, the differential lock valve was selected based on the flow rate and the flow permeability of the orifices. Supplier data was used in the simulation.

Maximum speed of simulation and theoretical maximum speed are observed in Figure 2.22 for simulation inputs, which are revolution of diesel engine, hydraulic pump displacement and hydraulic motors displacement. The pump stroke rate is at the maximum level, which equals the maximum displacement of hydraulic pump. 2200 RPM refers to maximum revolution of diesel engine. Hydraulic motors have minimum displacement to reach maximum speed. When examined at the maximum speed values, the theory and simulation values match each other. Comparison between theoretical and simulation values are given in Figure 2.23.

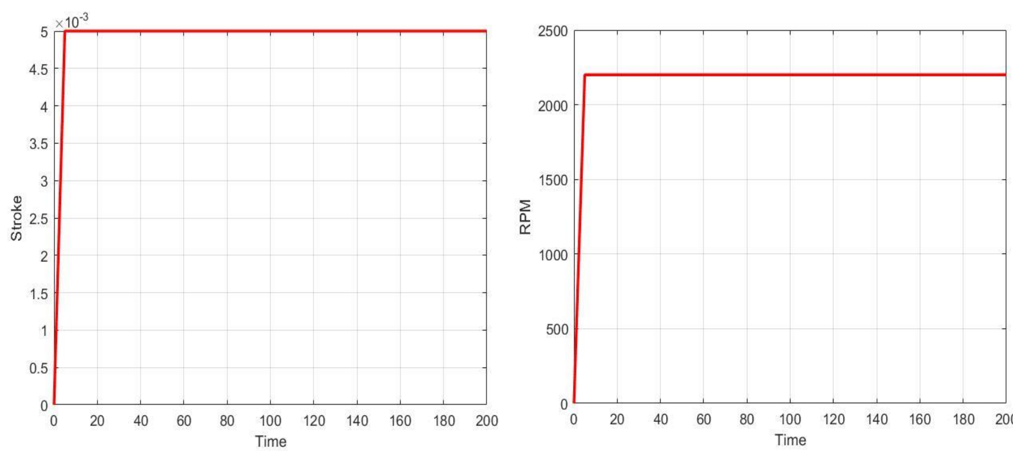

Figure 2.22. *Full Stroke of Pump and Maximum Engine RPM*

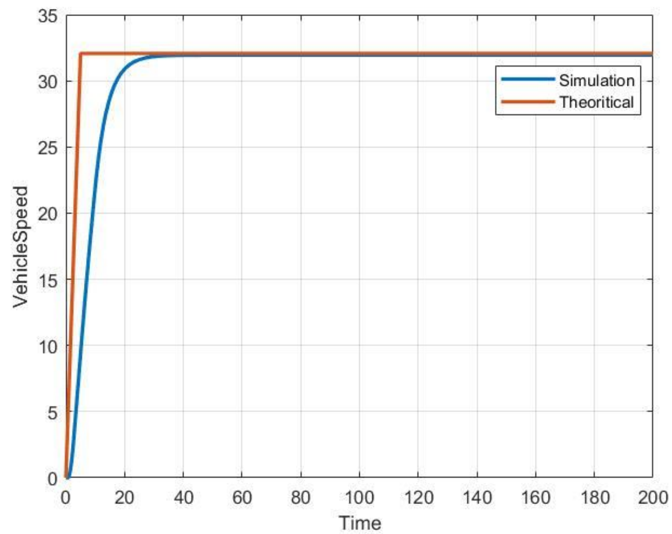

Figure 2.23. *Comparison Between Theoretical and Simulation Speed*

Also, for the two different positions of the differential lock valve that provides speed synchronization in the system, different load states are applied in the simulation and speed values are observed. Load inputs are given in Figure 2.24. In the first position, the valve should divide the flow evenly as the vehicle travels without any extra load that is illustrated in Figure 2.25 and 2.26. The position of the vehicle going straight was evaluated. During the steering, the flow to the motors will change according to the angle of rotation.

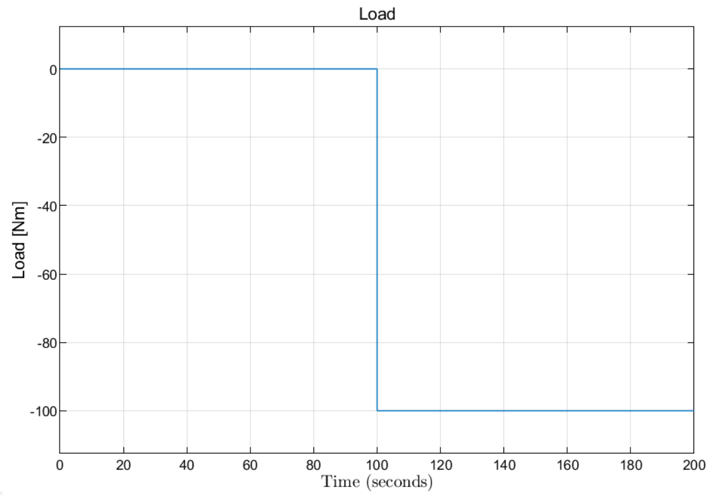

Figure 2.24. *Load Input*

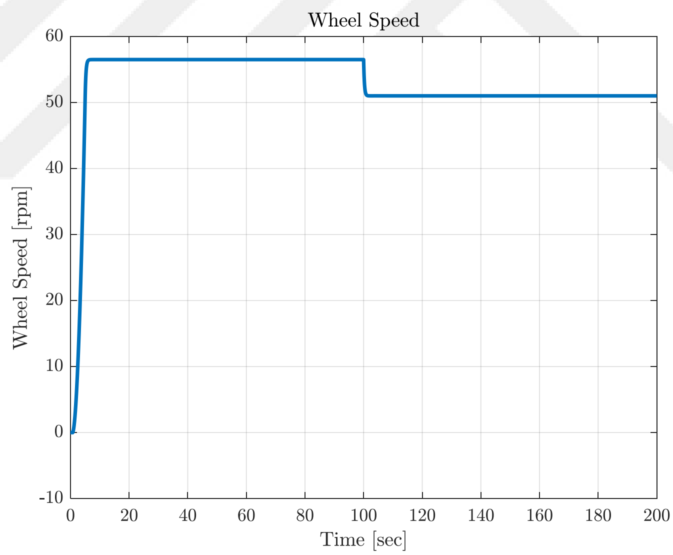

Figure 2.25. *Right Wheel RPM*

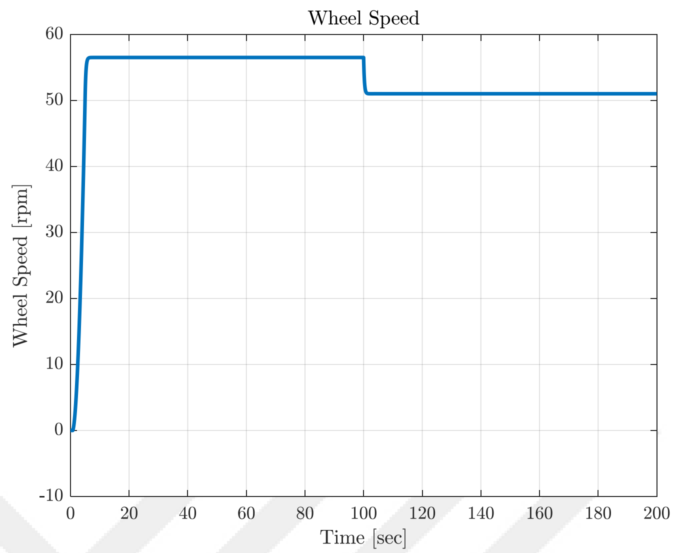

Figure 2.26. *Left Wheel RPM*

According to Figure 2.25 and 2.26, when first position of valve is activated, wheel speeds synchronize in same load cases through differential lock valve. Balanced orifice provides synchronization of right and left hydraulic motor speed. The flow variation of pump is observed in Figure 2.27.

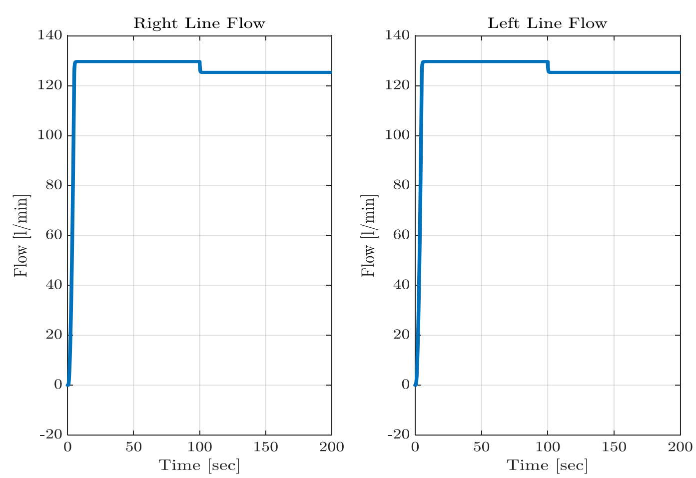

Figure 2.27. *Flow Changing of Pump*

In the second position, when the wheels are subjected to different loads, that is, when different loads are applied that can cause speed change, the position of the valve is activated and speed synchronization is performed. The applied load conditions and outputs are indicated in Figure 2.28. This position of the valve which has variable orifices provide synchronous speed status. Right and left wheel rpm values are given in Figure 2.29 and 2.30.

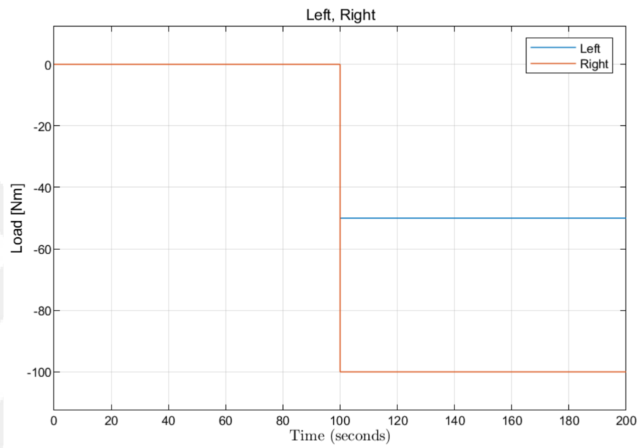

Figure 2.28. *Load Input of Right and Left Wheels*

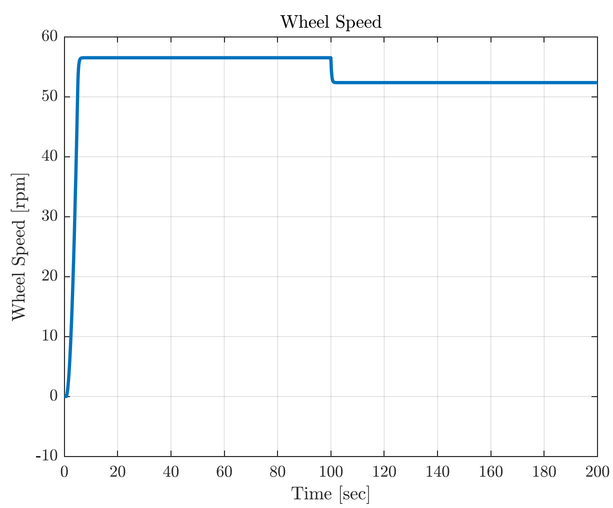

Figure 2.29. *Right Wheel RPM*

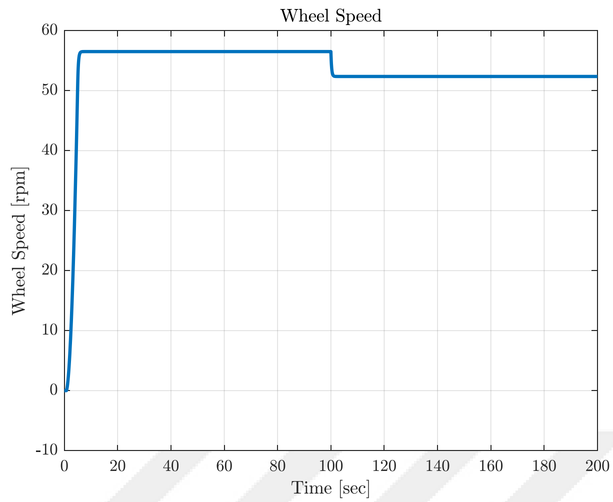

Figure 2.30. *Left Wheel RPM*

2.6.2. Flushing Valve

Flushing valve is used to cool the oil in the system by draining the oil in the system, and the charging pump is used in the complete oil that is decreased from the system. These components were evaluated to examine these two conditions during the simulation.

The flushing valve is driven by the pressure between the two lines of the pump in the hydraulic simulation. While the flushing valve drains some of the oil in the system into the tank, the charging pump must feed the system by meeting the leakage. The displacement of the charging pump in the system should be at a level to deal the leakage. The charging pump should provide the necessary flow for the system's losses. The flow that the flushing valve will send to the system is critical. Excessive discharge may affect the flow delivered to the front wheels, causing loss of speed. In this simulation, the charging pump should meet the amount of flow discharged by the flushing valve to the tank. Firstly, flow variation of flushing valve observed in load case. Load case is given in Figure 2.31 and flow variation is given in Figure 2.32.

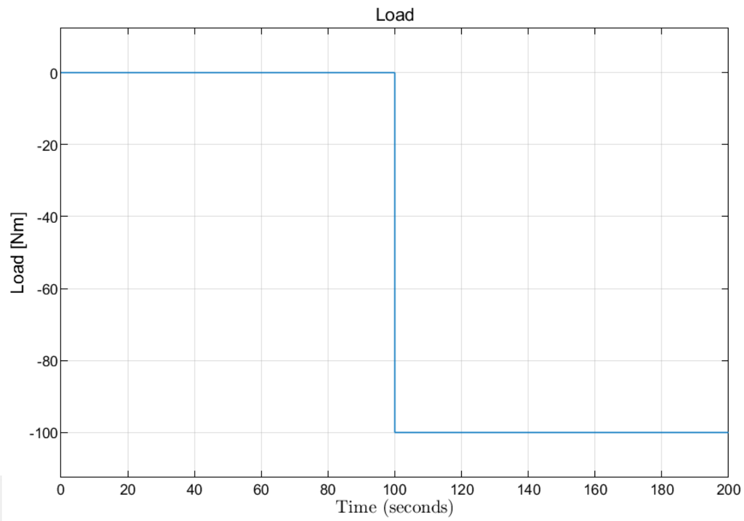

Figure 2.31. *Load Input*

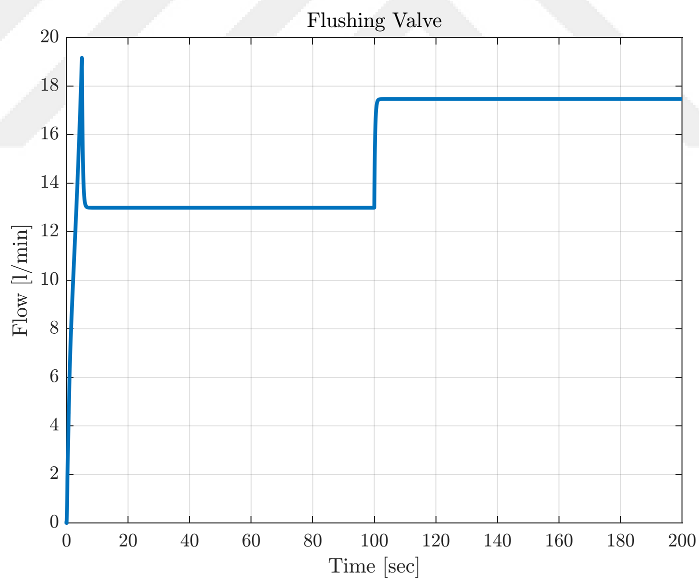

Figure 2.32. *Flow Variation of Flushing Valve*

When the load is applied, the flow rate sent by the flushing valve to the tank increases: the system pressure changes and besides the system should provide the necessary torque.

As this torque requirement will cause warming on the system, the flow rate of the flushing valve increases.

In order to emphasize the importance of the orifice element at the outlet of the flushing valve, flow variation was observed for the orifices selected in different diameters. In addition, the loss of speed in the system is shown when the flush valve discharges excess flow into the tank. The same load case is used for orifice analysis. If a control element such as orifice is not used at the outlet of the valve, excess flow loss occurs as seen in Figure 2.33.

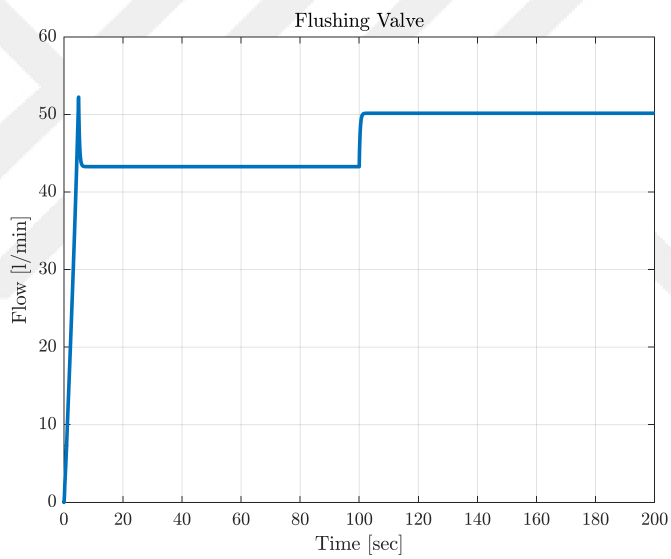

Figure 2.33. *Flow changing of Flushing Valve without Orifice*

2.6.3. Pressure Torque Relation

Pressure in the hydraulic system affects the torque generated by the system. The load consisting of wheels will directly affect the hydraulic system and cause changes in pressure.

The torque value of hydraulic motors at a specific motor displacement and under pressure will be compared with the theoretical calculation value and supplier data. Also, the variation of the traction force under a variable pressure is shown.

Firstly, same loads are applied to wheels, are given in Figure 2.34.

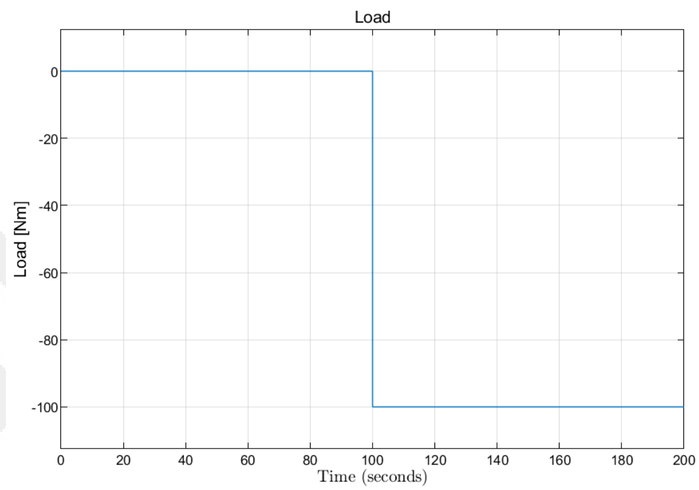

Figure 2.34. *Load Input*

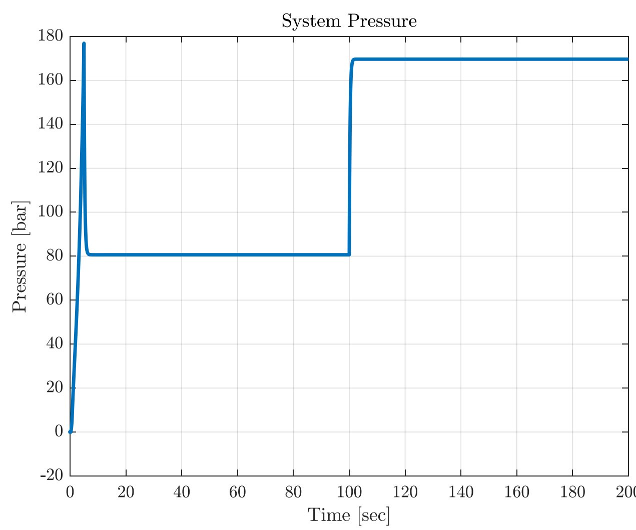

Figure 2.35. *Pressure difference Under the Same Wheel Load*

Secondly, different loads are applied to wheels, are given in Figure 2.35.

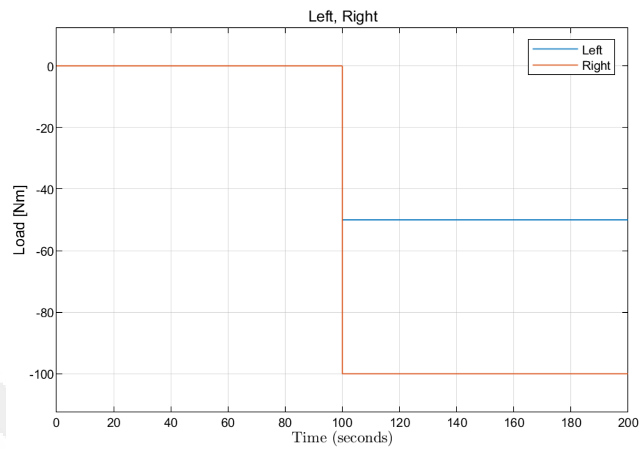

Figure 2.36. *Load Input of Right and Left Wheels*

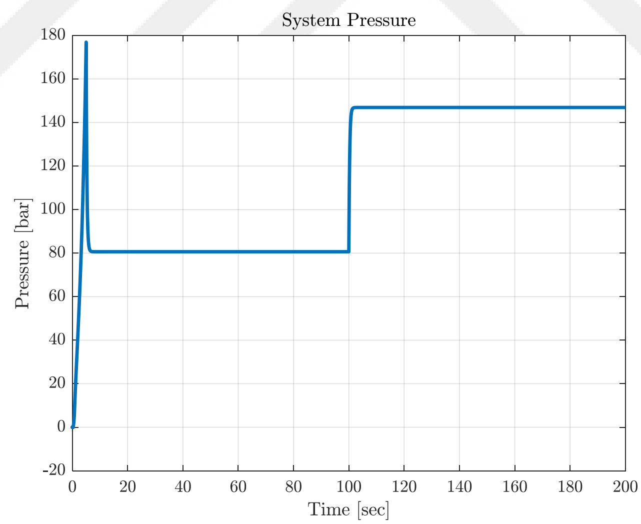

Figure 2.37. *Pressure difference Under the Different Loads*

As seen in Figure 2.37, 66.28 bar pressure change occurred under the applied load that is given in Figure 2.36. A total of 150 Nm load is applied and motor displacements are at maximum level and 75 cc/rev. The theoretically calculated formula is given in Equation

2.27. In equation 2.27, T is torque in Nm, ΔP is pressure difference in bar and V_m is hydraulic motor displacement in cc/rev.

$$T = \frac{\Delta P * V_m}{20 * \pi} \tag{2.27}$$

As a result of the theoretical calculation, a pressure difference of 62.83 bar was obtained. The pressure change resulting from the simulation and the pressure change resulting from the theoretical calculation are very close to each other. The same calculations can be made within the load case applied in the first graph, and again close results will be obtained.

Against the applied 150 Nm load, the pressure in the hydraulic system increased and in response to the load, the hydraulic motors produced about 150 Nm of torque. Torque comparison is given in Figure 2.38.

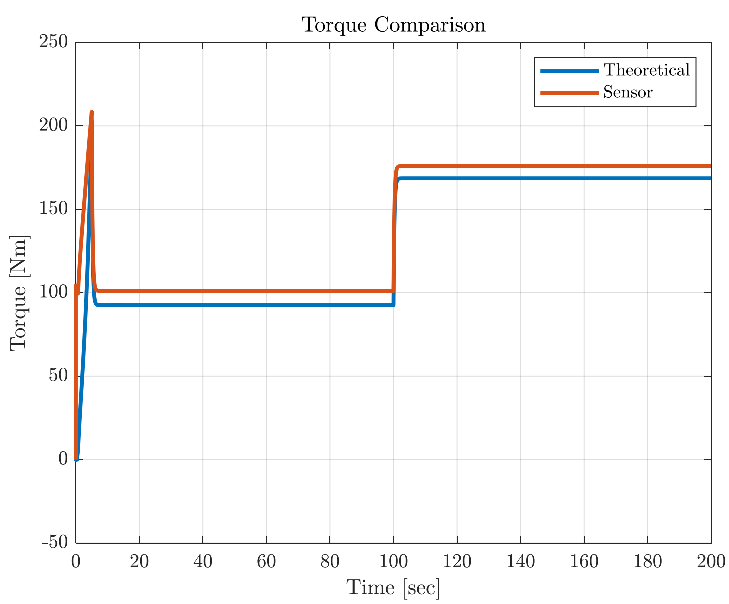

Figure 2.38. *Torque Comparison Between Theoretical and Sensor Values*

Along with the change of torque, changes in traction force were also observed in Figure 2.39. It has the same characteristics as hydraulic motors.

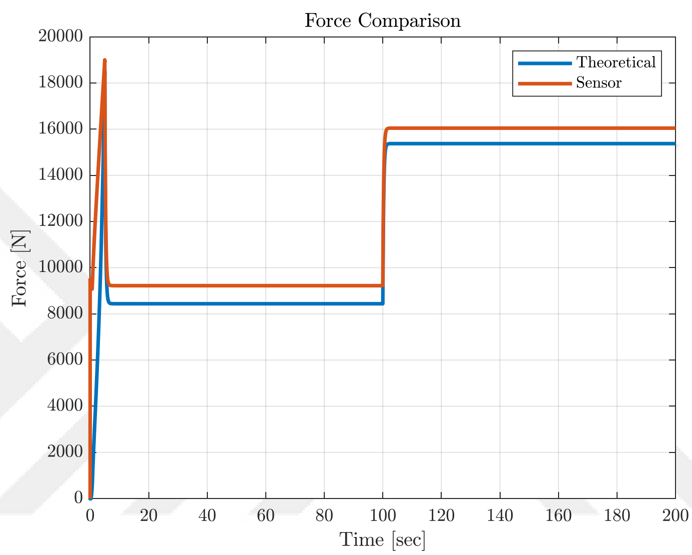

Figure 2.39. *Traction Force Comparison Between Theoretical and Sensor Values*

There are fixed differences between torque and force value measured form the sensors and calculated form the theoretical results. In reality, there always exists a minimum torque value produced by hydraulic motors without load. Differences occur due to this torque value and the selected efficiency.

CHAPTER 3

MATHEMATICAL MODEL

In this section, primarily the mathematical model of motor grader vehicle is constructed and the accuracy of this model is confirmed. The most important factor in the accuracy of this model is the diesel engine. The reaction of the designed diesel engine controller must be physically realistic. Then, a mathematical model of the hydrostatic drive system, which will add an additional traction force to the motor grader vehicle, is also created and it is integrated into the motor grader model. The AWD controller has been designed for the control of variable displacement pump and motors in the integrated AWD system.

In the motor grader model, the accelerator pedal value controlled by the operator is used as an input. When the hydrostatic driving model and the motor grader model are combined, the accelerator pedal will be the input of the entire model. This input depends on the diesel engine and changes the response of the diesel engine. This change was evaluated by modeling the controller of the diesel engine. In addition, the torque produced by the diesel engine is transferred to the wheels with power transmission elements. In order to observe the behavior of the vehicle, a subsystem including vehicle dynamics has been created. This subsystem includes the forces that move the vehicle and the forces that oppose it.

In the hydrostatic drive model, the flow and pressure parameters that will occur in the system are evaluated along with the flow produced by the pump. At the same time, the driving position of the differential locking valve, which is of great importance for this drive system, is also modeled.

3.1. Throttle Signal

The main input used by the operator to determine the response of the vehicle is the accelerator pedal value. Depending on the AWD system pump, the diesel engine has a drive element for the front drive system and the rear wheels are gained in relation to the value of the accelerator pedal.

There is a linear relationship between the accelerator pedal value of the vehicle and the angular speed of the diesel engine. The accelerator pedal value is expressed as a percentage. The idle speed of the diesel engine is 800 rpm and its maximum speed is 2200 rpm. The accelerator pedal value in the 0-100 range corresponds linearly to the 800-2200 rpm range. In the model, the relationship between them is expressed in Equation 3.1 and in Figure 3.1.

$$w_e = (\%Throotle * 14) + 800 \tag{3.1}$$

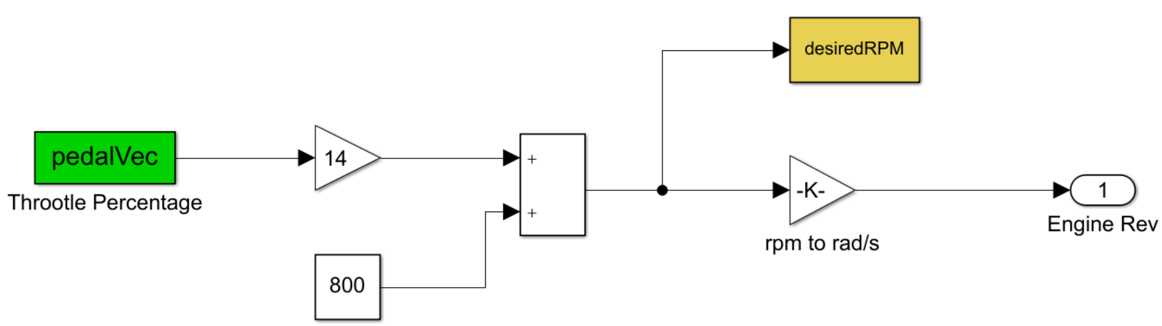

Figure 3.1. *Throttle Signal*

3.2. Engine Controller

The engine controller is designed to physically generate the response of the engine within the model. During this design, tests and system identification were used. According to the test data of the vehicle, dynamic reactions in the mathematical model were created by applying system identification to the diesel engine controller. The working principle of the traction system of the motor grader is shown in Figure 3.2. Torque for the longitudinal motion of the grader is provided by the engine and converted by the transmission depending on the selected gear. Hereby, the signal for the gear selection is provided by the transmission control unit (TCU). This signal comes from the driver. The TCU also received the pedal signal from the driver. Depending on the pedal position (in percent), the TCU computes the desired angular velocity of engine to be supplied by the engine. The desired angular velocity of engine is sent to the engine controller and the engine controller computes the desired torque.

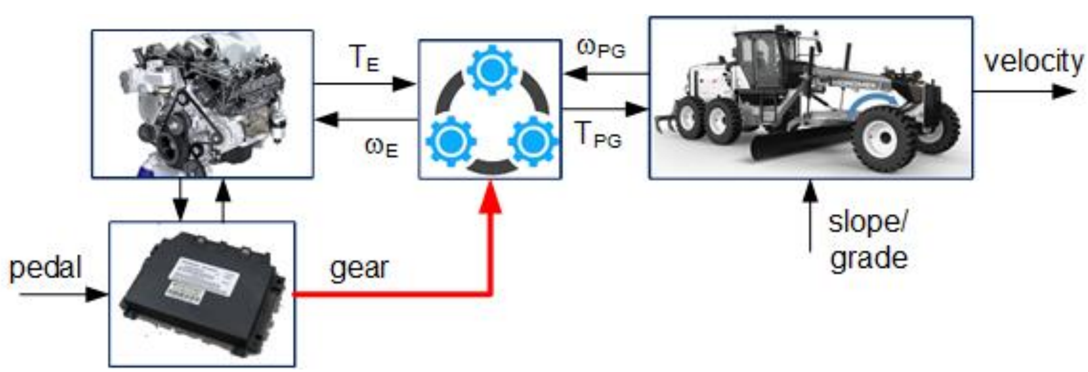

Figure 3.2. *Longitudinal Traction System of the Motor Grader*

In this context, it is important to note that the torque computation by the engine controller is implemented by the engine supplier and is unknown to HIDROMEK. However, the engine controller is needed in order to correctly model the traction system of the motor grader. Because of this reason, we performed a system identification of the engine controller for different gears using step response measurements. In these measurements, the motor grader is driven in a constant gear and the pedal position is increased step by step (for example around 10% or 20%) and tests were carried out according to the step function response of the accelerator pedal. The diesel engine speed and torque values were obtained as a result of these tests and a transfer function was obtained by making system identification in the time domain for the engine controller. In Figure 3.3 the data related with the experiment carried out for the 3rd gear is shown.

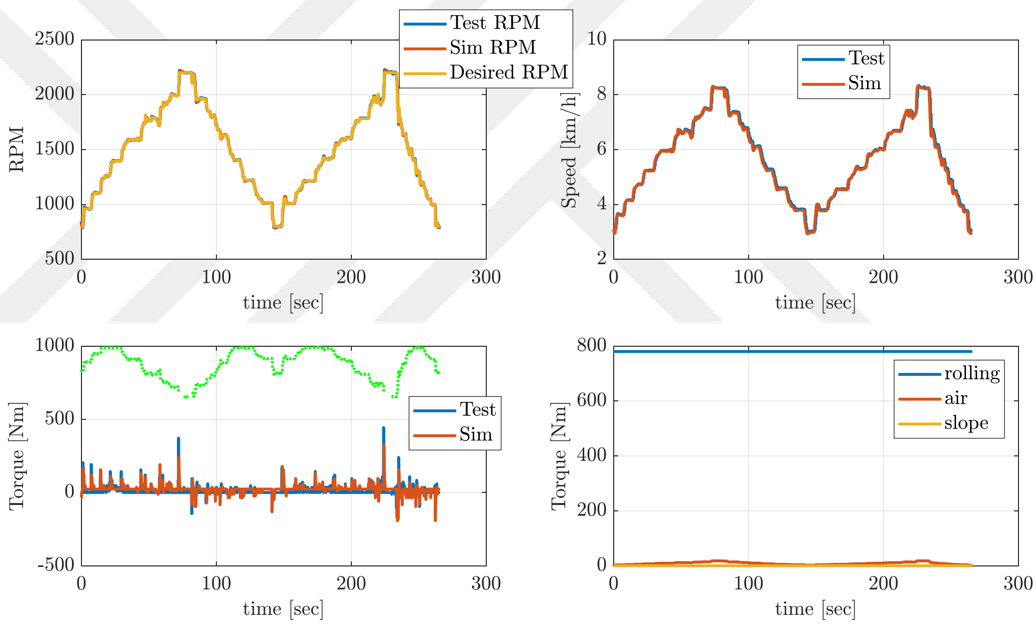

Figure 3.3. *Step Response Measurement in Gear 3*

From the identification experiments, we conclude that the engine controller is realized as a PI-controller with the following transfer function that is given in Equation 3.2.

$$C(s) = \frac{15 \cdot s + 8}{s} \tag{3.2}$$

The parameters of this transfer function were found by comparing the measured rpm values to the simulated rpm values as can be seen in Figure 3.3. In addition, the measured torque values and the simulated torque values are also shown in this figure. It can be seen that sum of squared residuals are minimized, which implies that the identified controller transfer function is accurate. A closer look at the rpm and torque plots is displayed in Figure 3.4. It can be observed that the simulated and the measured rpm values are almost identical. We also note that the yellow curve shows the desired rpm which is computed from the pedal position. Since all curves are very close to each other, this also implies that the engine controller performs well for the 3rd gear.

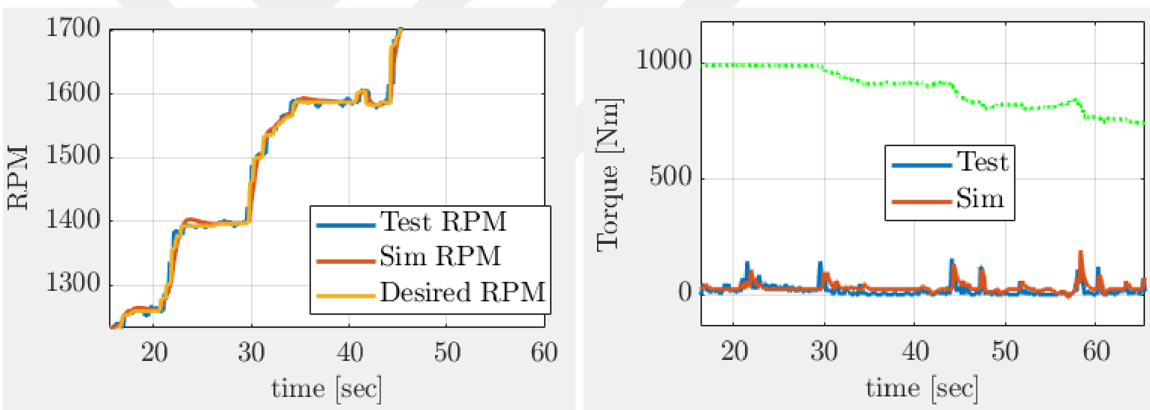

Figure 3.4. *Zoom in on the RPM and Torque Measurements and Simulations (3rd gear)*

Figure 3.5 also shows engine controller. The engine controller receives the desired rpm, actual gear and actual rpm as input signals and computed the engine torque as the output signal. In order to limit the maximum torque, the maximum torque curve of the supplier was used in the look up table. The controller values selected from the look-up table according to the gear value are multiplied by the difference between the desired engine speed and the actual engine speed. As shown in the figure, while one side represents proportional value, the other side represents the integral part of the controller and multiplied by the integrator to create the PI control design of the controller.

In addition, the torque due to friction was calculated to obtain the net torque value. The torque calculation caused by friction was made with the engine friction data received from the diesel engine. This data was obtained during the tests to design the engine controller. The friction that occurs in the diesel engine will also affect other components. Therefore the friction torque calculation depends on the rotation speed of the diesel engine. In Equation 3.3, T_f is friction torque in Nm and w_e is engine angular speed in rpm.

$$T_f = (((w_e - 800) / 350) + 7) * 12 \tag{3.3}$$

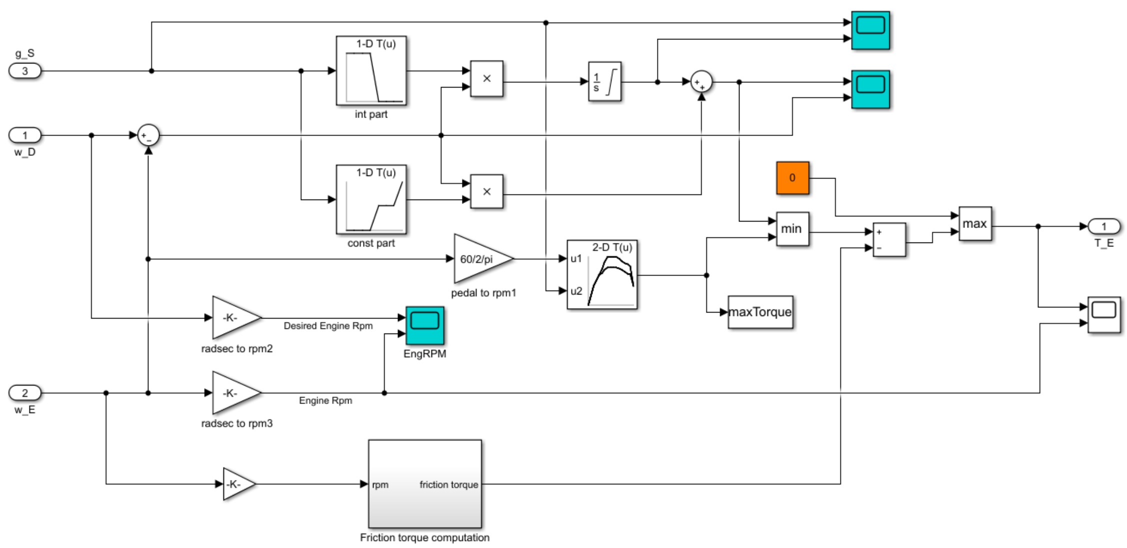

Figure 3.5. *Engine Controller*

The previous experiments were performed for the 3rd gear. Experiments for the 5th gear are also conducted. Figure 3.6 shows the comparison of the step response measurements and simulations. Again, it can be seen that the rpm measurements and simulations are very close to each other. Small deviations can be observed for the torque comparison. Nevertheless, it is clear that the peaks (which represent changes in the pedal position) are demonstrating the consistency between measurements and simulations. In addition, experiments for the 5th gear shown that the measured and simulated velocities are coherent.

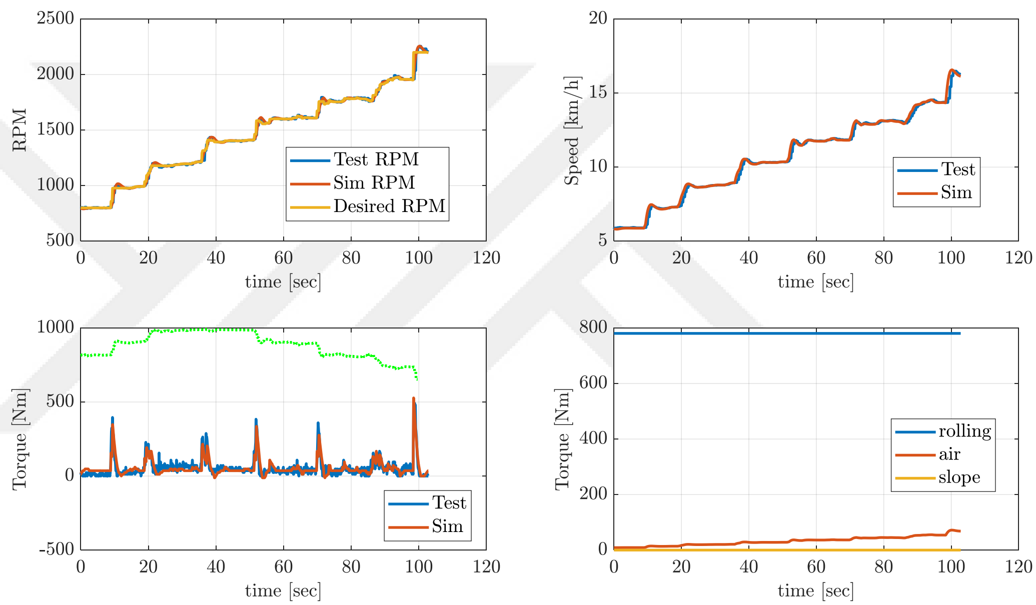

Figure 3.6. *Measurements and Simulation for the 5th Gear*

Figure 3.7 shows a zoom in on the rpm and torque comparison for the case of the 5th gear. Here, it can be observed that there is a slight overshoot of the measured and simulated rpm signal. This implies that the engine controller does not perform as well in the 5th gear as it performs in the 3rd gear (which is not a problem of our model but seems to be a problem of the pre-installed engine controller). Again, the torque measurements and simulations also agree well for the experiment in the 5th gear.

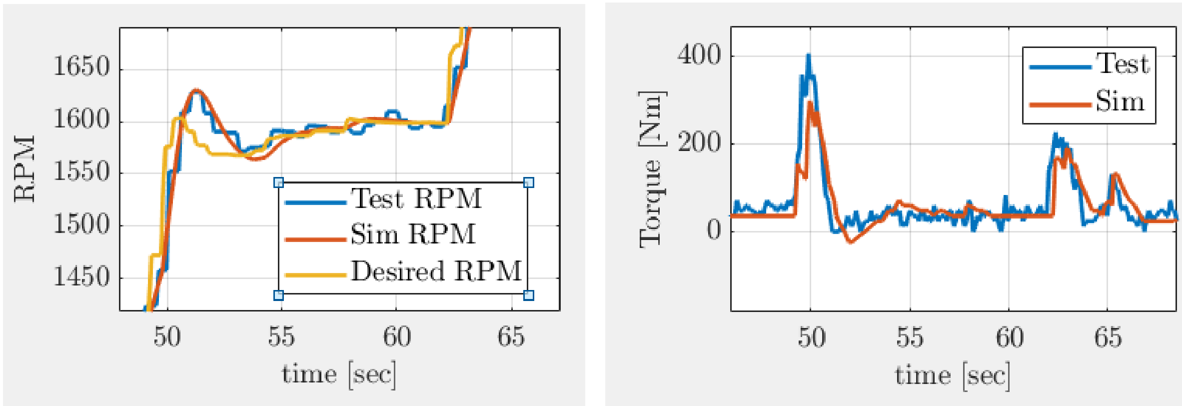

Figure 3.7*. Zoom in on the Measurements and Simulations in the 5th Gear*

In summary, it can be concluded that a suitable model of the engine controller is identified. This engine controller can be used in the simulation experiments to be conducted during the project.

3.3. Transmission and Other Driveline Components

The produced diesel engine torque is transmitted to the wheels through the transmission, differential and tandem, which are the power transmission components of the motor grader. In the model, the total gear ratio of these components according to gear information is determined in the look-up table. This torque value is transmitted to the wheels by considering the total efficiency of the components. Transmission subsystem is illustrated in Figure 3.8.

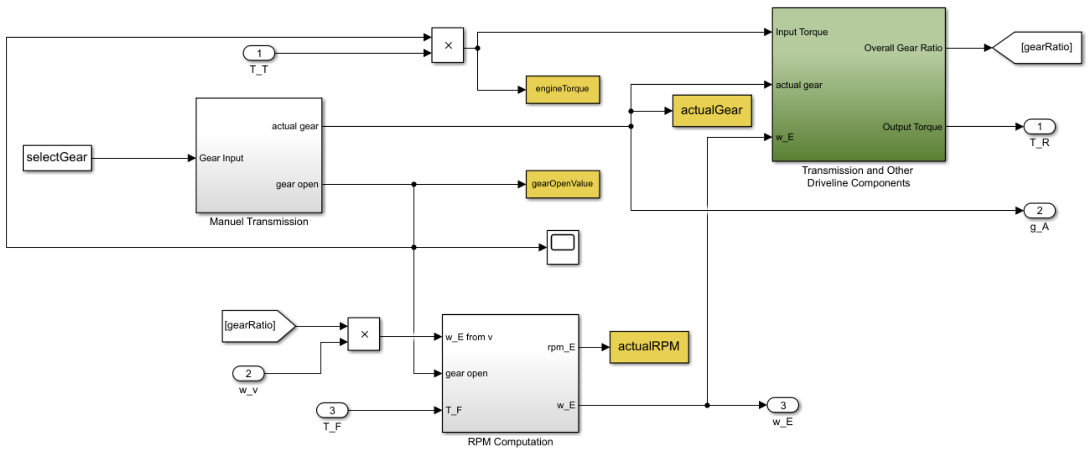

Figure 3.8. *Transmission and Other Driveline Components Subsystem*

The diesel engine and gearbox are directly connected. It separates and reunites during gear shifts. Therefore, this situation is modeled by means of a timer in the manual transmission subsystem and gear is expressed as open gear.

In transmission subsystem, torque values are calculated. The total gear ratio and torque calculation are given in Equation 3.4 and 3.5. i_{total} is total gear ratio, i_{tm} is transmission gear ratio, i_d is differential gear ratio and i_t is tandem gear ratio. T_w is wheel torque in Nm, T_e is engine torque in Nm and η is efficiency of powertrain components.

$$i_{total} = i_{tm} * i_d * i_t \tag{3.4}$$

$$T_w = T_e * i_{total} * \eta \tag{3.5}$$

The braking torque that may occur is indicated by a function. When the torque drops below a certain value in the function, the brake torque is activated. Apart from this, the braking torque is zero. Transmission subsystem is shown in Figure 3.9.

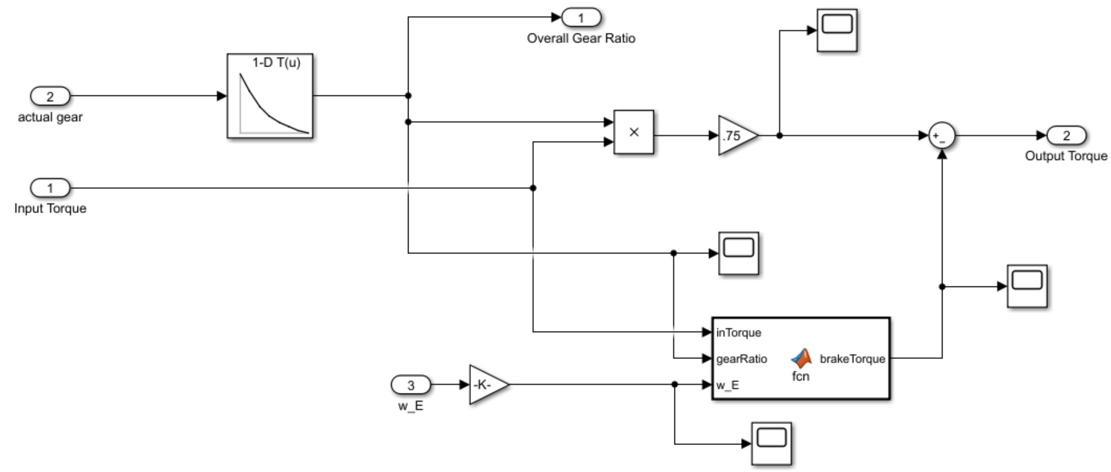

Figure 3.9. *Transmission Subsystem*

In addition, there is a sub-system that evaluates the engine speed in rpm in Figure 3.10. Vehicle speed is calculated in the vehicle dynamics subsystem. The diesel engine speed is calculated again from the calculated vehicle speed and comes to this rpm evaluation subsystem. In this subsystem, a coefficient is used to indicate the clutch the dynamics of the clutch between the diesel engine and the gearbox. Afterwards, a feedback structure was established by integrating it. Thus, the physical response of the engine speed in rpm value is indicated.

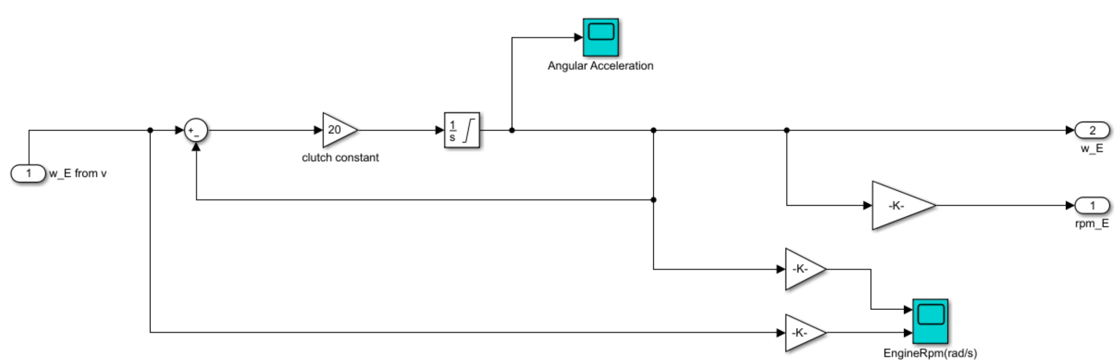

Figure 3.10. *RPM Computation Subsystem*

The change in the diesel engine angular velocity as a result of the operation performed in the engine speed in rpm evaluation subsystem is shown in Figure 3.11.

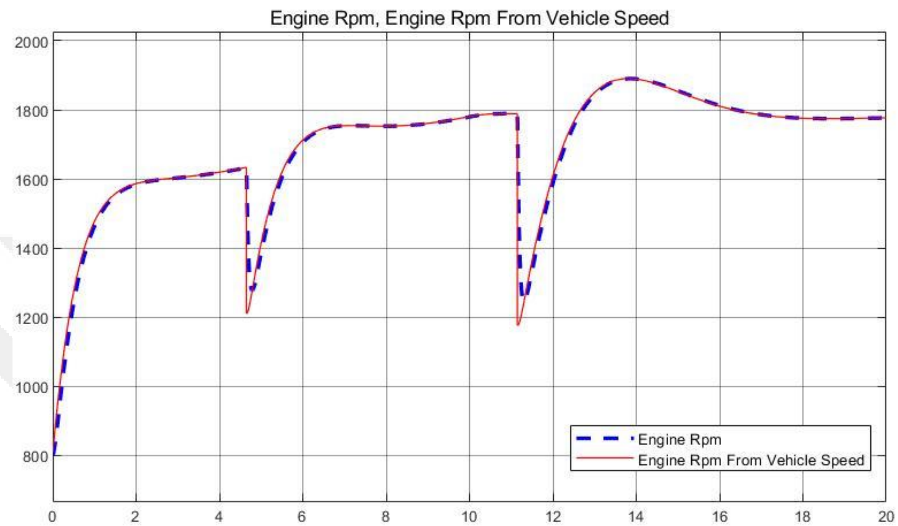

Figure 3.11. *Engine RPM Computation*

3.4. Vehicle Dynamics

This section examines the vehicle dynamics. A dynamic is created by modeling the vehicle movement on the longitudinal axis. In this dynamic structure, the positive and negative forces acting on the vehicle were evaluated. The torque transferred to the wheels creates a traction force. Rear traction force and front traction force are calculated separately. Also, there are slope resistance force, rolling resistance force and air resistance force that correspond to these traction forces. When the resistance forces are removed from the traction force, the net force that moves the vehicle emerges. The acceleration of the vehicle was calculated according to the net force acting. The mathematical representation of the resistance forces is expressed in Equation 3.6.

$$F_{air} = ((V_{wind} + V_{mg}) * 3.6)^2 * 0.5 * \rho * C_d * A_f \qquad (3.6)$$

In Equation 3.6, F_{air} is air resistance force in N, V_{wind} is wind velocity in km/h, V_{mg} is vehicle velocity in km/h, ρ is air density in kg/m^3, C_d is drag coefficient and A_f is frontal area in m^2. Wind speed input value is determined as positive if it is in the same direction with vehicle speed, and negative if it is opposite to vehicle speed.

$$F_{rollingres} = W_v * r \qquad (3.7)$$

In Equation 3.7, $F_{rollingres}$ is rolling resistance force in N, r is rolling resistance coefficient and W_v is vehicle weight in N. It is the resistance force resulting from rolling during the movement of the vehicle.

$$F_{slope} = \sin(\tan^{-1}(\%slope/100)) * W_v \qquad (3.8)$$

In Equation 3.8, F_{slope} is slope resistance force in N, %slope is percentage slope value and W_v is vehicle weight in N. This resistance force is parallel to road surface.

The traction force produced by the vehicles front and rear wheels is calculated as in Equations 3.9 and 3.10 and the net traction force of the vehicle performing the movement calculated using Equations 3.11 and 3.12.

$$F_f = \frac{\mathrm{T_{hm}} * i_g}{\mathrm{r_w}} \qquad (3.9)$$

$$F_r = \frac{\mathrm{T_e} * i_{total}}{\mathrm{r_w}} \qquad (3.10)$$

$$F_t = F_f + F_r \qquad (3.11)$$

$$F_{net} = F_t - F_{slope} - F_{rollingres} - F_{air} \tag{3.12}$$

Moreover, the inertia value of the vehicle was calculated to observe the dynamic effect of the forces acting on the vehicle. Inertia depends on vehicle mass, gear value and wheel radius and varies with varying gear ratio in each gear value. In equation 3.13 and 3.14, J_v is vehicle inertia in kgm^2, J_e is engine inertia in kgm^2, M_v is vehicle mass in kg, i_{total} is gear ratio of gear value and r_w is wheel radius in m.

$$J_v = \left(\frac{J_e * {i_{total}}^2}{{r_w}^2} + M_v\right) * {r_w}^2 \tag{3.13}$$

$$M_{vehicle} = \frac{J_v}{{r_w}^2} \tag{3.14}$$

The inertia of the vehicle changes during the movement of the vehicle. This change symbolizes the dynamic movement of the vehicle and will lead to acceleration changes. Using the 2^{nd} law of Newton here, the acceleration value of the vehicle was calculated in Equation 3.15. a is acceleration of vehicle in m/s^2. Acceleration computation is shown in Figure 3.12.

$$a = \frac{F_{net}}{M_{vehicle}} \tag{3.15}$$

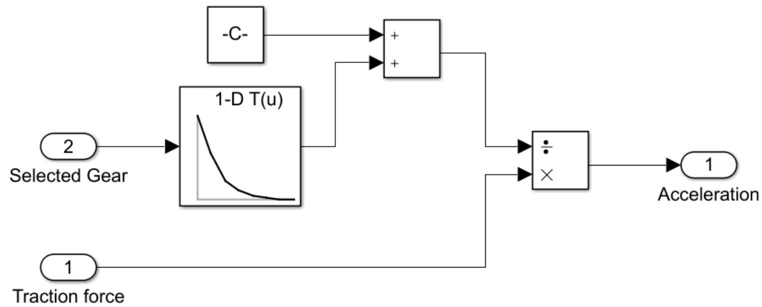

Figure 3.12. *Acceleration Computation*

In addition, the effect of the slip factor has been examined on the vehicle. The slip factor was selected the same for each gear value. The angular speed of the diesel engine was evaluated according to vehicle speed, wheel radius and slip factor. The physical response of angular speed of engine was determined by using the obtained angular speed in rpm evaluation subsystem. In Equation 3.16, 3.17 and 3.18, V_{mg} is vehicle speed in m/s, r_w is wheel radius in m and n_e is angular speed of diesel engine in rad/sec and s is the slip factor.

$$V_{mg} = r_w * n_w * (1 - S) \tag{3.16}$$

$$n_w = \frac{n_e}{i_{total}} \tag{3.17}$$

$$n_e = \frac{V_{mg} * i_{total}}{r_w * (1 - S)} \tag{3.18}$$

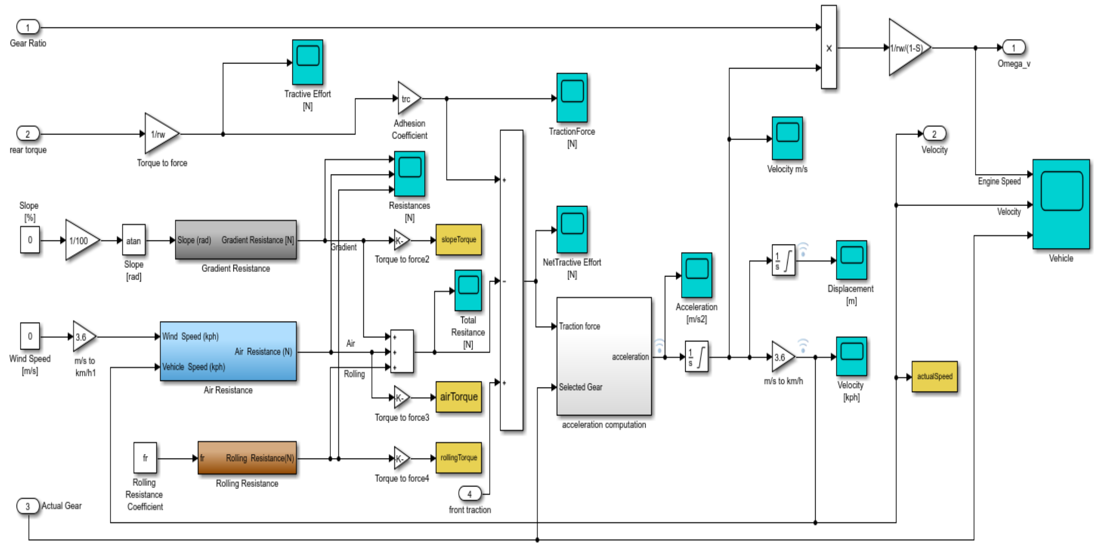

Figure 3.13. *Vehicle Dynamics Subsystem*

Traction force produced revealed the acceleration of the vehicle as it changes depending on the inertia value. To evaluate the acceleration, the gear value of the vehicle is significant. Vehicle dynamics subsystem is given in Figure 3.13.

3.5. Hydrostatic Front Drive System

A large number of studies are available in the literature for the mathematical model of the hydrostatic drive system. As a result of these studies, information about the relationship between hydraulic pump and motor has been obtained. Concepts such as flow produced by hydraulic pump, displacement of hydraulic motor according to displacement and incoming flow value are formulated. In addition, the formation of pressure in the hydrostatic system is modeled based on the compressibility of liquids. A bulk module suitable for the system has been determined so as to express the compression feature. The driving position, which is the first position of the differential lock valve, another element of the driving system, is modeled. In the mathematical model of this valve, the data provided by the supplier company were used.

Firstly, the flow produced by the hydraulic pump, which is the main drive element of the model, is calculated. Pump flow formulation is given in Equation 3.19. Q is flow in m^3/s, V is displacement in m^3, w_e is angular speed of engine in 1/s and η is volumetric efficiency.

$$Q = V * w_e * \eta \tag{3.19}$$

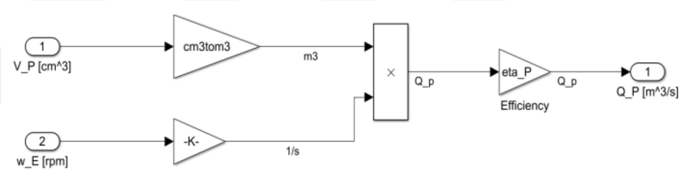

***Figure 3.14**. Pump Flow Calculation*

Pump subsystem is showed in Figure 3.14. w_E port is angular speed of pump shaft which is connected to directly diesel engine. That is to say, angular speed of pump and diesel engine are same. V_P is pump displacement value and Q_p is pump flow.

The flow from the pump creates a pressure in the hose according to the compressibility of the fluid. This pressure is calculated with bulk modulus. The bulk modulus is a measure of resistance to compressibility of a fluid. A flat slope signifies a fairly compressible fluid having a low bulk modulus. The formula showing this relationship is given in Equation 3.20.

$$Q_s = \frac{V_s}{E_s} * Dp \tag{3.20}$$

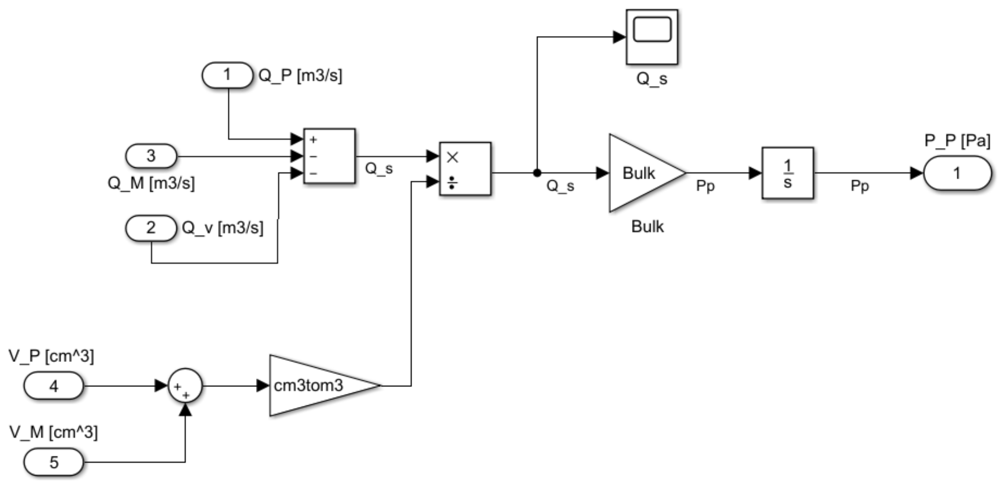

Figure 3.15. *Pressure Calculation*

In pipe subsystem, Q_P is pump flow in m^3/s, Q_M is hydraulic motor flow in m^3/s, Q_v is relief valve flow in m^3/s. Q_s is difference between pump flow and sum of relief valve flow and hydraulic motor flow. This relation is given in Equation 3.21. V_P is pump displacement, and V_M is motor displacement in m^3. Es is bulk modulus and P_p and p is pump pressure. Vs is total displacement of hydraulic system in m^3. Pipe subsystem is given in Figure 3.15.

$$Q_p = Q_s + Q_v + Q_m \tag{3.21}$$

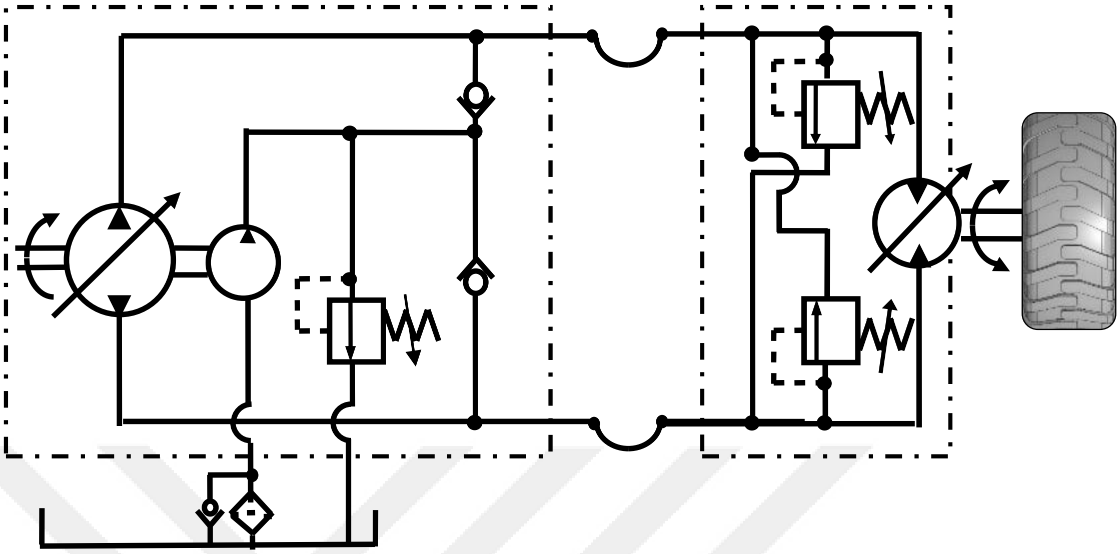

***Figure 3.16**. Hydrostatic Drive Representation [21]*

A hydrostatic transmission circuit having a single hydraulic pump and a single hydraulic motor is represented in Figure 3.16. It has a similar structure with the modeled system structure. Components and hydraulic lines followed by the fluid are visible on the Figure 3.16.

When the system pressure rises above the maximum pressure, relief valve is activated and discharges the flow to the tank. The Q_v relief represents the flow through the valve. Relief valve subsystem is given in Figure 3.17.

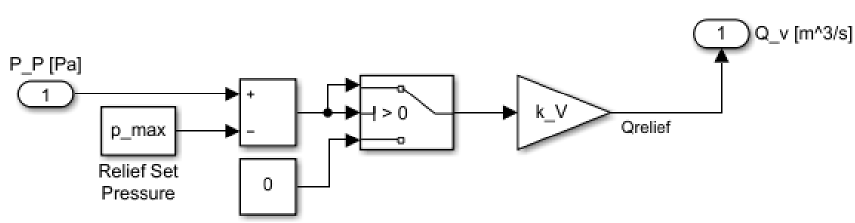

***Figure 3.17**. Relief Valve Subsystem*

If the difference between the value of the relief valve set and the pressure in the system is greater than zero, the switch becomes active and flow flows through the relief valve. A coefficient is used to determine the flow permeability of the relief valve. In Equation 3.22, Q_v is relief valve flow in m^3, p_max is relief set pressure in Pascal and it is equal to p_{set} and P_p is pump pressure in Pascal.

$$Q_v = k_v * (p_p - p_{set}) \tag{3.22}$$

Other significant component is differential lock valve (Flow Divider) which has two positions. The first position of the valve is its default position and is used for drive. In the first position, the balance orifice between the two hydraulic lines acts as a differential by sending different flows to the inner and outer wheel in turns. Pressure remains the same in this position. The second position of the valve is activated during skidding, ensuring equal flow to the wheels. In the model, the first position of the valve is modeled according to the supplier data with a Matlab function. QP is pump flow in L/min and pP is pressure in Pa. Flow divider first position function is given in Figure 3.18.

```
function [pA,pB] = fcn(QP,pP,flowDividerState1)
    pA = pP-(flowDividerState1(1)*QP^2 + flowDividerState1(2)*QP + flowDividerState1(3))*1e6;
    pB = pA;
```

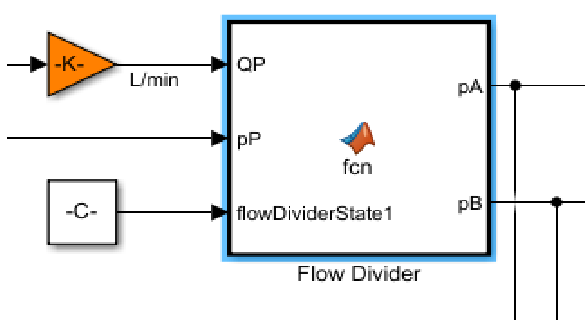

Figure 3.18. *Flow Divider Function*

The last subsystem is hydraulic motor subsystem that is shown in Figure 3.19. The torque values of friction and load have a negative effect against the torque value of the hydraulic motor. A speed calculation is made over the net torque released and this motor flow value is calculated according to the displacement and speed value. Hydraulic motor calculations are given in Equations 3.23, 3.24 and 3.25.

$$M_m = M_I + M_B + M_o \tag{3.23}$$

$$M_m = I_h * Dw_h + B_h * w_h + M_o \tag{3.24}$$

$$w_h = \frac{1}{D}\left((M_h - B_h * w_h - M_o)/I_h\right) \tag{3.25}$$

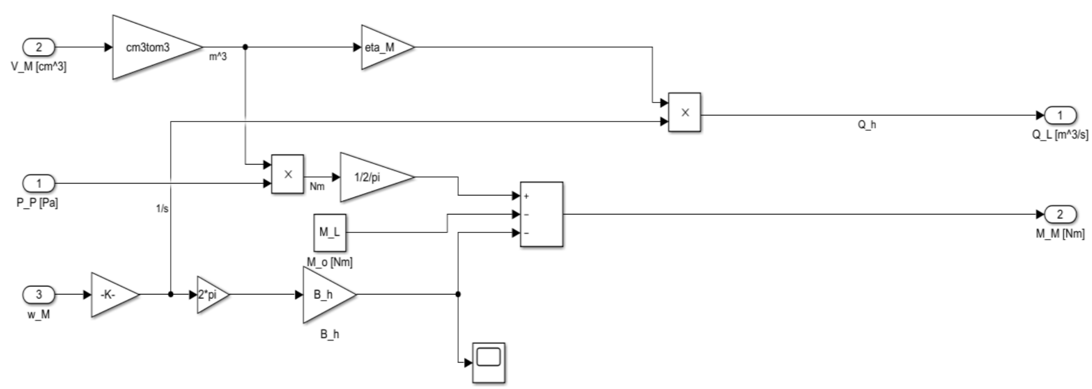

Figure 3.19. *Variable Hydraulic Motor Subsystem*

CHAPTER 4

CONTROLLER DESIGN

4.1. Controller Design Steps, Simulation and Test Results

4.1.1. Design Procedure

For the hydrostatic drive systems, controller designs based on speed synchronization and traction force have been realized in the literature. Traction force is the most important factor for the motor grader vehicle to perform efficiently on the field. Therefore, based on the traction force in the controller design, the torque produced by the diesel engine is distributed to the front and rear wheels according to the ratio obtained from the power regulation.

Firstly, a displacement value has been determined for the hydraulic motor according to each gear value of the vehicle. Vehicle speed measured from the rear wheels is the reference value for hydraulic motors located on the front wheels. However, the displacement of the pump was calculated based on gear ratios in front and rear transmission, diesel engine speed and torque control. The working principle created for the controller design is shaped in line with these parameters.

First of all, in the controller design, the first evaluations that can be made for the system have been observed in order to control the torque by creating a separate model with hydrostatic circuit and vehicle dynamics. In this model, constant values are determined for the parameters. Moreover, by combining this model with the motor grader model, variable values were created and simulations were made for the system on the vehicle.

After this integration, a feedback linearization process was performed on the hydrostatic circuit, and the controller block was updated.

With the new controller designed as a result of the feedback linearization process, it has been observed that the controller operates smoothly in all conditions in gear changes, fixed or variable gear values, speed increase and speed decrease.

4.1.2. First Evaluation of Torque Control

In the initial evaluation phase, a separate model including the vehicle dynamics and hydrostatic drive circuit of the front side was created and examined. The purpose of this model is to adjust the pump displacement by controlling the torque generated by the hydraulic motor with the desired engine displacement and the pressure generated in the hydrostatic system according to the desired torque value.

During these evaluations, a fixed value was determined for the hydraulic motor displacement, and at the same time, the gear ratio of the rear traction system was specified, assuming the vehicle was moving in the same gear. The ratio of the gearbox that gives the front traction force is constant. Only the weight and inertia values of the front of the vehicle are used in the vehicle dynamics block. The content of the vehicle dynamics subsystem is as described in the section on mathematical modeling. The torque generated in the hydrostatic drive circuit is transferred to the vehicle dynamics subsystem as the torque affecting the wheels, and the rotational speed and vehicle speed of the diesel engine are calculated. The calculated diesel engine rotation speed is specified as input for hydrostatic circuit. The hydraulic motor speed was calculated by multiplying the gear ratio in the hydrostatic drive circuit and the gear ratio of the rear drive components of the vehicle by the diesel engine speed. The model created for this evaluation is given in Figure 4.1.

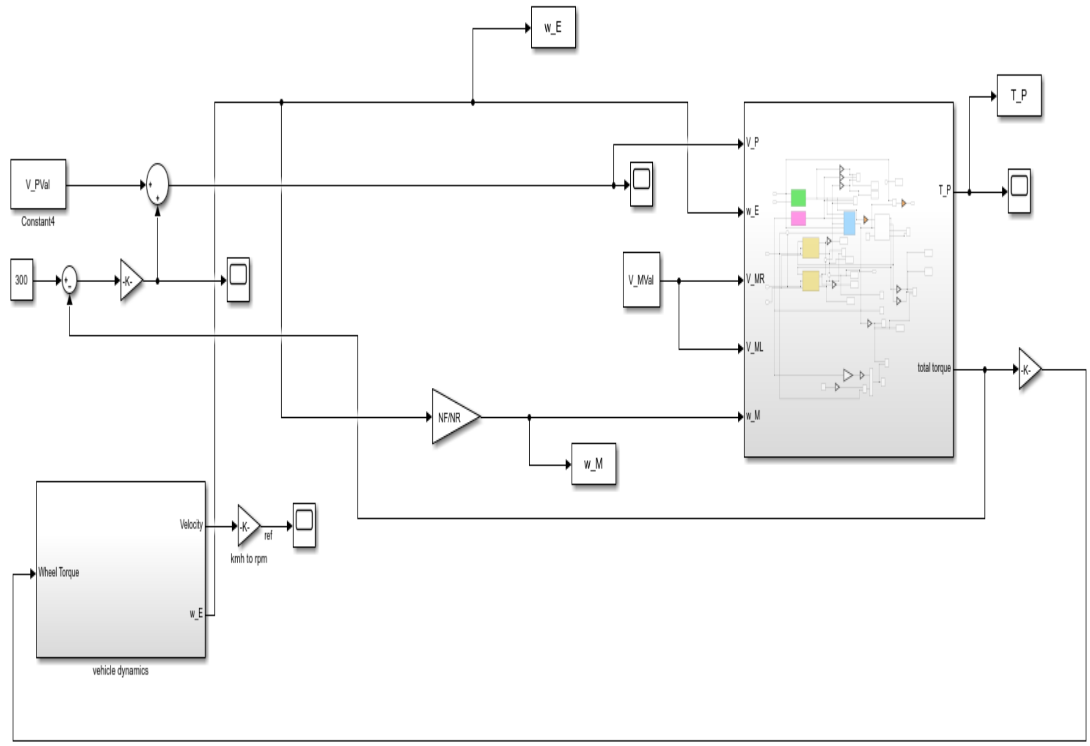

Figure 4.1. *First Evaluation*

The desired torque value has been determined as a constant value and a coefficient has been determined to minimize the error and reach this value. The feedforward cycle was created by summing the value obtained from this cycle with the calculated pump value. In Figures 4.2, pressure, angular speed of diesel engine and hydraulic motor, torque of hydraulic pump and hydraulic motor and flow of hydraulic pump and hydraulic motor are shown.

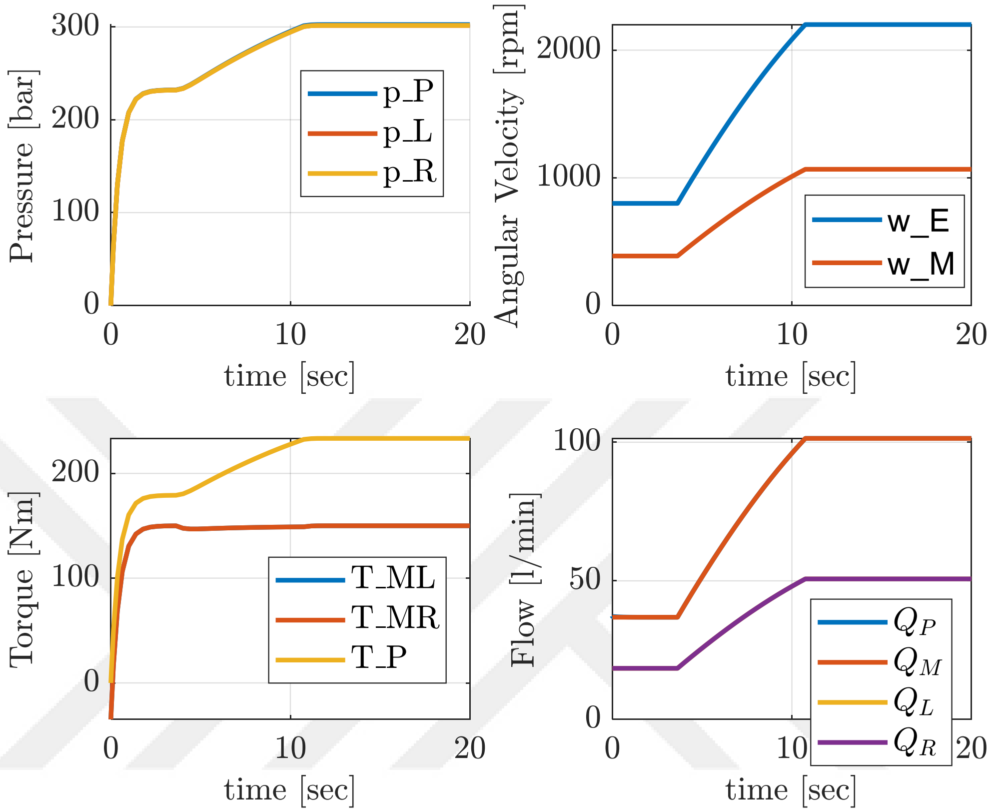

Figure 4.2. *First Evaluation Results*

The model made in this first evaluation system was integrated into the motor grader model and evaluated together with other variable parameters on the vehicle. The model is shown in the Figure 4.3. In the model, pump displacement was controlled according to constant gear and constant hydraulic motor displacement. Throttle percentage, diesel engine speed, hydraulic engine speed, front and rear wheels speed, margin of error and pump displacement were observed. The graphics are given in Figure 4.4.

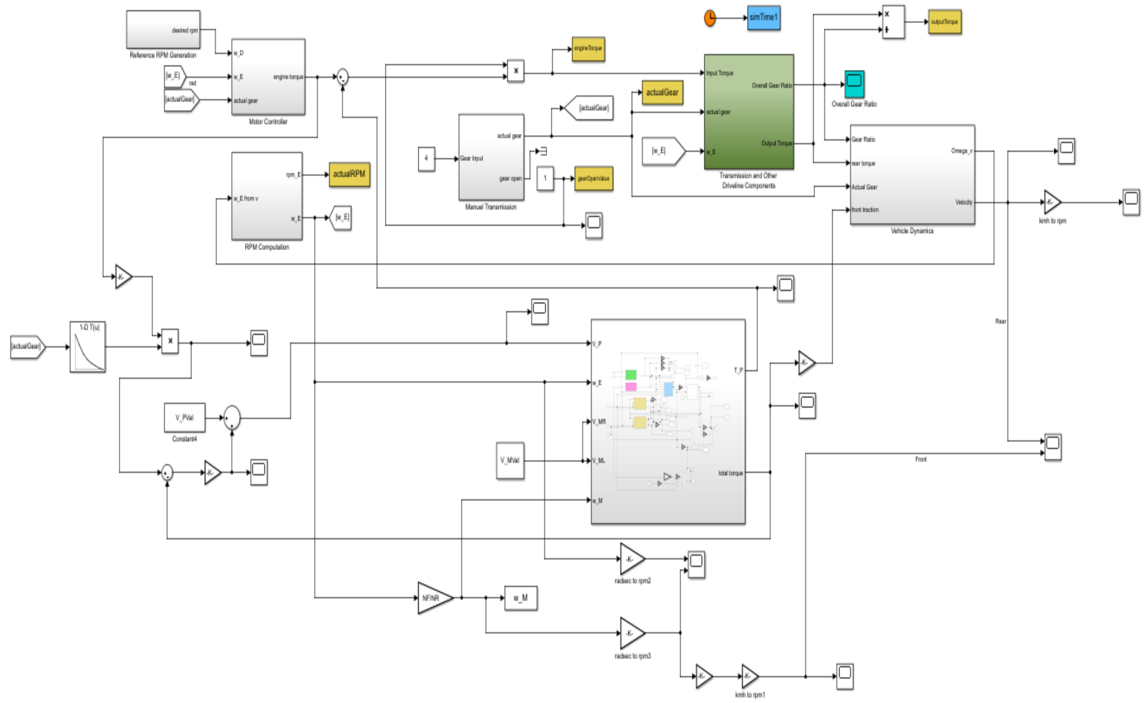

Figure 4.3. *First Evaluation Model*

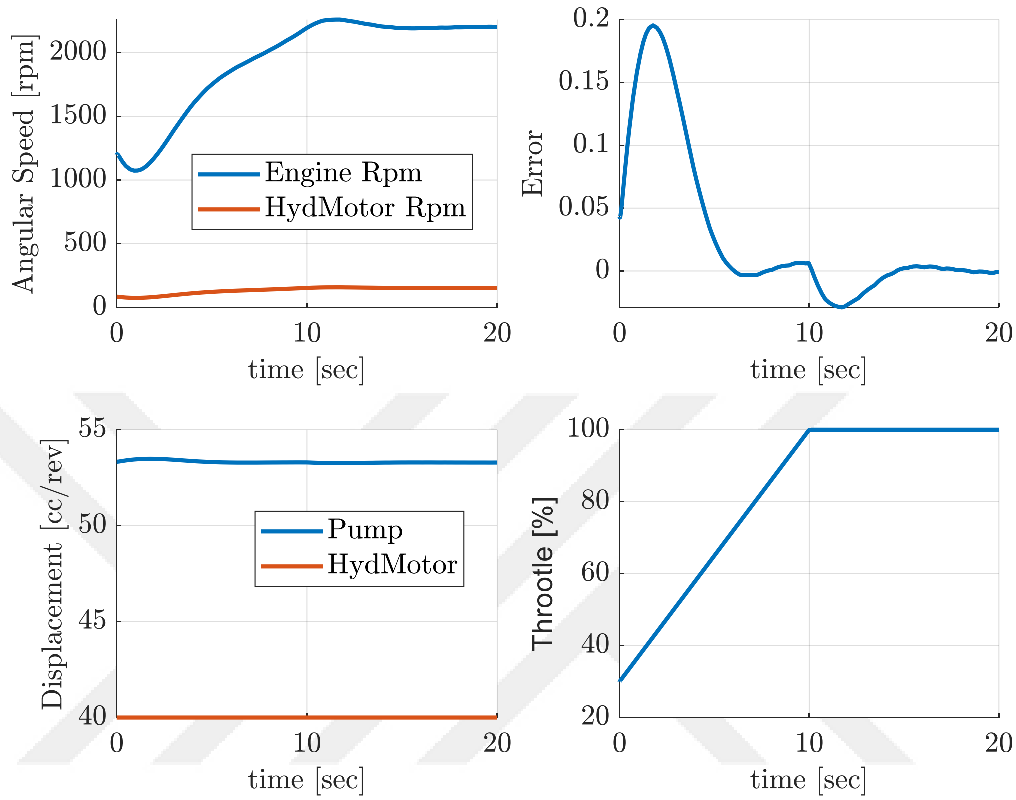

Figure 4.4. *Result of First Evaluation Model*

According to the results of the first evaluation model, diesel engine speed and hydraulic engine speed are related to gear ratios. In the first evaluation model, there is a hydraulic motor displacement value selected according to the gear. According to this hydraulic motor displacement, a relationship has been established between the ratio of gear ratios in the front and rear driving systems to each other. As seen in the graphs, the hydraulic motor displacement is constant and a hydraulic pump displacement value is determined by torque control.

4.1.3. Feedback Linearization

As a result of the evaluations made about the system, it was observed that the system should be made linear. Since hydrostatic drive is a non-linear system, it has been linearized with a feedback linearization method. Feedback linearization is expressed by the following Equations 4.1 and 4.2.

$$\dot{x} = f(x) + g(x)u \tag{4.1}$$

$$y = h(x) \tag{4.2}$$

In these Equations 4.1 and 4.2, $x \in R^n$, $u \in R$ and $y \in R$. u is input, x is state and y is output. Vector field are g: $R^n \rightarrow R^n$ and f: $R^n \rightarrow R^n$.

The torque parameter to be controlled varies depending on hydraulic motor displacement and system pressure. A constant hydraulic motor displacement value was determined for each gear value. In other words, hydraulic motor displacement value is known for each gear. Pressure parameter needs to be controlled. The torque formula is given below. T_m is hydraulic motor torque in Newton.m, V_m is hydraulic motor displacement in m^3 and P_m is pressure in Pascal. Q_p is pump flow in m^3/s, V_p is displacement of pump in m^3 and η_p is efficiency. Q_R and Q_L are right and left hydraulic motor flow in m^3/s, V_L and V_R are right and left displacement of hydraulic motors in m^3 and η_L and η_R are right and left hydraulic motor efficiencies. w_m is hydraulic motor speed in 1/s. Q_M is total flow of hydraulic motors in m^3/s. P_p is pump pressure in Pascal and B is bulk modulus. Function of Q_p represents pressure loss of flow divider. Feedback linearization of AWD system is expressed by the following equations.

$$T_m = V_m * P_m \tag{4.3}$$

$$Q_p = V_p * w_e * \eta_p \tag{4.4}$$

$$Q_L = V_L * w_m * \frac{1}{\eta_L} \tag{4.5}$$

$$Q_R = V_R * w_m * \frac{1}{\eta_R} \tag{4.6}$$

$$Q_M = Q_L + Q_R \tag{4.7}$$

$$Q_M = V_L * w_m * \frac{2}{\eta_L} = V_R * w_m * \frac{2}{\eta_R} \tag{4.8}$$

$$V_M = V_L + V_R \tag{4.9}$$

$$\eta_M = \eta_L = \eta_R \tag{4.10}$$

$$\dot{P_P} = B * (Q_p - Q_M) \tag{4.11}$$

$$P_M = P_P - f(Q_P) = P_P - \left(a + b * Q_p + c * Q_P^2\right) \tag{4.12}$$

$$T_M = V_M * p_M = V_M * p_p - V_M * \left(a + b * Q_p + c * Q_P^2\right) \tag{4.13}$$

Relation between w_e and w_M is given by following equations. w_e is angular speed of diesel engine in 1/s. g is rear drive gear ratio and N_F is front drive gear ratio.

$$w_E = \frac{g}{N_F} * w_M \tag{4.14}$$

$$\dot{P}_P = B * V_P * w_e * \eta_P - B * \frac{1}{\eta_M} * V_M * w_M \tag{4.15}$$

$$\dot{P}_P = B * V_P * w_e * \eta_P - B * \frac{1}{\eta_M} * V_M * \frac{N_F}{g} * w_e \tag{4.16}$$

$$\dot{P}_P = B * w_e * \left(V_P * \eta_P - \frac{V_M * N_F}{\eta_M * g}\right) \tag{4.17}$$

$$K = \frac{V_M * N_F}{\eta_M * g} \tag{4.18}$$

$$P_M = V_M * P_P - V_M * (a + b * \eta_P * V_P * w_e + c * \left(\eta_p * V_p * w_e\right)^2) \tag{4.19}$$

In this linearization, state parameter is P_p, input parameter is V_p, and output parameter is P_M. K is constant. With torque control, it is aimed to calculate the displacement value of the hydraulic pump. The torque in the hydrostatic drive system will vary according to the pressure. Therefore, the pump displacement and pressure values are used in linearization.

$$\dot{x} = B * w_e * (\eta_P * u - K) \tag{4.20}$$

$$y = V_M * x - V_M * (a + b * \eta_P * w_e * u + c * \eta_P^2 * w_e^2 * u^2) \tag{4.21}$$

Since the pressure loss in the valve is too low, the function dependent on the valve is neglected.

$$\dot{x} = B * w_e * \eta_P * u - B * w_e * K \tag{4.22}$$

$$y = V_m * x \tag{4.23}$$

$$\dot{x} = v \tag{4.24}$$

$$G(s) = \frac{V_M}{s} \tag{4.25}$$

$$u = \frac{v + B * w_e * K}{B * w_e * \eta_P} \tag{4.26}$$

4.1.4. Controller

AWD controller determines the most suitable hydraulic pump displacement and hydraulic motors displacement by calculating the torque requirement for the AWD system according to the torque produced by the diesel engine.

The vehicle has variable gear values, variable accelerator pedal value and different torque values that will occur depending on the accelerator pedal and gear variants. The controller designed by considering all these data calculates the parameters needed by the system under variable conditions. In order to prevent the vehicle from losing traction at variable gear values, the displacement values of hydraulic motors have been chosen as high as possible. At the same time, while making this selection, the maximum speed value that the vehicle can reach in each gear is a parameter that creates these selection criteria. In other words, there is a hydraulic motor displacement value for each gear value, and when the system is activated while the vehicle is walking, the hydraulic motor displacement value reaches its required value with a ramp function. The controller calculates a pump displacement based on the desired torque values for the AWD system, which is determined according to the hydraulic motor displacement values and power regulation selected according to gear value. The subsystems of the controller are shown in the Figure 4.5.

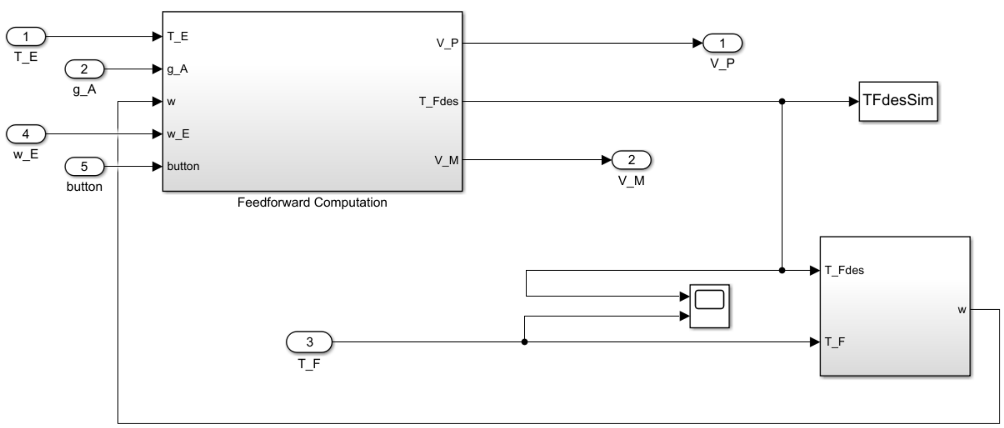

Figure 4.5. *Subsystems of Controller*

The working principle of the controller is based on the feedback linearization mentioned in the previous section. The controller contains the equations mentioned in the previous section. The mathematical model of the controller is shown in the Figure 4.6, Figure 4.7 and Figure 4.8. The whole model is given in Figure 4.9. Figure 4.6 includes hydraulic motor-gear look up table, maximum torque value for the torque value determined in power regulation, feedforward control and some part of feedback linearization. Other part of feedback linearization is located on Figure 4.7. This mathematical model includes formulas of feedback linearization section. The Figure 4.8 shows error computation. The difference between actual and desired torque is eliminated by multiplying it by the specified coefficient.

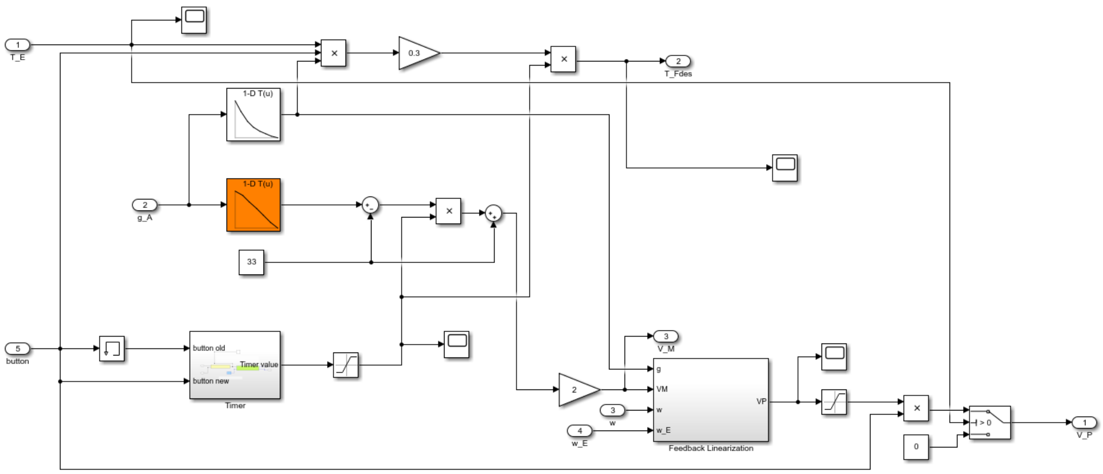

Figure 4.6. *Feedforward Computation of Controller*

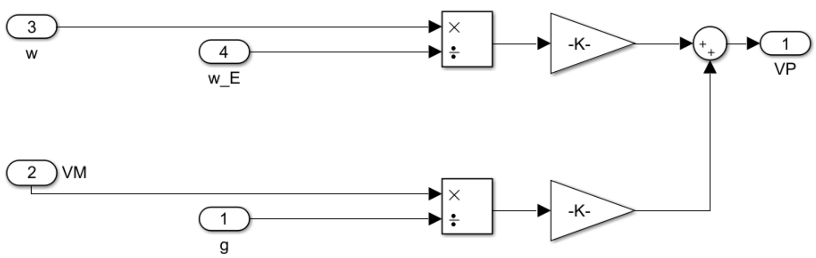

Figure 4.7. *Feedback Linearization of Controller*

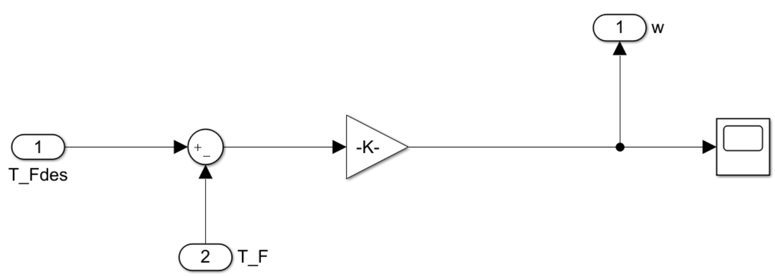

Figure 4.8. *Error Computation for Feedback Linearization of Controller*

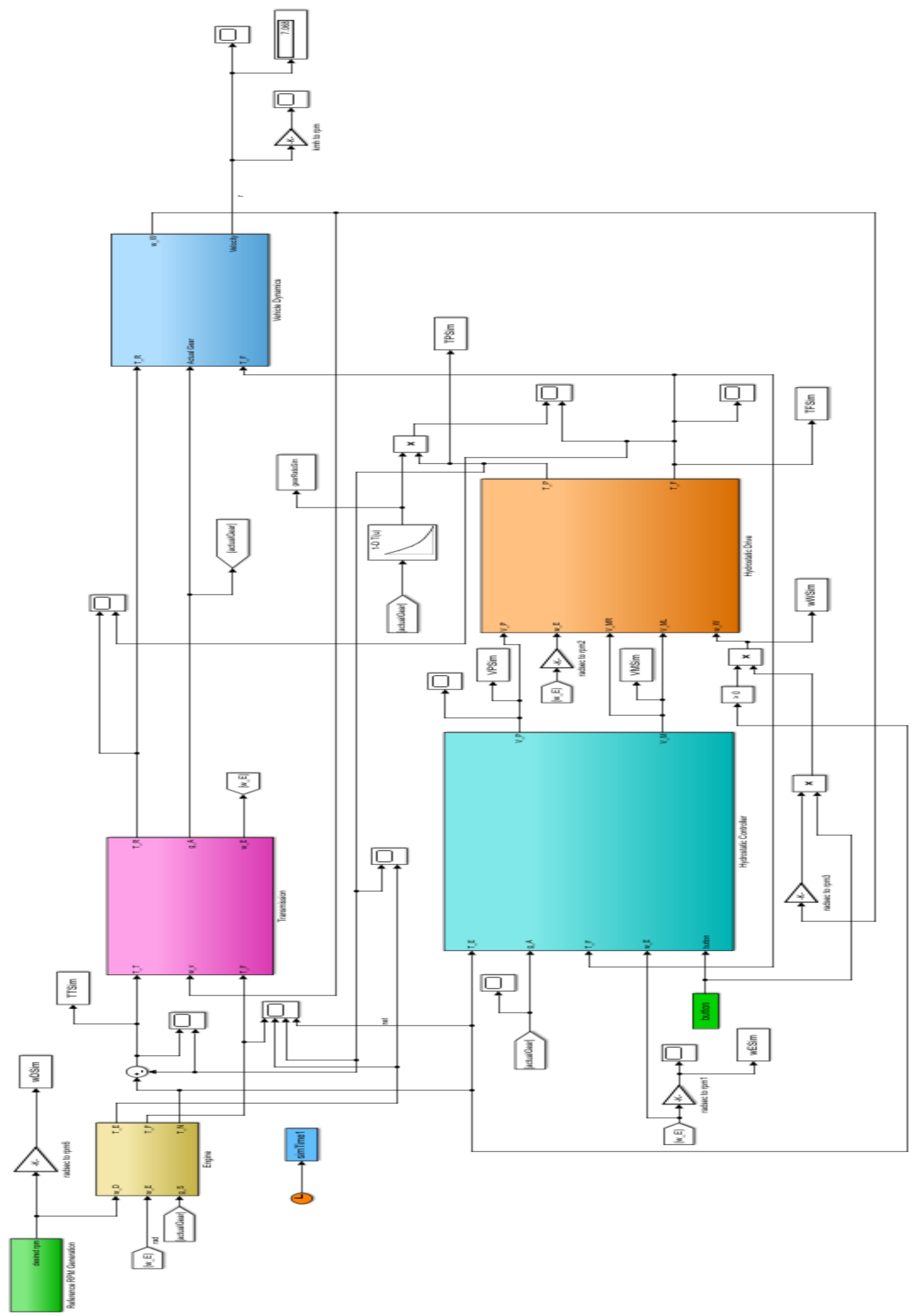

***Figure 4.9**. Mathematical Model of Motor Grader with AWD System*

4.1.5. Simulation

After the controller design was completed, it was combined with the physical system and simulations were performed under different scenarios. The scenarios performed were made according to the situations that the vehicle may encounter on the field. The simulation inputs and results are given in Figure 4.10, 4.11, 4.12, 4.13, 4.14, 4.15 and Table 4.1, 4.2 and 4.3.

In all simulations, the AWD system becomes active in the 5th second. In the first simulation, the accelerator pedal is constantly increasing and accordingly the vehicle tends to accelerate. With this speed increase, the flow rate of the hydraulic pump increases and the pressure increases as well. With this acceleration request, the desired torque value also increases with the increase in pressure. In Figure 4.10, the hydraulic pump and motor displacements, desired and actual torque values, pressure values and wheel and engine rpm values are shown.

Simulation 1:

Time	0	5	10	15	17	20
Gear	3	3	3	3	3	3
AWD Button	0	1	1	1	1	1
Throttle (%)	30	30	40	50	60	70

Table 4.1. *Simulation 1 Inputs*

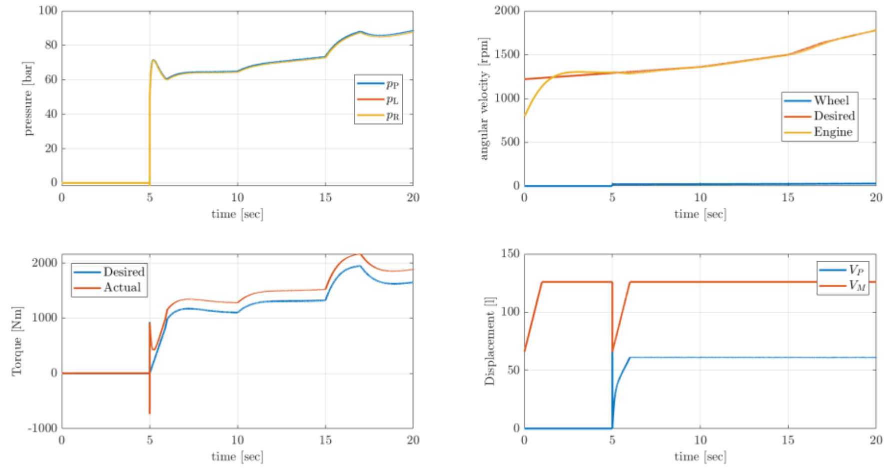

Figure 4.10. *Simulation 1 Torque, Pressure, Angular Velocity and Displacement Results*

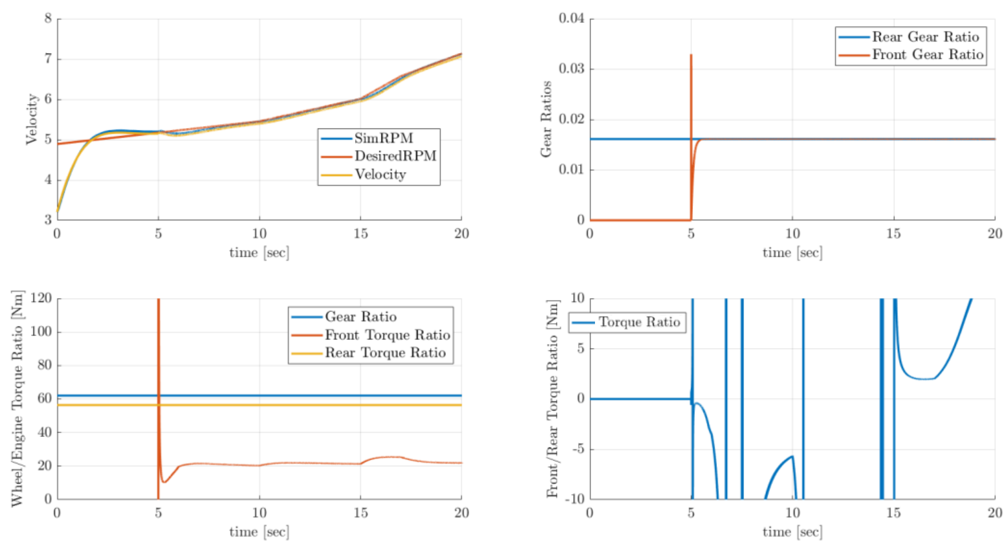

Figure 4.11. *Simulation 1 Velocity, Torque Ratios, and Gear Ratio Results*

In the second simulation, unlike the first simulation, gear upshifting was applied. The characteristic of the vehicle is as in the first simulation. Since the gear ratios also changed during the gear change, the vehicle needed more torque and a new hydraulic pump displacement value was calculated for the gear change. The hydraulic motor displacement varied according to the gear value and the system pressure increased with the increasing pump displacement and torque requirement.

Simulation 2:

Time	0	5	10	15	17	20
Gear	3	3	4	4	4	4
AWD Button	0	1	1	1	1	1
Throttle (%)	30	30	40	50	60	70

Table 4.2. *Simulation 2 Inputs*

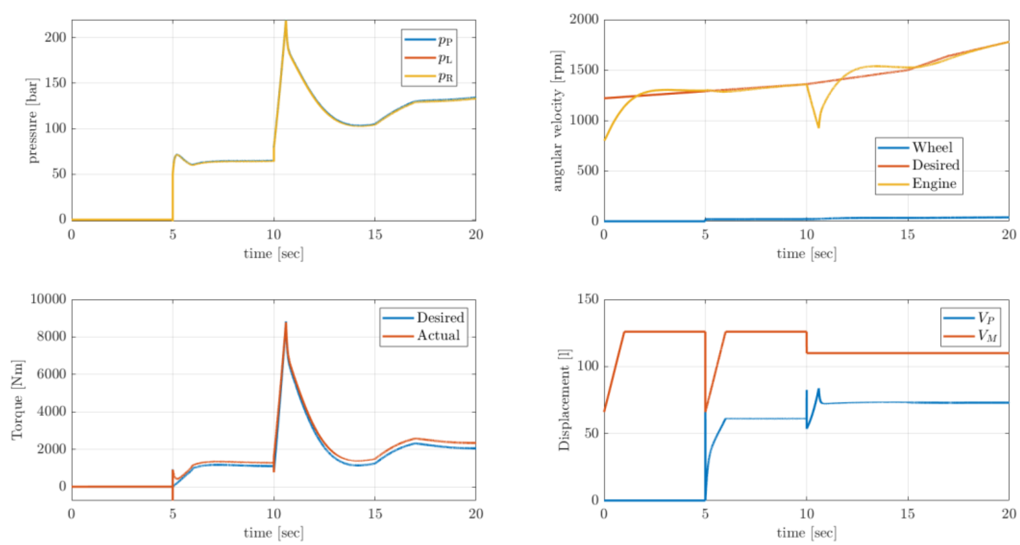

Figure 4.12. *Simulation 2 Torque, Pressure, Angular Velocity and Displacement Results*

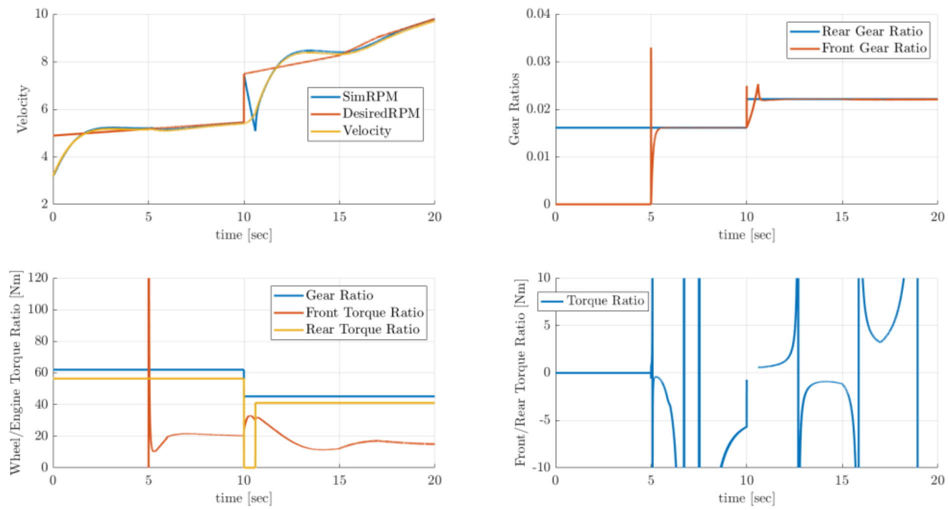

Figure 4.13. *Simulation 2 Velocity, Torque Ratios, and Gear Ratio Results*

In the third simulation, downshifting was performed. The vehicle tends to slow down, unlike the first two simulations. While the gear tends to slow down and the vehicle slows down, the hydraulic pump does not produce displacement. When the vehicle starts accelerating again, a new displacement value is determined for the hydraulic pump. The pressure value decreases during deceleration. Simulation 3 results are shown in Figure 4.14 and 4.15.

Simulation 3:

Time	0	5	10	15	17	20
Gear	3	3	2	2	2	2
AWD Button	0	1	1	1	1	1
Throttle (%)	30	30	30	30	30	40

Table 4.3. *Simulation 3 Inputs*

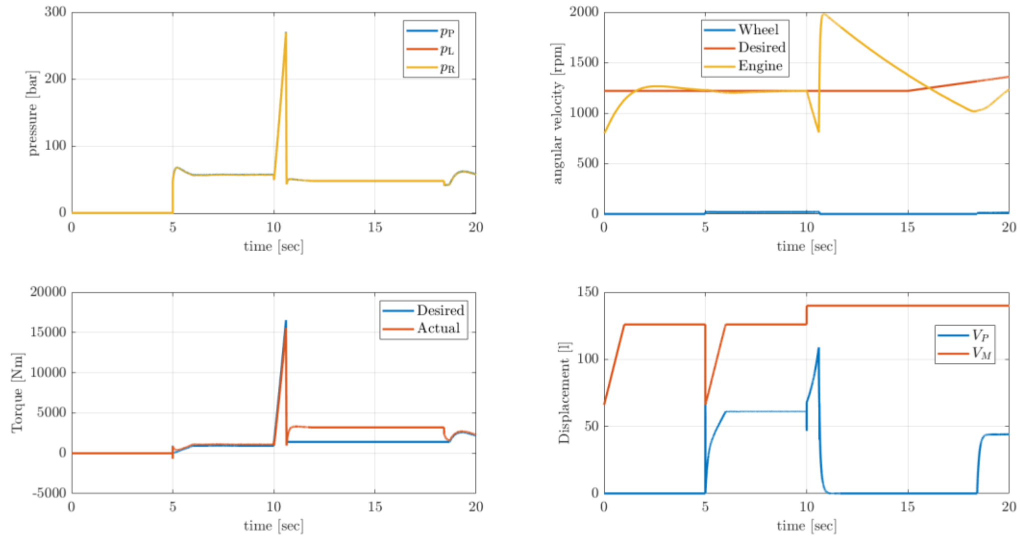

Figure 4.14. *Simulation 3 Torque, Pressure, Angular Velocity and Displacement Results*

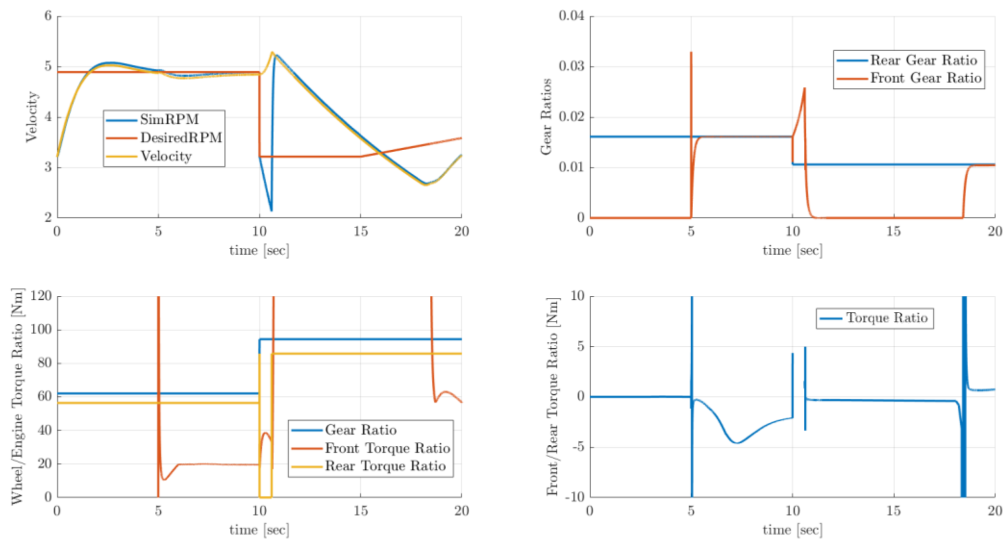

Figure 4.15. *Simulation 3 Velocity, Torque Ratios, and Gear Ratio Results*

4.1.6. Test Results and Comparison with Simulation

After the system was completed and the motor grader vehicle was operational, two different test environments were created for the system. In the first test environment, the vehicle was tested on a platform so that the wheels do not touch the ground. While the vehicle is on the platform, the system and its components have been verified. After this verification, the vehicle was prepared for testing on the site (with the wheels touching the ground). The first test platform is shown in the Figure 4.16.

Figure 4.16*. Test Platform for Initial Tests*

In the platform tests, firstly, hydraulic pump calibration was done. During the calibration, calibration was performed in accordance with the supplier instructions. During the testing phase, the percentage of hydraulic pump displacement has been increased at certain intervals, and pressure measurements and speed measurements have been performed from the speed sensors located on the hydraulic motors.

In tests, it is energized by sending the same PWM values to hydraulic motors. That is, hydraulic motor displacements are determined as the same and constant. Also, engine speed and gear is constant. Due to valve characteristics and efficiency, there is a small difference between hydraulic motor speeds. The current values of hydraulic motors powered by the same PWM signal are shown in the Figure 4.17 and 4.18. Additionally, the hydraulic pump's pressure values and wheel speeds are shown in the Figure 4.17 and 4.18.

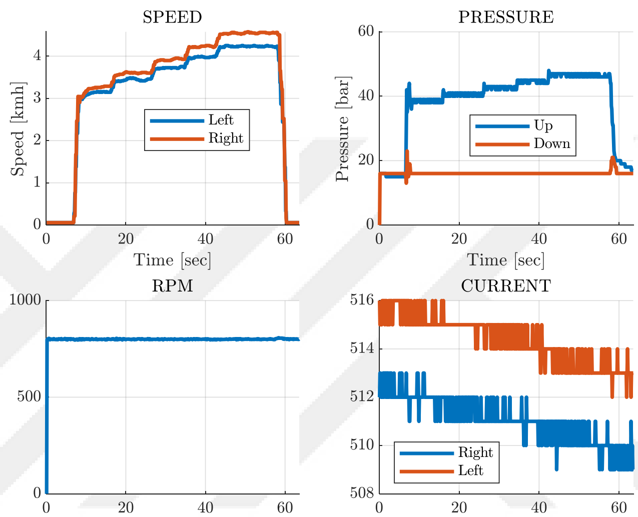

Figure 4.17. *First Test Results*

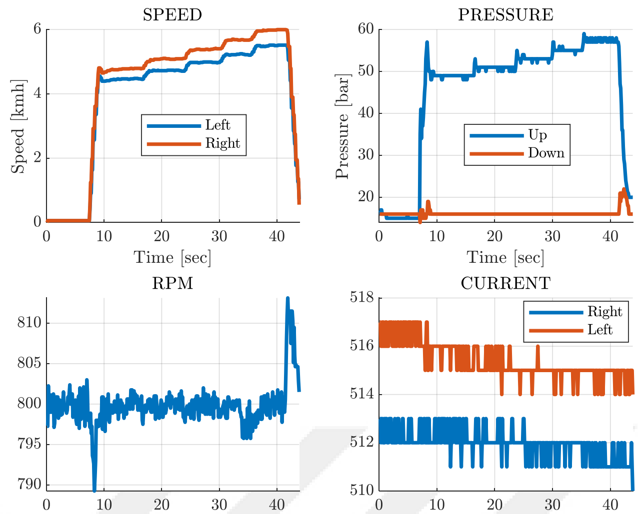

Figure 4.18. *Second Test Results*

The test data were applied as an input to the hydrostatic drive model and the test results and simulation outputs were compared. Test and simulation results are shown in the Figure 4.19, 4.20, 4.21 and 4.22.

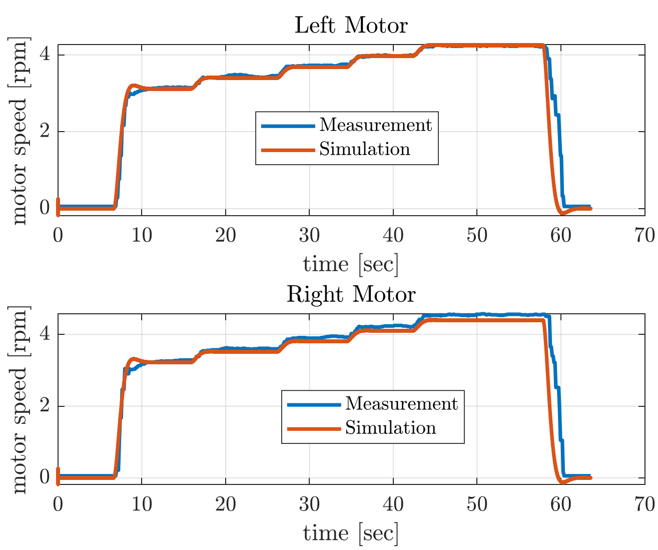

Figure 4.19. *Comparison of First Test-1 Results and Simulations*

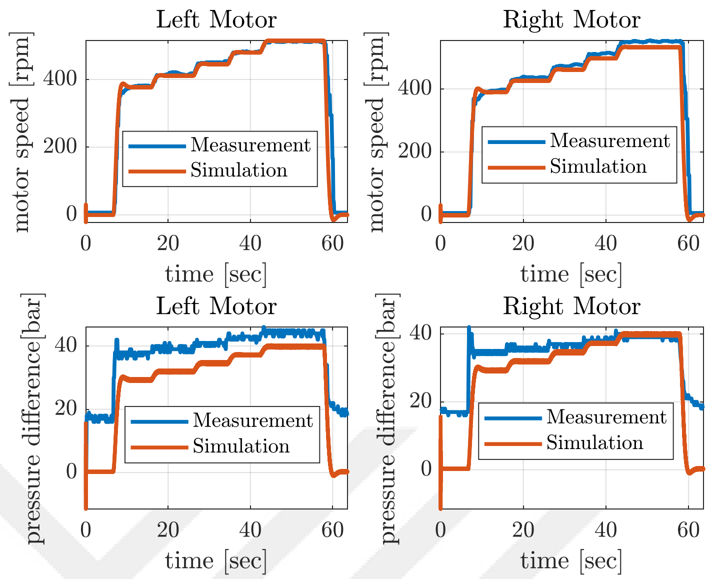

Figure 4.20. *Comparison of First Test-1 Results and Simulations*

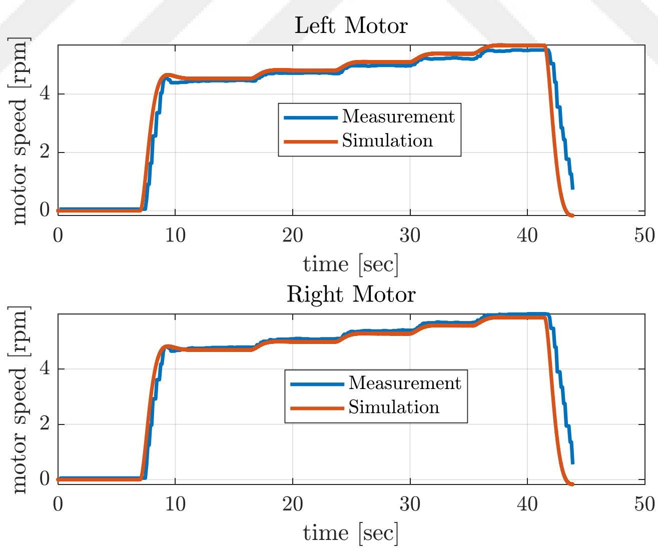

Figure 4.21. *Comparison of Second Test-1 Results and Simulations*

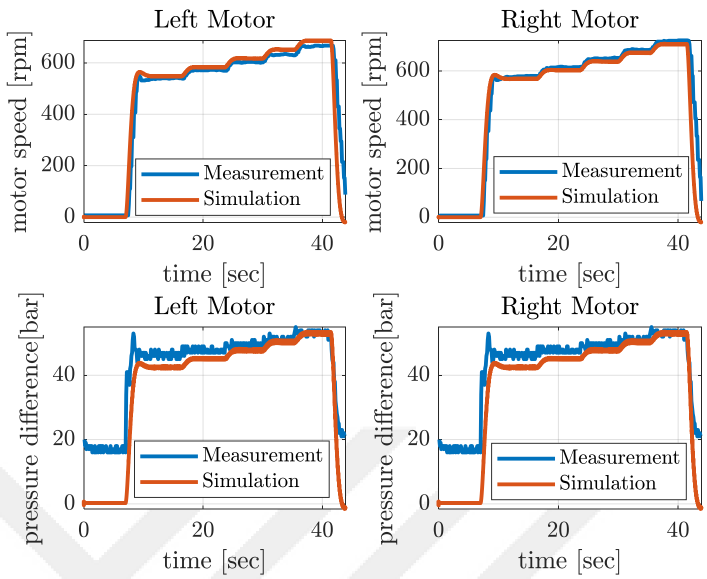

Figure 4.22. *Comparison of Second Test-1 Results and Simulations*

In order to integrate the controller structure designed for the AWD system into the embedded card, the software was realized in C environment. After the software was verified, the machine passed to the second test phase. The flow chart and software logic of the software are mentioned in the Algorithm section. Second test results are given in the Figure 4.23, 4.24 and 4.25. In tests, the vehicle gear value is constant and the vehicle accelerates and then decelerates.

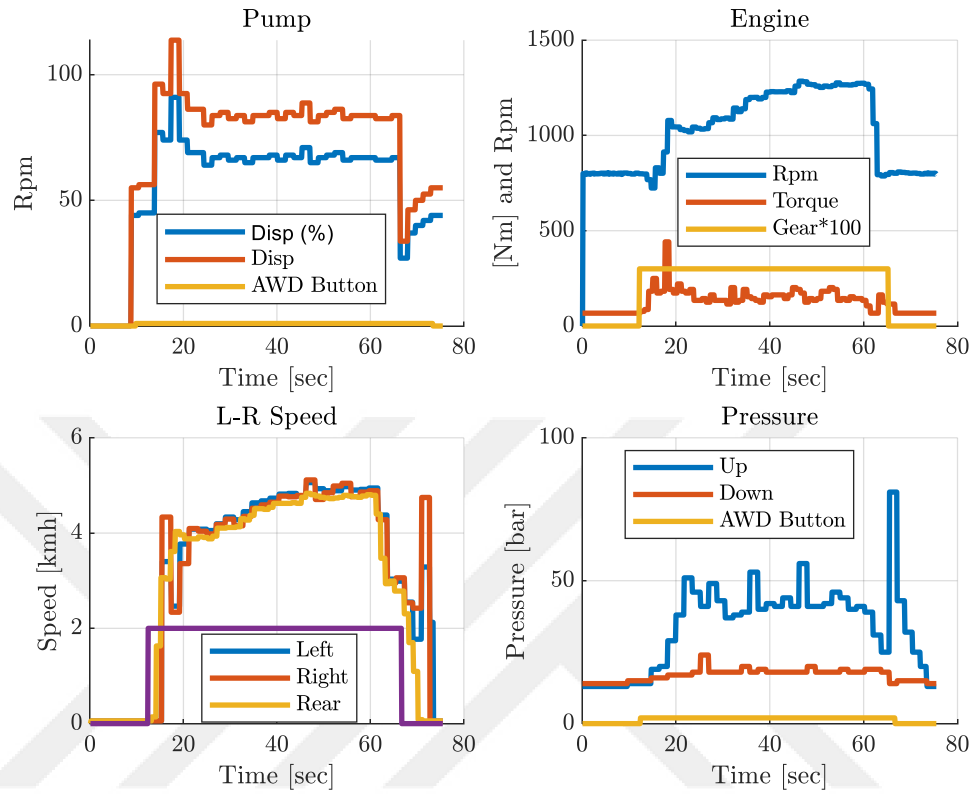

Figure 4.23. *First Test-2 Results*

As seen in the graphs, the AWD pump sends the displacement when the button is active and the vehicle is in gear. The first take-off moment is carried out with the inching pedal. The inching pedal acts as a clutch. The reason for the sudden increase of the speed value at the first take-off is related to the state of the inching pedal.

As seen in the test results, the front wheel speeds are slightly higher than the rear wheels. The front wheels of the vehicle lead the rear wheels. For this reason, a lead factor has been applied to make the front wheels turn faster. This is the reason for the speed difference between the front and rear wheels.

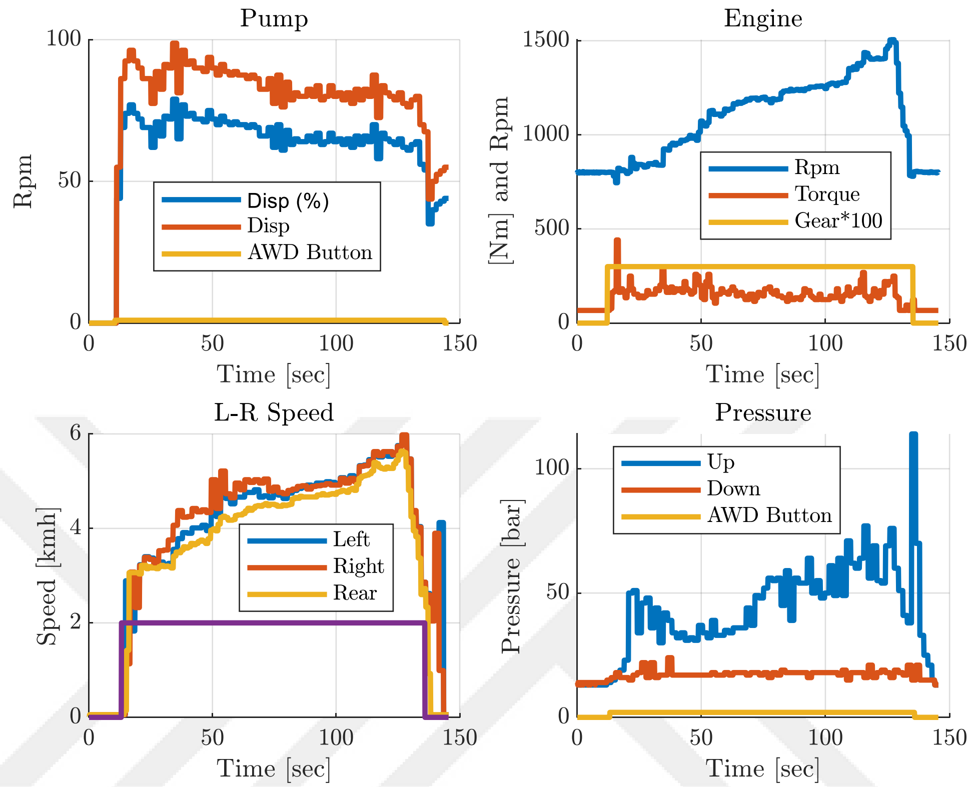

Figure 4.24. *Second Test-2 Results*

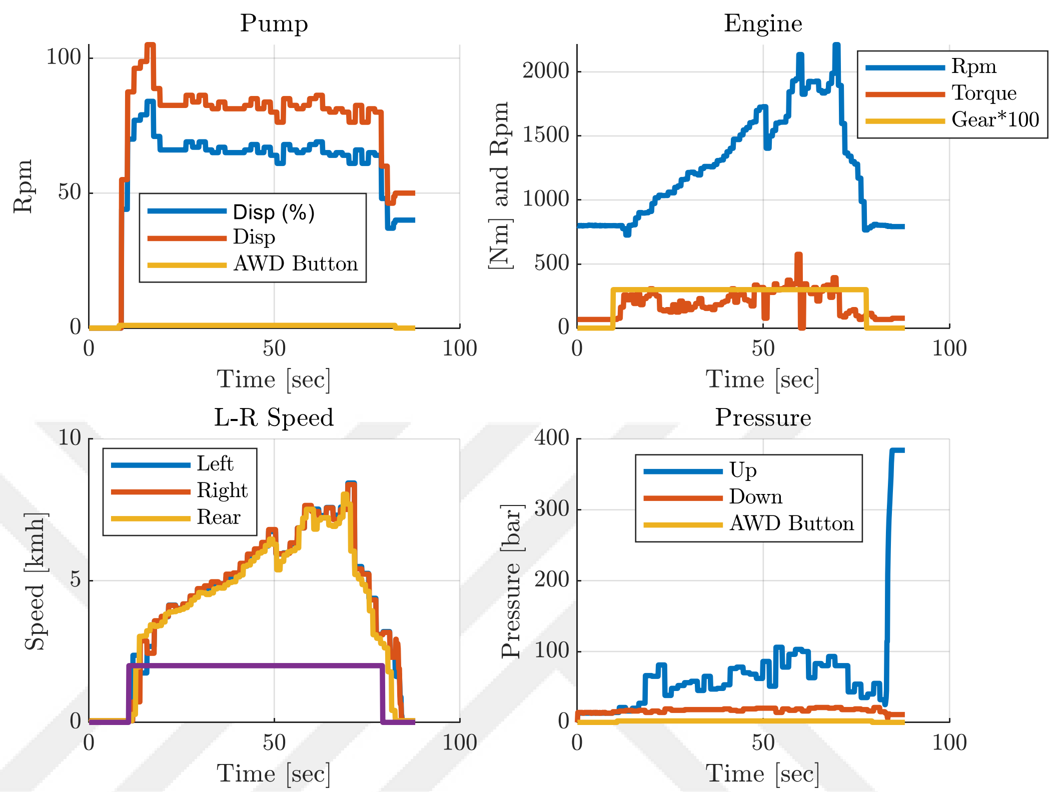

Figure 4.25. *Third Test-2 Results*

4.2. Algorithm

The software was created as a result of mathematical models and calculations. The torque control performed in the mathematical model was implemented in the software. The software's basic logic is based on the mathematically generated model and controller. The communication type used in the software is the Can-Bus communication network.

Can-Bus communication network, which is widely used in the automotive industry, is used in the motor grader vehicle. Communication with diesel engine control unit and other machine control units is provided by Can-Bus. J1939 standard was used in this communication system, which has different standards. Communication protocol has been carried out in accordance with this standard. A Can-Bus message has a 64-bit size. There are different numbers of data in a Can-bus message, depending on the size of the data used. There are two different cables in the Can-Bus communication protocol, Can-High and Can-Low. These cables have a line structure twisted around each other in the installation. In addition, the Can-bus is a differential signal. In the Can-Bus circuits, there is a resistance between the two lines so that the message transfer can be performed properly. In the Figure 4.26, the differential signal feature of the Can-Bus signal is highlighted. When a signal comes to the communication line, the Can-High and Can-Low signal lines change their voltage values in the opposite direction and have new voltage values. Since it is a differential signal, less noise occurs in the communication line.

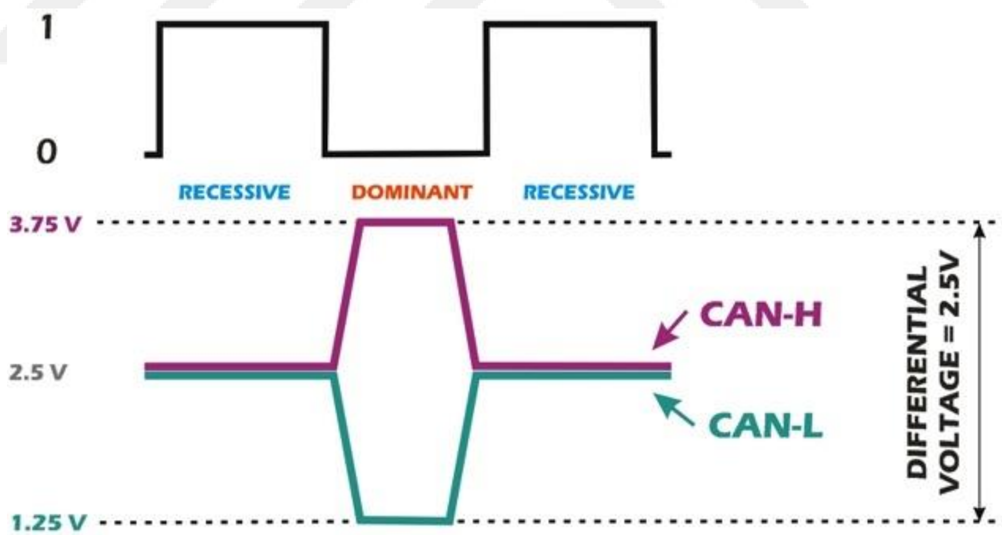

Figure 4.26. *Can-Bus Signal (22)*

The transmission of the messages contained in the algorithm is provided by Can-Bus. There are three different modes in the Motor Grader vehicle: park, work & travel and travel. The vehicle is stationary in parking mode. In work & travel mode, the blade functions of the motor grader can be controlled while the vehicle is in motion. Travel mode is used when the vehicle is traveling from one location to another. The functions of the vehicle cannot be controlled in Travel mode. AWD system is designed for work & travel mode.

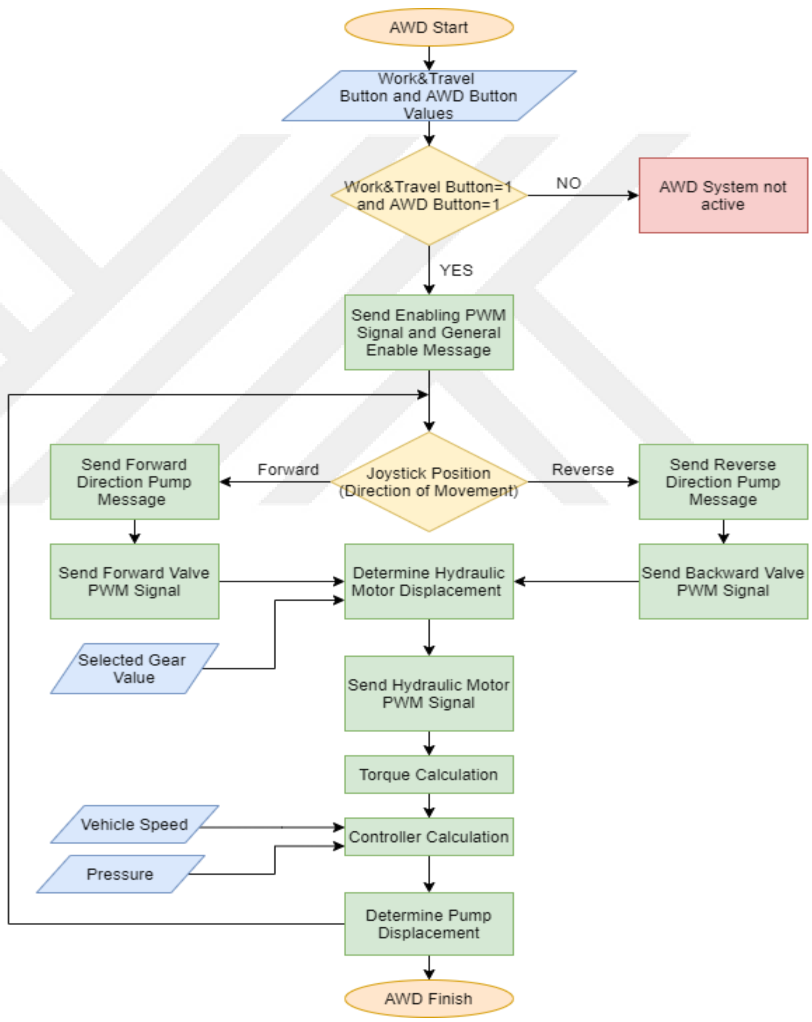

Figure 4.27. *Flowchart of Algorithm*

The system starts working provided that the work & travel button and the AWD button are active. The enable signal and message are activated so that the hydraulic pump can be activated. Depending on the direction of movement of the vehicle, gear is selected in the forward or reverse direction. With this selection, hydraulic pump direction is determined. A signal is sent to the valves representing the forward and reverse direction in the hydraulic control block. While the vehicle is in motion, a look up table has been created in which hydraulic engine displacement values are determined according to the gear value. PWM signal is sent to the valves in hydraulic motors by selecting a displacement value for hydraulic motors from this table according to the gear value. A torque calculation is made according to the torque data received from the diesel engine. In addition to these data, the designed controller calculates a value for pump displacement based on vehicle speed and hydraulic system pressure. The flowchart of the algorithm is shown in the Figure 4.27.

CHAPTER 5

CONCLUSION

In this study, the studies of a hydrostatic drive circuit, which provides traction force to the motor grader vehicle and provides a more efficient operation, were investigated. The hydrostatic drive circuit modeled in Simulink and Simscape environments has been made operational on the motor grader vehicle.

During the study, the requirements of the AWD system were determined first. Hydraulic pumps and hydraulic motors were selected according to these requirements. After the pre-feasibility and preliminary calculations are completed, the hydraulic system is designed. Mechanical, hydraulic and electronic components of the system have been identified. The system was first designed with blocks in the Simscape environment and a simulation was created. These simulation outputs are compared with theoretical calculations.

In the ongoing process, the AWD system and motor grader vehicle are modeled mathematically. The diesel engine and its controller, transmission and power transmission components, the dynamic structure of the vehicle, the hydrostatic walking system (AWD) and the controller of the AWD system are elements of the mathematical model. The dynamic behavior of the diesel engine modeled with its controller has been verified by test data. Transmission and powertrain components are modeled after the diesel engine. The dynamic structure of the vehicle includes the positive and negative forces acting on the vehicle. Depending on these forces, the inertia of the vehicle was brought together and the dynamic behavior of the vehicle was modeled. The AWD system is modeled in line with the calculations and literature studies. A controller design was then carried out by applying feedback linearization. Simulations of a motor grader vehicle with AWD system were observed.

After the modeling is completed, the assembly of the prototype vehicle has been completed and the accuracy of the components has been tested. It was observed that the results were close to each other by comparing the tests and simulation outputs. Afterwards, the software of the vehicle was completed to perform field tests and the results on the field were observed. It was observed that the system was working correctly by providing speed synchronization with torque control.

During the study, activities related to the AWD system are included. AWD system has been verified by testing the studies in the field as an academic and a real system.

REFERENCES

[1] https://en.wikipedia.org/wiki/Grader

[2] http://www.intrac.ee/uploads/products/buvnieciba/graders-brochure-en.pdf

[3] J. Backas, R. Ghabcheloo, ve K. Huhtala, “Gain scheduled state feedback velocity control of hydrostatic drive transmissions”, *Control Engineering Practice*, vol. 58, pp. 214-224, Jan. 2017, doi: 10.1016/j.conengprac.2016.10.016.

[4] P. Zeman, W. Kemmetmüller, ve A. Kugi, “Mathematical Modeling and Analysis of a Hydrostatic Drive Train”, *IFAC-PapersOnLine*, vol. 48, no.1, pp. 508-513, 2015, doi: 10.1016/j.ifacol.2015.05.064.

[5] K. A. Mistry, B. A. Patel, D. J. Patel, P. M. Parsana, ve J. P. Patel, “Design and Analysis of Hydrostatic Transmission System”, *IOP Conf. Ser.: Mater. Sci. Eng.*, vol. 310, p. 012048, Feb. 2018, doi: 10.1088/1757-899X/310/1/012048.

[6] R. Likaj ve A. Shala, “DESIGN OF AUTOMATIC SYSTEM WITH HYDROSTATIC TRANSMISSION”, p. 5.

[7] P. J. Stroempl, “Flow Divider and Flow Divider/Combiner Valves for Closed Loop Hydrostatic Transmissions”, Sep. 1990, p. 901554, doi: 10.4271/901554.

[8] M. S. Kumbasar, “HİDROSTATİK TAHRİK VE KAPALI DEVRELERDE

TASARIM KRİTERLERİ”, p. 7.

[9] R. Prabel ve H. Aschemann, “Torque Control of a Hydrostatic Transmission Using Extended Linearisation Techniques”, Dec. 2017, pp. 352-359, doi: 10.3384/ecp17144352.

[10] D. Song *et al.*., “Hardware-in-the-loop validation of speed synchronization controller for a heavy vehicle with Hydraulics AddiDrive System”, *Advances in Mechanical Engineering*, vol. 10, no. 4, p. 168781401876716, Apr. 2018, doi: 10.1177/1687814018767169.

[11] H. Aschemann, J. Ritzke, ve H. Schulte, “Model-Based Nonlinear Trajectory Control of a Drive Chain with Hydrostatic Transmission”, *IFAC Proceedings Volumes*, vol. 42, no. 13, ss. 461-466, 2009, doi: 10.3182/20090819-3-PL-3002.00080.

[12] Y. Wang, Z. Zhang, ve X. Qin, “Modeling and control for hydraulic transmission of unmanned ground vehicle”, *J. Cent. South Univ.*, vol. 21, no. 1, pp. 124-129, Jan. 2014, doi: 10.1007/s11771-014-1923-6.

[13] Z. Jedrzykiewicz, J. Pluta and J.Stojek, "Application of the MATLAB - Simulink package in the simulation tests on hydrostatic systems", *Acta Montanistica Slovaca*, pp. 29-37, Jan. 1998.

[14] A. V. Akkaya, “Effect of bulk modulus on performance of a hydrostatic transmission control system”, *Sadhana*, vol. 31, no. 5, pp. 543-556, Oct. 2006, doi: 10.1007/BF02715913.

[15] MODULE-6: HYDROSTATIC TRANSMISSION SYSTEMS, http://content.inflibnet.ac.in/data-server/eacharya-documents/55d31af3e413010f24d8f40c_INFIEP_201/2014/ET/201-2014-ET-V1-S1__m6l23.pdf

[16] https://loganclutch.com/saepto-typical-applications?print=true

[17] Handbook for Mobile Transmissions Calculation Details, Calculation of Hydromatik Mobile Transmissions.

[18] J. Grabbel and M. Ivantysynova, ‘An Investigation of Swash Plate Control Concepts for Displacement Controlled Actuators’, International Journal of Fluid Power, vol. 6, no. 2, pp. 19–36, Jan. 2005, doi: 10.1080/14399776.2005.10781217.

[19] A. Değirmencioğlu, ' Tek Pompa ve Çok Motorlu Kapalı Devre Hidrostatik Sistemleri Şarj Pompası ve Loop Flushing Debisinin Belirlenmesi', Uluslararası Katılımlı VII. Ulusal Hidrolik Pnömatik Kongresi, pp. 125-137, 2014.

[20] U. Akpınarlı, E. Çakır, Ç. Kaltalıoğlu, İ. Varol, ' Tüm Tekerlerden Çekişli Motor Greyder Hidrostatik Ön Aksının Tasarımı', 1. Ulusal Mühendislik ve Teknoloji Kongresi, 2019.

[21] https://www.quora.com/What-is-a-CAN-bus